THE ROLE OF A LOCUS CONTROL REGION UPSTREAM OF *Bcl6* IN GERMINAL CENTER FORMATION

A Dissertation

Presented to the Faculty of the Weill Cornell Graduate School

of Medical Sciences

in Partial Fulfilment of the Requirements for the Degree of

Doctor of Philosophy

by

Rajat Singh

August 2018

THE ROLE OF A LOCUS CONTROL REGION UPSTREAM OF Bcl6 IN GERMINAL CENTER FORMATION

Rajat Singh, Ph.D.

August 2018

Germinal Center B-cells (GCB) arise upon antigen stimulation and undergo somatic hypermutation (SHM) in order to produce high-affinity antibodies. BCL6, a transcriptional repressor, sustains GCB survival despite the genotoxic stress associated with SHM by repressing apoptosis and cell cycle arrest genes.

Studies from our lab show intra-chromosomal interactions between a putative locus control region (LCR) and the *BCL6* promoter in human GCBs. In both human and mice, this LCR is characterized by histone modifications associated with active enhancers, DNase hypersensitive regions, and increased binding of transcription factors and chromatin modifiers. This evidence suggested that the LCR is 'switched on' during the transition from naïve B-cells to GCBs and led us to hypothesize that the LCR plays a role in the transcriptional re-programming characterizing this stage of B-cell differentiation. We utilized CRISPR-Cas9 technology, to knock out the LCR in mice, which resulted in complete abrogation of GC formation. Additionally, we found that this defect is GCB intrinsic, and the loss of the LCR does not affect other tissues that require BCL6. We also discovered that a single copy of the LCR, in cis with *Bcl6*, is sufficient for GCB formation. However, when the LCR is in *trans* with *Bcl6* it results in the loss of GC formation.

Furthermore, to study the effect of this LCR on gene regulation we tried to utilize an ex-vivo culture system that mimics aspects of B-cell differentiation into GC B-cells. These B-cell follicle cultures or GC 'organoids' were extensively utilized to

grow and differentiate murine B-cells. During the course of this investigation, we optimized many aspects of the culture conditions. However, the ex-vivo system did not phenocopy the in-vivo observations made in LCR KO mice. Our current efforts are focused on identifying the necessary functional motifs within the LCR by utilizing lymphoma cell lines.

This work adds to our current understanding of how chromatin architectural modulation may be controlled by critical loci around master transcription factors, thereby influencing widespread transcriptional regulation required for differentiation. Additionally, an understanding of this particular LCR upstream of *Bcl6* has the potential to guide investigations into the manner in which chromosomal translocations—like the 3q27 translocations frequently observed in diffuse large B-cell lymphomas (DLBCL)—play a role in lymphomagenesis and the maintenance of such pathologies.

BIOGRAPHICAL SKETCH

Rajat Singh obtained a Bachelor of Science (Biochemistry) from Sri Venkateswara College, University of Delhi, New Delhi, India in May 2006. Rajat then moved to the United States and joined Washington State University, Pullman, WA (WSU), where he obtained his second Bachelor of Science (Neuroscience) in May 2008.

During the last year of his undergraduate studies at Washington State University, Rajat received the National Cancer Institute-Cancer Research Training Award (NCI-CRTA). With this fellowship, he started working at the NCI in Bethesda, MD under the guidance of Dr. Robert J. Kreitman. His research in the clinical immunotherapy section of the Lab of Molecular Biology (CCR, NCI) involved a pre-clinical investigation of the recombinant immunotoxin LMB-2 (*Pseudomonas exotoxin conjugated to a single change Fv antibody targeting CD25*) combined with chemotherapeutic agents targeting solid tumors. His work spanned a period of two years and led to a first author publication.

Rajat continued working at the National Institutes of Health with another fellowship (Technical-Intramural Research Trainee Award) in Dr. Craig Blackstone's lab at the National Institute of Neurological Disorders and Stroke (NINDS, NIH) in Bethesda, MD. Here he contributed towards multiple projects focused on a group of genetic disorders known as hereditary spastic paraplegias. Specifically, he investigated the role of genes implicated in the disease-SPG11, SPG15 and SPG20. The 20-month tenure at NINDS resulted in three publications.

Rajat left the NIH in the summer of 2012 to join the Immunology and Microbial Pathogenesis graduate program at Weill Cornell Medical College. He

became a member of Dr. Ari M. Melnick's lab in July 2013 and decided to study the role of a putative locus control region (LCR) in the transition from Naïve B-Cells to Germinal Center B-Cells. During his time as a graduate student Rajat has been involved in additional teaching and volunteering activities which include working as a teaching assistant for *Cell Biology and Development* over two years, the *Fundamentals of Immunology* for a year, and volunteering as a peer-counselor with the '*Peers Advocating Wellness*' (PAWs) program at Weill Cornell among other training, mentoring and community service activities.

Rajat's graduate research has led to one co-first author publication (August 2016), and is on track to contribute to another manuscript (expected publication between 2018-2019). After obtaining a Ph.D., Rajat is continuing his academic pursuits as a medical student at Sidney Kimmel Medical College, Thomas Jefferson University, Philadelphia, PA. He ultimately looking forward to a career in academic medicine and hopes to further contribute to the field of Immunology and Hematology as his career progresses.

This work is dedicated to my parents.

ACKNOWLEDGEMENTS

I want to express my deepest gratitude for all the support I have received throughout my Ph.D. starting with my thesis advisor, Dr. Ari M. Melnick. I owe my most sincere thanks to Ari for his guidance and encouragement over the last 5 years. Ari's zeal for science is best reflected in the manner through which he enthusiastically encourages us to incorporate new technologies and methods into our scientific pursuits. The freedom he allowed me to pursue any outlet to discover something new, his ever-present encouragement to collaborate, and his insightful mentoring have been vital in the progress I have made as a graduate student. I would like to add that it is only towards the end, when I started taking stock of all that I have learned in the last 5 years in the lab that I started truly appreciating the extent to which Ari's mentoring has been instrumental in shaping the manner in which I think about science. I will forever be in his debt for the role he has played in making me the scientist I am today.

I would also like to thank my thesis committee members Dr. Jayanta Chaudhuri, Dr. Effie Apostolou, and Dr. Olivier Elemento. Dr. Chaudhuri has been an incredible mentor in his own right with his cheerful disposition, passionate encouragement to pursue questions in B-cell biology and at the very beginning, being one of the faculty members who influenced my decision to join Weill Cornell Graduate School of Medical Sciences. Dr. Apostolou has been a constant source of inspiration as the resident mentor on our floor. Effie's guidance and help have been indispensable especially with respect to the assistance she has consistently offered in tackling the nuances of chromatin biology. Dr. Elemento has also been instrumental in shaping the course of my project and providing insightful comments and suggestions to keep my project on the right track. He had been present from the very beginning of

my project, and his work led me to the questions I ultimately addressed in my Ph.D. thesis research.

An incredible source of inspiration has been the collective force that is represented in the past and current members of the Melnick lab. From my first lab mentor, Karen Bunting, who laid the ground work for the work I ended up pursuing, to Wendy Beguelin who helped me through the most critical phase of my project. Both individuals have been scientific and personal sources of inspiration, and I shall forever remain grateful for their help. I would also like to thank Yanwen Jiang, Katerina Hatzi and Martin Rivas for their contributions through discussions and suggestions in guiding my project and providing the umbrella of general vigilance required from mentors. I would also like to thank Johannes C. Hellmuth for his contributions to the *Bcl6* LCR project. His keen eye and willingness to move forward into the sparsely charted territory of CRISPR screens breathed life into the LCR project at a critical time.

There are many members of the lab who have directly provided valuable assistance in various times of need. For their support and help, I would like to thank Tak Lee, Coraline Mlynarczyk, Leandro Venturutti, Hsia-Yuan Ying, Matt Challman, Maria Teresa Calvo Fernandez, Darko Barisic, David Poloway, Ashley Doane and Brandon Swed. I would also like to thank Hao Shen and Ling Wang for all the help they have provided with mouse work and bench experiments over the last 5 years.

I would like to specially thank Juliet Philips for her unwavering support and friendship through the years in the Melnick lab. Juliet in her excellent management of the lab, and extraordinary dedication to the people she works with has been a life mentor. The attention to detail she pours into every aspect of her work transcends an ordinary level of commitment and I hope to emulate her work ethic and kindness in my own career.

I would like to thank members of the Apostolou lab including Dafne Campigli di Giammartino and Boaz Aronson who have been immensely helpful in guiding chromosomal conformation capture experiments over the last couple of years. I would also like to thank Dr. John Schimenti from the center of vertebrate genomics at Cornell University (Ithaca), and members of his lab—Dr. Priti Singh, Rob Munroe and Christian Abatte for their help in the generation of the LCR KO mice.

Another facility that has played a critical role in my work has been the Flow Cytometry Core led by Jason McCormick at Weill Cornell. Jason in his unique passion for the work in the field of flow cytometry made my frequent visits to the core a joy and for that I am grateful to him.

My time in graduate school has been enriched through the friends I have made here. I would like to specially thank Suveg Pandey, Abhijeet Sharma and Chaitanya Badwe. Our shared passion for football (specifically Arsenal Football Club), admiration for the greatest manager to ever live—'Le Professeur' Arsene Wenger, and general camaraderie played an instrumental role in maintaining sanity through my time as a Ph.D. candidate.

I would like to thank my parents for their patience and unwavering love. While having lived half a world away from them for over a decade has been a challenge in many respects, I constantly feel their presence and support. Without the sacrifices they made to offer me the opportunities I have benefitted from, none of my achievements would have been possible.

Lastly, I owe the greatest debt to my wife, Jaime Eberle-Singh who has stood by me over the last 8 years. In her own right, a talented, hard-working scientist, her demeanour, tenacity and dedication to every single endeavour challenges and inspires me. Her love and support are the pillars on which I have frequently leaned on in times of need, and it is fair to say that without her I would not be where I am today

TABLE OF CONTENTS

LIST OF FIGURES

CHAPTER 1

CHAPTER 2

CHAPTER 3

CHAPTER 4

CHAPTER 5

LIST OF ABBREVIATIONS

ATAC	Assay for Transposase-Accessible Chromatin
BCR	B-cell Receptor
BCL6	B-cell Lymphoma 6
Cas	CRISPR associated
CD	Cluster of Differentiation
ChIP	Chromatin Immunoprecipitation
cLP	Common Lymphoid Progenitor
CRISPR	Clustered Regularly Interspaced Short Palindromic Repeats
DLBCL	Diffuse Large B-cell Lymphoma
DNA	Deoxyribonucleic Acid
DZ	Dark Zone
FDC	Follicular Dendritic Cells
FL	Follicular Lymphoma
GC	Germinal Center
GCB	Germinal Center B-cells
g	Grams
H3K4me2	Histone-3 Lysine-4 di-methylation
H3K4me3	Histone-3 Lysine-4 tri-methylation
H3K27me3	Histone-3 Lysine-27 tri-methylation
H3K27Ac	Histone-3 Lysine-27 Acetylation
HDAC	Histone Deacetylase
Het	Heterozygous
Homo	Homozygous

HSC	Hematopoietic Stem Cells
Ig	Immunoglobulin
IL	Interleukins
IVT	In-vitro Transcription
Kb	Kilo base
KO	Knock-out
LCR	Locus Control Region
LZ	Light Zone
Mb	Mega base
mg	Milligram
ml	Millilitre
NB	Naïve B-cells
NHEJ	Non-Homologous End Joining
qPCR	Quantitative Polymerase Chain Reaction
RAG-1/RAG-2	Recombination Activating Gene 1 and 2
RCF	Relative Centrifugal Force
RNA	Ribonucleic Acid
RPM	Rotations per minute
RSS	Recombination Signal Sequence
seq	Sequencing
sgRNA	Single Guide RNA
SHM	Somatic Hypermutation
TCR	T-cell Receptor
WT	Wild Type

LIST OF SYMBOLS

α	alpha
β	beta
γ	gamma
μ	micro
K	Lysine

Chapter 1-A Brief History of Immunology

1.1 Early theurgic understandings of immunity

In 61 AD, the Roman poet Marcus Annaeus Lucanus started work on his unfinished epic 'Pharsalia' that tells the story of the civil war between Julius Caesar and the Roman senate forces led by Pompey. In book IX, after the assassination of Pompey, Cato the Younger embarks on a journey from Dyrrhachium to Utica, where he would make one last stand against Caesar (Ridley, 1905). Lucan describes an encounter with members of the Psyllian tribe who come to their aid during the perilous trek. Here, with some artistic liberties the great poet uses—arguably for the first time—the word '*immunes*' to describe the famous resistance to snake venom that the tribe possessed. While Lucan has often been touted as an example of a great classical poet who stripped the role of the supernatural from historical events, here he succumbed to the allure of the magical powers of the Psyllian's when he wrote

"*Of all who till the earth*
The Psyllians only are by snakes unharmed.
Potent as herbs their song; safe is their blood,
Nor gives admission to the poison germ
E'en when the chant has ceased. Their home itself
Placed in such venomous tract and serpent-thronged
Gained them this vantage, and a truce with death…"

Up until the 19th century, the term 'i*mmunitas*' and '*immunis*', which were originally used in Latin legal texts to refer to 'exempt status', rarely ever alluded to incidents of resistance to poisons or plagues (Silverstein, 2009). However, the

observations were inevitably noted all along. In describing the Plague of Justinian (spread of the plague described in figure 1.1), 541 AD, Procopius said

"*It started from the Aegyptians who dwell in Pelusium. Then it divided and moved in one direction…it spread over the whole world, always moving forward and travelling at times favourable to it…For it left neither island nor cave nor mountain ridge which had human inhabitants; and if it had passed by any land, either not affecting the men there or touching them in indifferent fashion, still at a later time it came back; then those who dwelt round about this land, whom formerly it had 'afflicted most sorely, it did not touch at all…*" (Dewing, 1914).

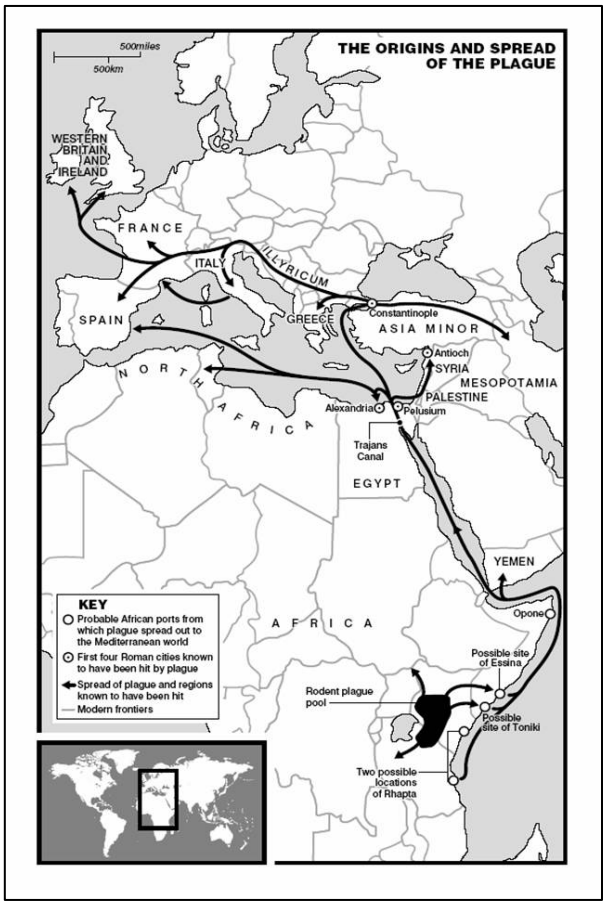

Figure 1.1 Possible origin and spread of the Justinian plague as described by Procopius (Keys, 2000)

While curiosity around the phenomenon we refer to today, as 'acquired immunity' remained alive, another pertinent and related question was being tackled in parallel—what was the source of diseases? As one might guess, the earliest explanations were theurgic, i.e. the agency of divine or supernatural intervention was the source of all illness. In ancient Greece, Asclepius, the God of Medicine and healing was revered for centuries. Although Hippocrates (460-377 BC), the father of medicine, himself was considered to be a follower of Asclepius, he rejected the supernatural causations of ailments, and established empiricism, rational thought and science as virtues to be extolled in the search for explanations of disease (Savel & Munro, 2014). As is with family recipes passed down through generations that experience subtle evolution not through outright replacement but by the addition of newly acquired spices, the theurgic ideas made room for the Hippocratic tradition of medicine and slowly, and reluctantly (but never completely) gave way to western medicine. The blending of rational thought to a cogent belief in the power of the supernatural is the template of early medical prescriptions that can be found in historical texts of almost every culture around the world. The physicians and healers of the time walked the line between cautious prescription of strategies understood through observation and analysis, and explaining everything else with the help of the mood of Mother Nature, the alignments of stars, and when all else failed, the Gods.

1.2 Early theories of immunity and disease

History does not speak of a watershed moment that may have cause a drastic paradigm shift. The Asclepius to Hippocrates transition had been gradual, and is arguably ongoing. However, mankind had found value in empiricism and the

philosophy of the Hippocratic school of thought caught on. An early theory from that period—pertinent to this discussion—advanced the idea that illnesses were a result of imbalances between the humors—blood (sanguine), phlegm (phlegmatic), yellow bile (choleric) and black bile (melancholic). These imbalances were initially thought to be in the actual amount of the humors. However, a 'rediscovery' of Hippocratic teachings by Galen (2nd century AD) along with a better understanding of physiology, anatomy, and pathology resulted in a shift in the paradigm from quantitative to qualitative imperfections of the humors. Between the 5th and 10th centuries AD, a gradually improving understanding of smallpox helped refine these early theories of disease. An illustrious Arab physician by the name of Rhazes, not only gave a thorough description of the clinical symptoms of smallpox but also put forward, possibly for the first time, a theory for 'acquired immunity' (even though he didn't use these terms) (Abu Bekr Mohammad ibn Zakariya al-Razi, n.d.). In 1546, Girolamo Fracostoro, believed that small seeds (seminaria) were the cause of disease, that they spread from person to person, and had distinct tissue affinities. He also concluded that the differential affinities were the reason for 'natural immunity'.

In the sixteenth and seventeenth centuries, two schools of medicine arose as a result of the scientific persuasions of physicists and chemists: iatrophysics—touting that all bodily functions have a mechanical characteristics; and iatrochemical—whereby physiology was a product of chemical reactions. Most of the theories of acquired immunity were founded from the iatrochemical perspective (Silverstein, 2009).

By the end of the seventeenth century, Western Europe had become seriously concerned with smallpox, and in 1714 the news of the eastern practice of *variolation*

had arrived in letters to the Royal Society of London that focused efforts on acquired immunity to the disease. These letters from Timoni and Pylarni, described the strategy of establishing a benign infection by inoculating pustule derived crusts from 'favorable' cases of smallpox. What followed was the rapid popularity of this strategy that ultimately led to the first clinical trial in immunology—performed on a group of prisoners and another group of orphans in 1721. The success of these 'Royal Experiments' brought about renewed interest into the mechanisms of immunity facilitated by variolation. Around this time, the practice also spread to Colonial America thanks to the efforts of Cotton Mather who regularly read the Proceedings of the Royal Society of London, and learned of the letters from Timoni and Pylarni. Mather, with the help of other physicians spread the word via published documents from the New England region and addressed concerns that were raised in objections to the practice of inoculation (Figure 1.2). The text in the title page of the document reads "*Some account of what is said of inoculating or transplanting the small pox / by the learned Dr. Emanuel Timonius, and Jacobus Pylarinus ; with some remarks thereon ; to which are added, a few in answer to the scruples of many about the lawfulness of this method ; published by Dr. Zabdiel Boylstone*." (Mather, 1721).

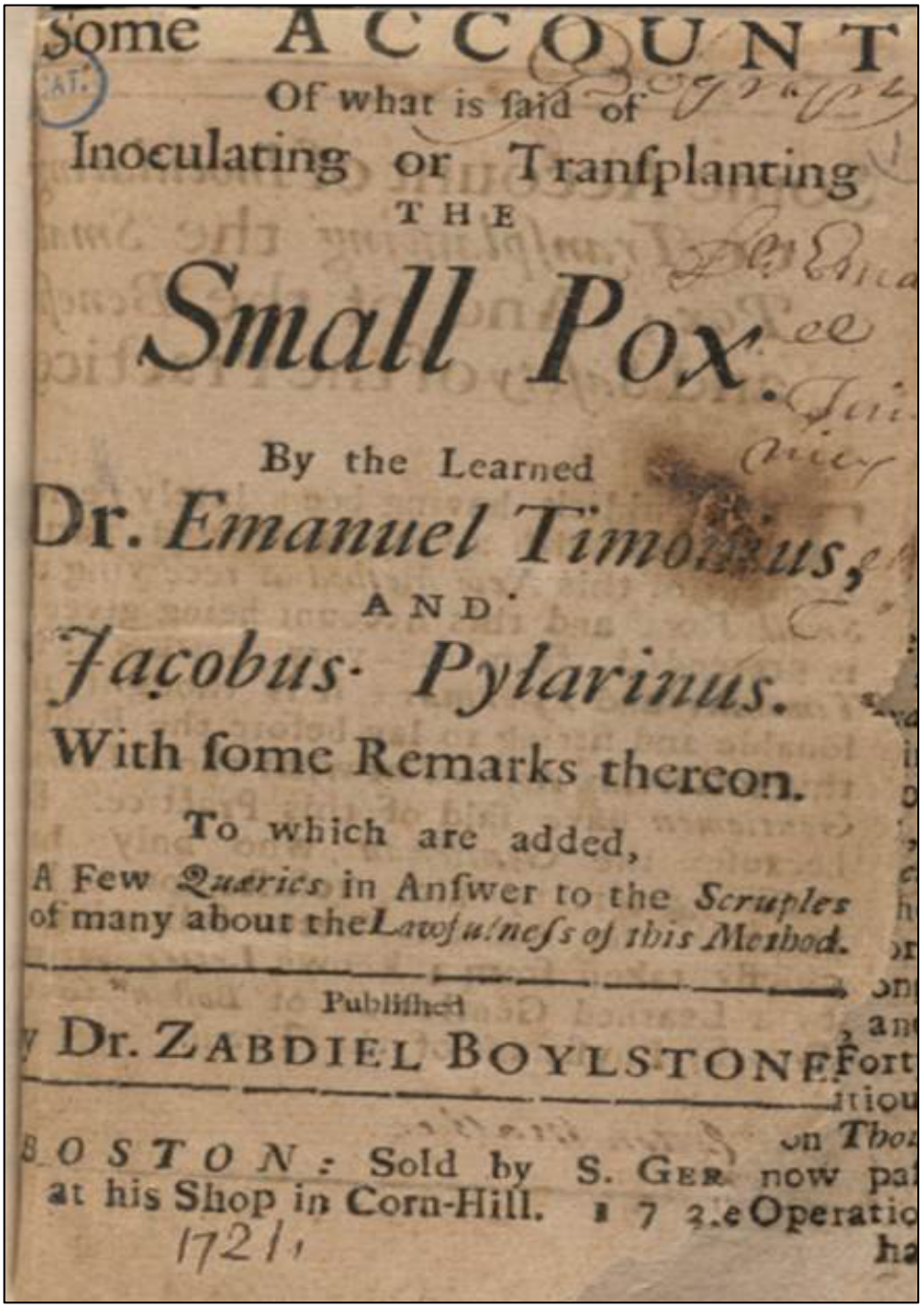

Some ACCOUNT
Of what is said of
Inoculating or Transplanting
THE
Small Pox.
By the Learned
Dr. Emanuel Timonius,
AND
Jacobus Pylarinus.
With some Remarks thereon.
To which are added,
A Few Queries in Answer to the Scruples of many about the Lawfulness of this Method.
Published
by Dr. ZABDIEL BOYLSTON.
BOSTON: Sold by S. Gerrish at his Shop in Corn-Hill.
1721.

Figure 1.2 Title page from 'Some account of what is said of inoculating or transplanting the small pox. Boston: Sold by S. Gerrish at his shop in Corn-Hill.' (Mather, 1721)

One of the main theories of the time, explaining the acquired resistance to smallpox, was the Depletion Theory that suggested that the basis of this immunity was the depletion of a particular resource specifically required by the disease-causing agent. According to this view, the reintroduction of the causal agent or seed expedited the loss of said resource. Proponents of this theory included Thomas Fuller (Fuller, 1730), James Kirkpatrick, Louis Pasteur (Pasteur L., Chamberland C., 1880), and even Paul Ehrlich who extended the idea to tumor immunity.

An inflection point in the history of disease and immunity came from the work of Louis Pasteur and Robert Koch. They provided experimental evidence for bacterial agents as the root cause for infectious diseases and a rubric for establishing them as such. Critical discoveries were made in the ten years from 1880, when Pasteur published his experiments on acquired immunity to fowl cholera via attenuated organisms (Pasteur, 1880), to 1890 when von Behring and Kitasato had discovered anti-toxins against diphtheria and tetanus (Behring & Kitasato, 1890). However, the investigators of the time ignored the role of the host in establishing the immunity, therefore producing a list of 'passive theories' as classified by Sauerback (Sauerbeck, 1909). The time for 'active theories' was on the horizon and were bolstered by the discovery of the antibody and complement.

1.3 Humoralists versus Cellularists

Towards the end of the 19th century, there were two major debates within the field of immunology that split the scientists of the time in two factions. The first issue pertained to the role of inflammation—was it a physiological response that was ultimately beneficial to the organism or was it a deleterious side effect that contributed to the pathology of illness. The second debate, which was more of a battle, had to do

with the mechanisms that explained the basis of innate and acquired immunity—was it humoral or cellular.

At the beginning of the debate there was a prevailing bias towards the humoral school of thought. After all, the history of the humors and their perceived role could be traced back to the early tradition of empirical medicine starting from Hippocrates. However, in 1858, Rudolph Virchow challenged the humoral basis of disease when he claimed that all pathology was a result of cellular malfunction and not that of maladjusted humors (Virchow, 1858). While his work gradually gained acceptance, the events that followed and the allegiances that scientists picked were peculiar. In the late 1870s, Robert Koch's work on the etiology of wound infections further bolstered the germ theory of disease (Koch, 1876). In 1884, Ilya (Elie) Metchnikoff proposed the phagocytic theory (Metschnikoff & Freund, 1884), which initially, had more to do with the questions surrounding inflammation—a question that was primarily within the purview of pathologists. While this might make it seem that both Koch and Metchnikoff would have held similar ideas, you would be gravely mistaken in that assumption

Metchnikoff, who was by training a zoologist, had an early interest in the digestive processes of invertebrates. While studying 'mobile cells' in starfish he formulated the idea that those cells could provide protection to the organism when challenged with a foreign, invasive object or organism. He performed a pilot experiment, in which he inserted a splinter into the starfish and then waited overnight to see how the mobile cells would respond. What he noticed was the cells (phagocytes) moving into the region of the injury. He postulated that the role was protective, and in that idea was the foundation of what would become the cellular

basis of inflammation. This was also the beginning of a protracted attack on his cellularist viewpoint which lasted decades. His early assertions from the platform of the phagocytic theory pertained to the nature of inflammation, which he claimed was not a deleterious response. This met with strong opposition from pathologists who viewed macrophages to be associated with purulent discharge and inflammation associated with poor prognoses. Such was the reaction to his ideas that Rudolph Virchow during a visit in 1883 cautioned Metchnikoff against advancing his theories at the time (Metchnikoff, 1921).

As one might imagine, the phagocytic theory had immunological implications and soon came under attack from the humoralists. The tale that followed is multilayered and complex and had serious implications for the trajectory of research in immunology. The debate that should have remained within the hallways of scientific discussion bled into political and nationalistic ideologies of the factions—the humoralists were primarily German and generally took their cues from Robert Koch, while the cellularists were mostly French who followed the lead of Metchnikoff (Silverstein, 2009). A long held divide between the nations had come to a head during the Franco-Prussian war of 1870, which the French lost to the Germans, and led to beliefs and biases that compromised objectivity in the assessment of science.

Pasteur, who had received an honorary M.D. from the University of Bonn, returned the degree in the aftermath of the war. Ten years later, Koch and Pasteur engaged in an unpleasant debate over the etiology and pathogenesis of anthrax and other diseases, which eventually lost all sense of civility. This enmity between the two countries played out once again in the form of a scientific argument between Jules Bordet and Paul Ehrlich many years later (Zinnser, 1914).

A number of observations came in quick succession in the last two decades of the 19th century from both sides, which in retrospect, hinted at the importance of both mechanisms. However, at the time, this possibility was forcibly overlooked and, in the end, the cellularists lost traction as a number of papers showing that cell-free fluids of normal and immunized animals could kill bacteria started surfacing. The humoralists held the view that the phagocytes that did show up were there to clean up debris and not actively involved in protective activities. The most important discovery that stalled the development of Metchnikoff's ideas, was the discovery that antibodies conferred immunity against diphtheria and tetanus exotoxins (Behring & Kitasato, 1890). Another study showed that this serum could be passively transferred to another organism to confer protection against diphtheria without the involvement of any cellular components. This led Koch to proclaim the end of the phagocytic theory. Subsequent work from Paul Ehrlich showing the titration of anti-diphtheria antibodies (Ehrlich, 1897) emphasized the nature of antibodies as an entity that could be studied ex-vivo in the test tube—a convenience that immunologists readily found an affinity for—and heralded the age of antibody and complement research, a major step in the evolution of immunology, albeit at the cost of ignoring the cellular basis of immunity to the chagrin of many modern immunologists.

All that remained for the field to latch onto the idea of antibodies was a theoretical framework that could be the foundation of future work. To that extent, Ehrlich did not disappoint, and in a remarkable set of postulates, gave the world the idea of the side-chain theory. It should be added that the while the majority of the field shifted its focus to antibodies, there was an appreciation for the cellularist viewpoint for a number of reason including of course, legitimate curiosity around the phagocyte

theory but also in recognition of Metchnikoff as a relentless and brilliant scientist. This was reflected in the 1908 Nobel Prize that was jointly awarded to Metchnikoff and Ehrlich for their work on immunity (Nobelprize.org, 2014a).

From this point on, a relative hiatus in research surrounding cellularist ideas followed. Questions around delayed hypersensitivity (or bacterial allergy) were being half-heartedly addressed. Landsteiner and Chase demonstrated the importance of mononuclear cells in cellular immunity in 1942 through their famous cell transfer experiments (Landsteiner & Chase, 1942) but these experiments amongst many others were coming late in terms of what was technically possible earlier in the 20th century. This half a century long lull was turned around in the 1960s when questions about allograft rejection, tolerance, viral infections, immune deficiencies and autoimmune diseases started surfacing.

1.4 Early theories of antibody formation

The next step in the antibody story starts with the academic masses huddled around the new door that had just appeared—the question of where the antibodies came from and how were they made?

On March 22, 1900, Paul Ehrlich, presented the "side-chain theory" in the Croonian lecture to the Royal Society of London. The theory, which later evolved into one of the foundational tenets of adaptive immunity, postulated that blood cells presented on their surface a variety of "side-chain receptors" that bound to toxic/infectious agents and inactivated them. He went on to suggest that the interaction between the foreign substance and the cell-bound receptor activated the cell, resulting in the large scale production and release of the receptor with the same specificity into

the blood stream of the organism. He further noted that the specificity of the receptor for the infectious agent was pre-determined (Ehrlich, 1900). An interesting observation about Ehrlich's work has been made which suggests that a part of Ehrlich's lay in the pictures he drew to convey his ideas. Figure 1.3 below is one of his illustrations depicting the side chain theory (Himmelweit, n.d.).

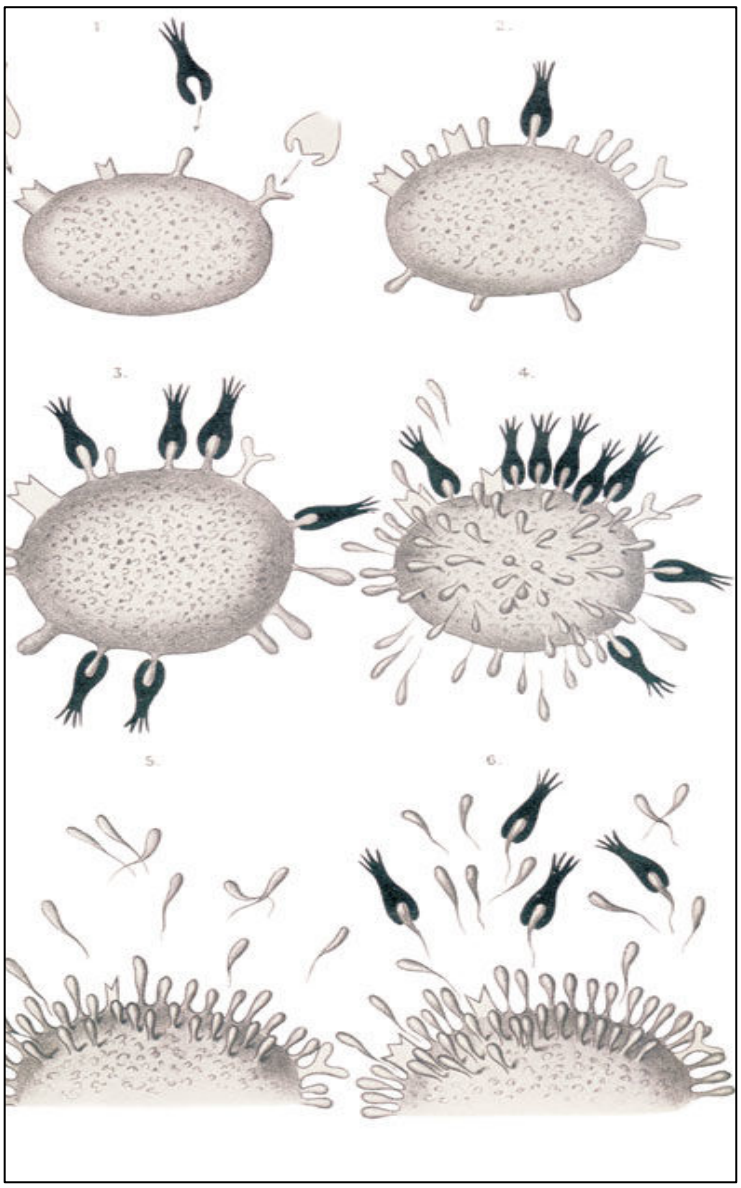

Figure 1.3 Ehrlich's side chain theory depicting the antibody-producing cell as having receptors for more than one type of antigen (black). Each antigen has a receptor with a different specificity. The antigen selects for increased production of the antibody.

The side-chain theory soon faced significant opposition by immunologists who believed in an instructional model of antibody production. According to these instructional theories, the antigen itself had a role to play in determining the specificity of the anti-toxin/antibody (Bordet, 1940).

It wasn't until the second half of the 20th century that selective theories re-emerged. Eventually, the work of N. Jerne, D. Talmadge and F.M. Burnet resulted in the acceptance of the "clonal selection theory" as a paradigm for adaptive immunity (Goldsby, Kindt, Osborne, & Kuby, 2003). This theory confirmed most of Ehrlich's predictions (with modifications), and in its current form states that the origin of the diverse repertoire of specific antibodies is independent of the antigen pool and each lymphocyte (both B and T cells) expresses only one kind of antigen receptor on its surface (Burnet, 1957). The antigen receptor diversity is attributed to a somatic gene rearrangement process that Burnet alluded to in 1957 when he proposed the clonal selection theory. According to him "The [clonal selection] theory requires at some stage in early embryonic development a genetic process for which there is no available precedence". This speculative remark proved to be largely correct as was shown by a series of discoveries and the formal proposal of a somatic recombination process known as V(D)J recombination in 1976.

The history described thus far in this text has, for the sake of brevity, skipped over the minutia of the discoveries that were made up until the mid 1900s. However, a component of this story that may seem more pertinent are the cells of the immune system that we refer to as lymphocytes, and in the next section I will briefly recount the trajectory of work that was done that led to the discovery of lymphocytes, and the distinction that was made between T and B-cells.

1.5 The discovery of B and T lymphocytes

It is clear now that before the identification of lymphocytes, we had an understanding of the nature of the antibody, and its role in immunity had gradually been unravelled. It was in 1948, when Astrid Fagraeus showed that antibody formation correlated with the appearance of plasma cells in the spleen (Fagraeus, 1948). The source of antibodies being plasma cells was subsequently confirmed via immunofluorescence microscopy (Coons, Leduc, & Connoly, 1955). Antibodies had already been shown to be gamma globulins through electrophoretic studies (Tiselius & Kabat, 1939), and between 1952-1955, immunodeficient patients were identified as lacking gamma globulins (Bruton, 1952), and more specifically not having germinal-centers and plasma cells (Good & Varco, 1955).

A curious observation of great implication was reported by Bruce Glick, when he showed that the removal of the bursa of fabricus from newly hatched chicks led to a defect in antibody formation. In retrospect, it is clear that the observation was initially overlooked, in part due to the publication of his work in *Poultry Science*, a journal of little consequence to immunologists (Glick, Chang, & Jaap, 1956).

While the clonal selection theory was being proposed to the world, a better understanding of the composition of the antibody molecule was emerging—it was shown to possess 4 chains—paired heavy and light chains that were connected via disulphide bridges (Edelman, 1959; Porter, 1959). It was also shown that the heavy and light chains had a homogenous, crystallisable fragment (F_c) and a variable, non-homogenous fragment (F_{ab}). New questions about the genetic makeup of higher organisms and the manner in which the variable and constant regions could potentially arise in an antibody molecule were coming up and in 1965, Dreyer and Bennett

postulated that different variable and constant region genes could combine to make specific light chain or heavy chain of the antibody (Dreyer & Bennett, 1965).

The idea of the thymus as an organ critical for immune function had also been emerging. Jacques Miller noticed that thymectomized mice had severe immunodeficiencies. Independently, Good, who had studied agammaglobulinemia picked up clues from Glick's work and combined them with the observations made in patients with thymoma. He also thymectomized mice and came up with similar defects in lymphocyte development. The observations made, initially projected the idea that the thymus gave rise to the cells that became lymphocytes and these populated various lymphoid tissues—the *single lineage model*. However, this model did not hold water as different phenotypes emerged from the removal of the bursa and the thymus. In 1966, Max Cooper showed that the specific ablation of thymus in conjunction with whole body irradiation of chicks left them lymphopenic, with impaired cell mediated immunity and also had problems in their ability to reject grafts. These animals had lower antibody titers but still had plasma cells and formed germinal centers. On the other hand, when the bursa was removed along with whole body irradiation the inverse phenotype was observed (Cooper, Raymond, Peterson, South, & Good, 1966). This clarified the distinct roles of the two organs and also paved the way for the *two-lineage model*—lymphocytes were B and T-cells.

In 1974, a number of publications showed that the mammalian equivalent of the avian bursa of fabricus was the bone marrow (and fetal liver) (Owen, Cooper, & Raff, 1974; Ryser & Vassalli, 1974; Stocker, Osmond, & Nossal, 1974). In 1976, Susumu Tonegawa and Nobumichi Hozumi heralded the new era of immunology when they published their findings on the somatic rearrangement of variable and

constant genes in the process of forming an antibody light chain (Hozumi & Tonegawa, 1976), work for which Tonegawa was awarded the Nobel Prize in 1987 (Nobelprize.org, 2014b).

The discovery of VDJ recombination by Tonegawa seems to be an appropriate place to conclude the historical introduction to the field of immunology. This is in part due to the idea that the discoveries made since the late 1970's fall under the category of modern molecular immunology. While the subject matter of this thesis falls within the purview of epigenetic mechanisms involved in the regulation of gene expression between two specific stages of B-cell development, there is, yet again, a need for context around B-cell biology. To this extent, the next chapter will include descriptions of VDJ recombination and the manner in which it is tied to early B-cell development. I will then switch to the particular stage of B-cell development that is relevant to my graduate thesis work—Germinal Center B-cells.

Chapter 1 References

Abu Bekr Mohammad ibn Zakariya al-Razi. (n.d.). *Rhazes. A Treatise on the Smallpox and Measles, translated by W A Greenhill.* London: Sydenham Society. http://doi.org/1848

Behring, & Kitasato. (1890). Ueber das Zustandekommen der Diphtherie-Immunität und der Tetanus-Immunität bei Thieren. *Deutsche Medizinische Wochenschrift*, *16*(49), 1113–1114. http://doi.org/10.1055/s-0029-1207589

Bordet, J. (1940). Traité de l'immunité dans les maladies infectieuses. *Journal of the American Medical Association*, *115*(17), 1479. Retrieved from http://dx.doi.org/10.1001/jama.1940.02810430069033

Bruton, O. C. (1952). Agammaglobulinemia. *Pediatrics*, *9*(6), 722–728. Retrieved from http://pediatrics.aappublications.org/content/9/6/722.short%5Cnhttp://pediatrics.aappublications.org/content/9/6/722.abstract?ijkey=67f94c80d6add1255791ad3f3ee7880e7f045a84&keytype2=tf_ipsecsha

Burnet, F. M. (1957). A modification of Jerne's theory of antibody production using the concept of clonal selection. *Australian Journal of Science*, *20*, 67–69.

Coons, A. H., Leduc, E. H., & Connoly, J. M. (1955). Studies on antibody production. I. A method for the histochemical demonstration of specific antibody and its application to a study of the hyperimmune rabbit. *The Journal of Experimental Medicine*, *102*(1), 49–60. http://doi.org/10.1084/jem.102.1.49

Cooper, M. D., Raymond, D. A., Peterson, R. D., South, M. A., & Good, R. A. (1966). The functions of the thymus system and the bursa system in the chicken. *The Journal of Experimental Medicine*, *123*(1), 75–102.

Dewing, H. B. (1914). *Procopius' History of the Wars, Books I and II*. *The Loeb Classical Library* (Vol. 1).

Dreyer, W. J., & Bennett, J. C. (1965, September). The molecular basis of antibody formation: a paradox. *Proceedings of the National Academy of Sciences of the United States of America*.

Edelman, G. M. (1959). DISSOCIATION OF γ-GLOBULIN. *Journal of the American Chemical Society*, *81*(12), 3155–3156. http://doi.org/10.1021/ja01521a071

Ehrlich, P. (1897). The value assessment of diphtheria and its theoretical foundations. *Clinical Yearbook*, *6*, 299–326.

Ehrlich, P. (1900). *On Immunity with Special Reference to Cell Life*. London.

Fagraeus, A. (1948). The plasma cellular reaction and its relation to the formation of antibodies in vitro. *Journal of Immunology (Baltimore, Md. : 1950)*, *58*(1), 1–13.

Fuller, T. (1730). *Exanthematologia: or, an attempt to give a rational account of eruptive fevers.* London.

Glick, B., Chang, T. S., & Jaap, R. G. (1956). The Bursa of Fabricius and Antibody Production. *Poultry Science*, *35*(1), 224–225. http://doi.org/10.3382/ps.0350224

Goldsby, R. A., Kindt, T. J., Osborne, B. A., & Kuby, J. (2003). *Immunology* (5th ed.). New York: W.H Freeman & Company.

Good, R. A., & Varco, R. L. (1955). A clinical and experimental study of agammaglobulinemia. *The Journal-Lancet*, *75*(6), 245–271.

Himmelweit, F. (n.d.). *The collected papers of Paul Ehrlich. Volume III, Chemotherapy*. Retrieved from https://www.sciencedirect.com/science/book/9780080090566

Hozumi, N., & Tonegawa, S. (1976, October). Evidence for somatic rearrangement of immunoglobulin genes coding for variable and constant regions. *Proceedings of the National Academy of Sciences of the United States of America*.

Keys, D. (2000). *Catastrophe: An investigation into the Origins of the Modern World* (1st ed.). New York: The Ballantine Publishing Group.

Koch, R. (1876). Untersuchungen ueber Bakterien V. Die Aetiologie der Milzbrand-Krankheit, begruendent auf die Entwicklungsgeschichte des Bacillus Anthracis. *Beitrage Zur Biologie Der Pflanzen*, 277–310. http://doi.org/http://edoc.rki.de/documents/rk/508-5-26/PDF/5-26.pdf

Landsteiner, K., & Chase, M. W. (1942). Experiments on Transfer of Cutaneous Sensitivity to Simple Compounds. *Experimental Biology and Medicine*, *49*(4), 688–690. http://doi.org/10.3181/00379727-49-13670

Mather, C. (1721). Some account of what is said of inoculating or transplanting the small pox. In Z. Boylstone (Ed.), . Boston.

Metchnikoff, O. (1921). *Life of Elie Metchnikoff 1845-1916*. *Houghton Mifflin Company*. Boston and New York: HOUGHTON MIFFLIN COMPANY. http://doi.org/10.1017/CBO9781107415324.004

Metschnikoff, E., & Freund, M. B. (1884). Ueber eine Sprosspilzkrankheit der Daphnien. Beitrag zur Lehre über den Kampf der Phagocyten gegen Krankheitserreger. *Deutsche Medizinische Wochenschrift*, *10*(43), 699–700. http://doi.org/10.1055/s-0029-1209659

Nobelprize.org. (2014a). The Nobel Prize in Physiology or Medicine 1908. Retrieved from http://www.nobelprize.org/nobel_prizes/medicine/laureates/1908

Nobelprize.org. (2014b). The Nobel Prize in Physiology or Medicine 1987.

Owen, J. J., Cooper, M. D., & Raff, M. C. (1974). In vitro generation of B lymphocytes in mouse foetal liver, a mammalian “bursa equivalent”. *Nature*, *249*(455), 361–363.

Pasteur, L. (1880). The attenuation of the causal agent of fowl cholera. *C. R. Acad. Sci.*, *91*.

Pasteur L., Chamberland C., R. E. (1880). Sur les maladies virulentes, et en particulier sur la maladie appelee vulgairement cholera des poules. C. R. Acad. Sci. 90, 249–

248. *C. R. Acad. Sci.*, (90), 239.

Porter, R. R. (1959). The hydrolysis of rabbit y-globulin and antibodies with crystalline papain. *The Biochemical Journal*, *73*, 119–126.

Ridley, S. E. (1905). *Pharsalia by M. Annaeus Lucanus*. London: Longmans, Green & Co.

Ryser, J.-E., & Vassalli, P. (1974). Mouse Bone Marrow Lymphocytes and Their Differentiation. *The Journal of Immunology*, *113*(3), 719 LP-728. Retrieved from http://www.jimmunol.org/content/113/3/719.abstract

Sauerbeck, E. (1909). *Die krise in der Immunitatsforschung*. Leipzig: Werner Klinkhardt.

Savel, R. H., & Munro, C. L. (2014). From asclepius to hippocrates: The art and science of healing. *American Journal of Critical Care*, *23*(6), 437–439. http://doi.org/10.4037/ajcc2014993

Silverstein, A. (2009). *A History of Immunology*. *A History of Immunology*. http://doi.org/10.1016/B978-0-12-370586-0.X0001-7

Stocker, J. W., Osmond, D. G., & Nossal, G. J. V. (1974, November). Differentiation of lymphocytes in the mouse bone marrow: III. The adoptive response of bone marrow cells to a thymus cell-independent antigen. *Immunology*.

Tiselius, A., & Kabat, E. A. (1939, January). AN ELECTROPHORETIC STUDY OF IMMUNE SERA AND PURIFIED ANTIBODY PREPARATIONS. *The Journal of Experimental Medicine*.

Virchow, R. (1858). Die Cellularpathologie in ihrer Begründung auf physiologische and pathologische Gewebelehre. *Verlag von August Hirschfeld, Berlin.*, 1858.

Zinnser, H. (1914). *Infection and resistance-An exposition of the biological phenomena underlying the occurrence of infection and the recovery of the animal body from infectious disease*. The Macmillan Co. Retrieved from

https://archive.org/stream/infectionresist00zinsrich/infectionresist00zinsrich_djvu.txt

Chapter 2: From the Bone Marrow to the Spleen and Things in Between

2.1 Introduction

While the selective historical description of immunology and the critical early discoveries described in chapter 1 are unquestionably important, the subject matter of this thesis requires an introduction to a specific subset of information around B-cells. Research over the last 50 years has provided us an incredible amount of insight into the stages of B-cell development. As a student of immunology, I found B-cells to be a fascinating biological system to study as it forces us to reimagine the evolutionary pressures in a completely unconventional fashion.

It is generally accepted that most organisms have developed mechanisms to tackle insults to genomic DNA. These mechanisms range from prevention to repair modalities; and the manner in which these complex molecular systems came to be are intuitive as they rarely defy logic. In the adaptive immune system, we have come to appreciate the jawed vertebrates to represent an evolutionary inflection point where lymphocytes first appeared (Pancer & Cooper, 2006). What makes the T and B-cells complete head turners are two distinct stages of somatic DNA alterations that challenge the 'lets not mess with the genome' wisdom: VDJ recombination and somatic hypermutation. Both of these processes coupled with class switch recombination involve manipulation of DNA in a manner, which requires precarious and dangerous regulatory processes that are now known to be associated with a number of pathologies including cancer.

Among the many explanations surrounding the emergence of lymphocytes is the idea that the emergence of warm-blooded animals concurrently created the

evolutionary pressure of defense mechanisms against rapidly multiplying microbes that preferred warmer temperatures as well. The pressure, more specifically, required plasticity and diversity in its ability to respond. The development of this plasticity may have been preceded by the ability to simply employ phagocytic means of defense against microbes, a feature that is--assuming this hypothesis to be true—retained in B-cells (Parra, Takizawa, & Sunyer, 2013).

While a definitive narrative of the events that led to the emergence of the lymphocytes will likely never be revealed, the research that addresses their biology is akin to unravelling a magical puzzle like no other. This chapter summarizes some of the key features of the molecular events that occur at the genetic and epigenetic level in B-cells as we understand them today. Towards the end I present the rationale behind my research that is described in subsequent chapters.

2.2 Early stages of B-cell development and V(D)J recombination

Collectively, the B-cell antigen receptor (immunoglobulin) repertoire enables the immune system to mount a protective response against a wide range of antigens. The immunoglobulin molecule or antibody is composed of 4 polypeptide chains: two identical light (L) chains and two identical heavy (H) chains that are held together by non-covalent bonds and covalent di-sulfide linkages. Each H and L chain can be sub-divided into a constant (C) and a variable (V) region. The constant region is the determinant of the effector function for the particular antibody and can be one of five biochemically distinguishable immunoglobulin classes. The variable region of the heavy chain (VH) and the light chain (VL) fold together in the antibody molecule to form the antigen-binding site. The diversity in antigen recognition ability of antibodies is due to the variation in the amino acid sequence at the antigen-binding site. This

diversity is generated from a limited number of V region gene segment rearrangements resulting in the VH and VL portions of the heavy and light chains.

The immunoglobulin heavy chain locus (Igh) in the mammalian genome is comprised of three discontinuous gene segments known as variable (V_H), diversity (D_H) and joining (J_H) gene segments (Tonegawa, 1983). The number of genes in each segment vary between species, for example, in C57BL/6 mice, the Igh locus is on chromosome 12, is about 2.7Mb and contains 195 V_H, 13 D_H, 4 J_H and 8 C_H gene segments; whereas in humans the Igh locus is a 957 kb region on chromosome 14 and has 44 V_H, 27 D_H and 6 J_H gene segments (Ebert et al., 2011; Matsuda et al., 1998). Figure 2.1 depicts the general organization of the Igh locus along with some of the epigenetic regulatory elements.

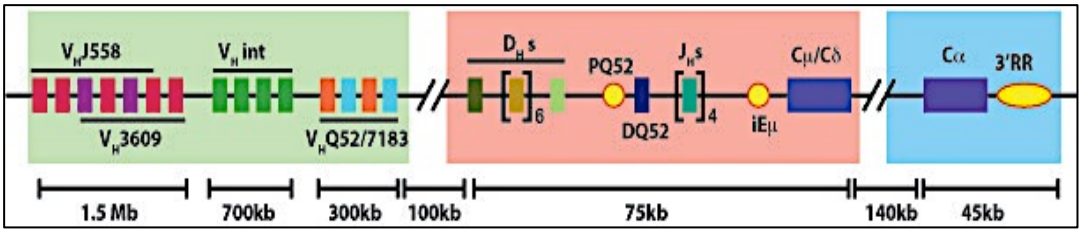

Figure 2.1 A schematic of the organization of the Immunoglobulin heavy chain in mice (not to scale). The locus is ~ 3Mb in length with the V_H gene segments occupying about 2.44Mb starting at the 5' end of the locus (green shaded area). This region is further divided into distal (V_HJ558 and V_H3609), intermediate and proximal (V_HQ52 and V_H7183) families. The length of the different V_H gene segment families is depicted. The intronic enhancer "iEμ" (between the J_Hs and Cμ segment) and the promoter upstream of DQ52 (PQ52) are shown as yellow circles. The remaining constant regions are represented in the blue shaded area along with the 3' regulatory region shown as a yellow oval.

The immunoglobulin light chain locus (Igl) differs from the Igh locus in that it does not have a diversity gene segment and the recombination is only between the V_L and J_L gene segments (Bernard, Hozumi, & Tonegawa, 1978; Early, Huang, Davis,

Calame, & Hood, 1980). The light chain itself is of two kinds: kappa and lambda, and their recombination does not occur during the pro-B cell stage. Instead, Igl locus VJ recombination occurs in the small-pre-B cell stage when the Igh recombination has been completed. The mechanism of recombination of the Igl locus is similar to that of the Igh locus (Murphy, 2011).

The process of recombination of the gene segments is guided through recombination signal sequences (RSS) that are recognized by V(D)J recombinase enzymes known as RAG-1 and RAG-2. These enzymes bind to the RSS that flank gene segments to be recombined and subsequently align them next to each other (McBlane et al., 1995). The RAG-1/RAG-2 complex then cuts a single strand of both DNA backbones between the RSS and the coding region creating two hairpin structures. The cells non-homologous end joining (NHEJ) DNA repair proteins (like Artemis, Ku70:Ku80 heterodimer, XRCC4, DNA ligase IV and DNA Protein Kinase) help in resolving the hairpin structure. This leaves the two gene segments recombined and cleaves out the intermediate DNA to form the extra-chromosomal circular DNA known as the signal joint.

The RSS can come in two different flavours and the basic construction includes a conserved seven nucleotide sequence (5'CACAGTG3') contiguous with the gene segment coding region, followed by either a 12 or a 23 bp non-conserved spacer region, finally followed by another conserved block of nine nucleotides (5'ACAAAAACC3'). A gene segment flanked by an RSS with the 12-bp spacer can only combine with another gene segment with an RSS that has a 23-bp spacer. This is known as the 12/23 rule (Eastman, Leu, & Schatz, 1996; Van Gent, Ramsden, & Gellert, 1996).

The sequence of gene rearrangements of the Igh locus during the pro-B cell stage is D_H to J_H resulting in the DJ_H followed by V_H to DJ_H. The sequential gene rearrangement is achieved in part, by the specific arrangement of RSS in the Igh locus: the V_H and J_H segments are all flanked by the 23-bp RSS motifs whereas the D_H gene segments are flanked on both sides by the 12-bp RSS. The 12/23-rule ensures that one D_H gene segment recombines with another J_H segment first to form DJ_H, and the second recombination occurs between a V_H segment and the DJ_H segment (Murphy, 2011). V(D)J recombination is now known to be a highly regulated process that is not only important for the generation of the diverse repertoire of antibodies but also for its role in lineage specification of B-cells.

One of the hallmarks of a B-cell is its antigen receptor with unique antigen specificity. The fate of the B-cell is intricately tied to the assembly of a viable antigen receptor. B cells undergo most of their development in the bone marrow, and V(D)J recombination of the Immunoglobulin heavy chain locus occurs during the early stages of the differentiation process followed by the recombination of the light chain locus in a highly ordered and regulated manner (Figure 2.2). Built into these systems are backup plans and error fixing opportunities that are also summarized below.

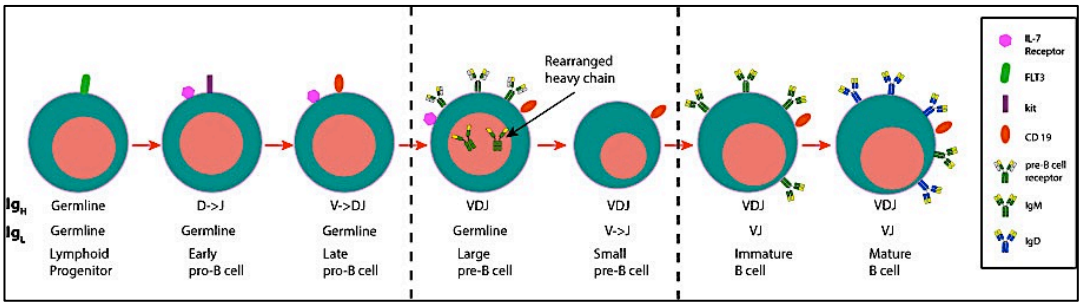

Figure 2.2 B-cell development from lymphoid progenitors to mature B cells depicting the sequential recombination of Ig genes during VDJ recombination.

Lymphopoiesis starts in the bone marrow of adult mammals, where a hematopoietic stem cell (HSC) interacts with bone marrow stromal cells to give rise to a common lymphoid progenitor (cLP). The cLP can have many different fates, one of which is the formation of an early-pro-B cell. This stage is marked by the initiation of Igh rearrangements, specifically the recombination of D_H to J_H on both alleles. The early pro-B cell stage is characterized by a high expression of CD117 (kit), $CD24^{low}$ and a lack of CD25 on the surface (Murphy, 2011).

Once the D_H to J_H recombination is complete, the cell moves to the late-pro-B cell stage. The Igh locus V(D)J recombination is completed during this stage. V_H to DJ_H recombination is attempted on one of the alleles, and if an intact μ-heavy chain mRNA is produced, V(D)J recombination stops and the cell transitions into a large pre-B cell. This transition is marked by the surface expression of a pre-B cell receptor, which is Igμ protein along with two surrogate light chains. Pre-B cell receptor signalling is known to prevent the second allele from undergoing V(D)J recombination—also known as allelic exclusion—through Ca^{2+}-Calmodulin mediated binding of the E2A transcription factor. This inhibitory interaction results in the down-regulation of components of the recombination machinery (Hauser, Grundström, & Grundström, 2014). If the initial V(D)J recombination does not produce a μ chain the cell makes another attempt on the other allele. If the second attempt fails as well the cell undergoes apoptosis.

After the expression of the pre-B cell receptor, the late-pro-B cell starts proliferating and the cells are now referred to as large-pre-B cell stage. Rag1/2 expression is significantly reduced during this stage, as there is no further recombination at any of the immunoglobulin loci. Once proliferation stops, the cells become small-pre-B cells

and the recombination of the V_L and J_L of the Igl begins. After the completion of the light chain recombination, both the heavy and the light chain are expressed as surface IgM molecules and the cell becomes an immature-B cell. B cells with self-reactive IgM molecules are negatively selected in the bone marrow at this stage while the surviving B cells leave the bone marrow to become mature-B cells (Jung & Alt, 2004).

As mouse models are used extensively to study the immune response, it is important to point out that B-cell development is remarkably similar in humans and mice. A schematic with an overview of the major stages of B-cell development is shown in figure 2.3.

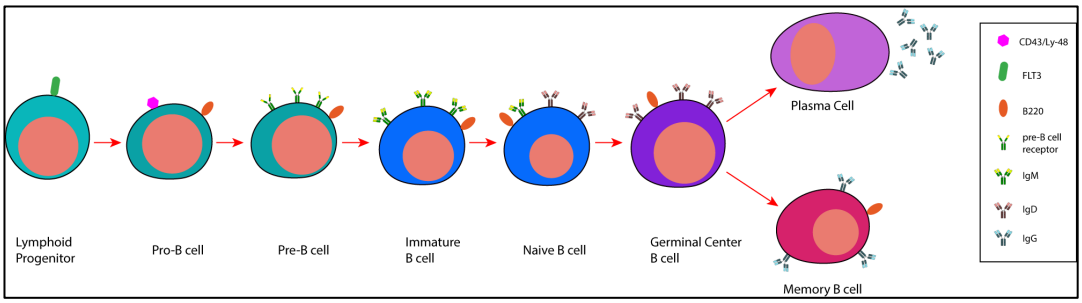

Figure 2.3 Major stages of B-cell development to the formation of Memory B-cells and Plasma Cells.

In both species, B-cells originate from fetal liver (B-1) and bone marrow (B-2) (Nuñez et al., 1996). The underlying molecular mechanisms that lead to the expression of the BCRs are similar between mice and humans (LeBien, 2000). Of note is one distinction during the pre and pro-B-cell stages. While in mice the differentiation and survival of the early B-cells is dependent on IL-7, human B-cells do not show any dependency on IL-7 (Namen et al., 1988; Noguchi et al., 1993; Prieyl & LeBien, 1996; Puel, Ziegler, Buckley, & Leonard, 1998). Over the last few decades, extensive research has led to the discovery of a number of differentially expressed surface markers that can be utilized to distinguish different B-cell compartments. While these

markers are analogous between the two species, there are occasional differences in expression (and sometimes nomenclature). Here on, the markers mentioned will pertain to mice.

Once an IgM expressing immature B-cells are formed they exit the bone marrow and are referred to as transitional B-cells. These cells can be subcategorized as T1, T2 or T3 cells based on their different surface marker profiles and functions (Allman et al., 2001; Carsetti, Köhler, & Lamers, 1995; Loder et al., 1999). Transitional B-cells do not enter the lymphatics and are confined to circulation in the blood and spleen. These cells have two potential fates as they further differentiate: Follicular B-cells (FOB) or Marginal Zone B-cells (MZB) (Pillai & Cariappa, 2009). These two cell types have distinct functions, localize to specific and separate niches, and even though they both have BCRs, display different signalling outcomes. The mechanisms that are involved in these two separate fates are not completely understood. MZBs (IgM^{hi}, IgD^{lo}, $CD21^{hi}$, $CD23^{lo}$) localize to the marginal zone of the spleen and can act in a T-cell independent fashion to offer a first wave of defense against blood borne pathogens (Balazs, Martin, Zhou, & Kearney, 2002). T-independent antigen responses also fall under the purview of B-1 cells which will not be discussed in this work. FOBs (IgM^{lo}, IgD^{hi}, $CD21^{lo}$, $CD23^{hi}$) are the lineage of cells arising from transitional B-cells that are involved in T-dependent antigens. The T-cell dependence is explained with the help of the two-signal model of the humoral immune response (Bretscher & Cohn, 1970). Signal 1 is the antigen binding to the BCR, while signal 2 is the 'help' that is offered to the B-cells after they internalize the antigen, process them into smaller fragments, and subsequently present them on the cell surface to either CD4+ T-cells, thereby following the T-dependent response. On the other hand, T-independent responses involve the interaction of innate immune cells

with B-cells for signal 2. T-dependent responses lead to a response that lasts longer and results in a profound increase in the affinity of the BCR for its cognate antigen.

The FOB-cells are the freely recirculating B-cells in the peripheral immune system. These 'mature' B-cells are referred to as 'follicular' as they are found in organized aggregates within secondary lymph organs (white pulp of spleen and cortical regions of lymph nodes) known as primary B-cell follicles (labelled 'F' in Figure 2.4, left panel). Within these follicles exist a complex network of stromal cells known as follicular dendritic cells (FDCs) interspersed with tangible body macrophages and T-follicular helper cells (Figure 2.4, right panel). FDCs produce the chemokine CXCL13 (Vermi et al., 2008) and attract CXCR5 expressing B and T-cells to organize the follicular structure (Ansel et al., 2000). FDCs also express IL-6 and BAFF which are important for the survival of GCBs, as well as adhesion molecules that are required for interactions with the B-cells in the follicle. Upon activation with antigen the B-cells will put in motion the process that leads to the formation of the germinal center.

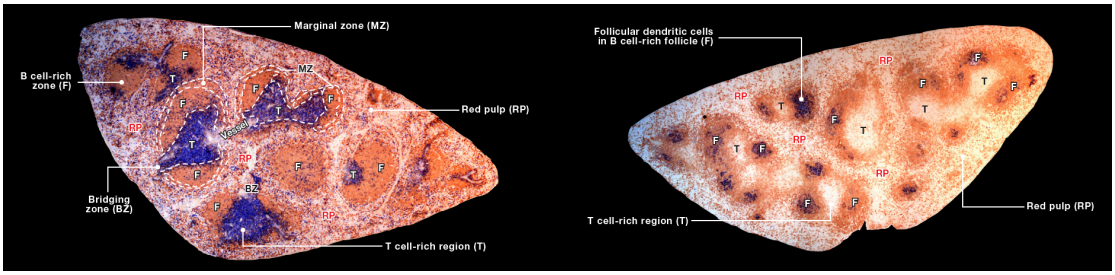

Figure 2.4 (LEFT) Cross-section of spleen from 8-week old C57BL/6 mouse. B-cells in brown (anti-B220), T-cells in blue (anti-CD3), and B-cell follicles are dark brown due to a high density of FOBs. Marginal Zone (MZ), Red Pulp (RP), Bridging Zone (BZ) are also indicated. (RIGHT) Cross-section of a mouse spleen showing follicular dendritic cells in dark blue (anti-CD35) within individual B cell follicles stained brown (anti-IgD). The position of the adjacent T zones and surrounding red pulp are labeled for clarity. The spleen is from an un-immunized mouse and the follicles lack GCs, and are thus primary follicles. Image is from the open source 'Immunology Image Resource'. The sections were submitted by Xiaoming Wang and Jason Cyster. Howard Hughes Medical Institute and Department of Microbiology and Immunology, UCSF.

2.3 Cells and functions of the Germinal Center

The T-dependent response is similar to the T-independent in that a few days after the initial antigenic challenge, appear plasma cells in the extra-follicular regions of the spleen. These express low affinity IgM just like that of the T-independent response. However, around that time an entirely different and complex sequence of events starts in parallel. T-cells in the spleen that have been independently activated by antigen interact with activated B-cells for the same antigen. The site of this interaction is the border of the follicle adjacent to the T-cell zone known as the T:B border (Jacob, Kassir, & Kelsoe, 1991; Nieuwenhuis & Opstelten, 1984). Here, the processed antigen is expressed on the activated B-cell with MHC II complex for the CD4+ T-cells to recognize via their TCRs. The B-cells expressing B7-1(CD80) and B7-2 (CD86) interact with CD28 on the T-cells. This leads to bi-directional activation signals that facilitate proliferation of T-cells and the B-cells (Coffey, Alabyev, &

Manser, 2009; Garside et al., 1998; Okada et al., 2005). In addition to these signals, the T-cells now start expressing CD40L (CD154) which binds to CD40 on the B-cells. This interaction leads to downstream signalling which results in the transcription of immunoglobulin genes and class-switching from IgM/IgD to IgG. Secreted cytokines dictate the specific type of class switching that occurs. A cluster of rapidly proliferating B-cells will start forming from the T:B border which organizes itself into a dark zone (DZ) and a light zone (LZ). Figure 2.5 shows a secondary follicle in a tonsillar section stained for Ki-67, the region the GC with a denser population of cells at the bottom is the DZ while the sparsely stained (non-proliferating region) is the LZ.

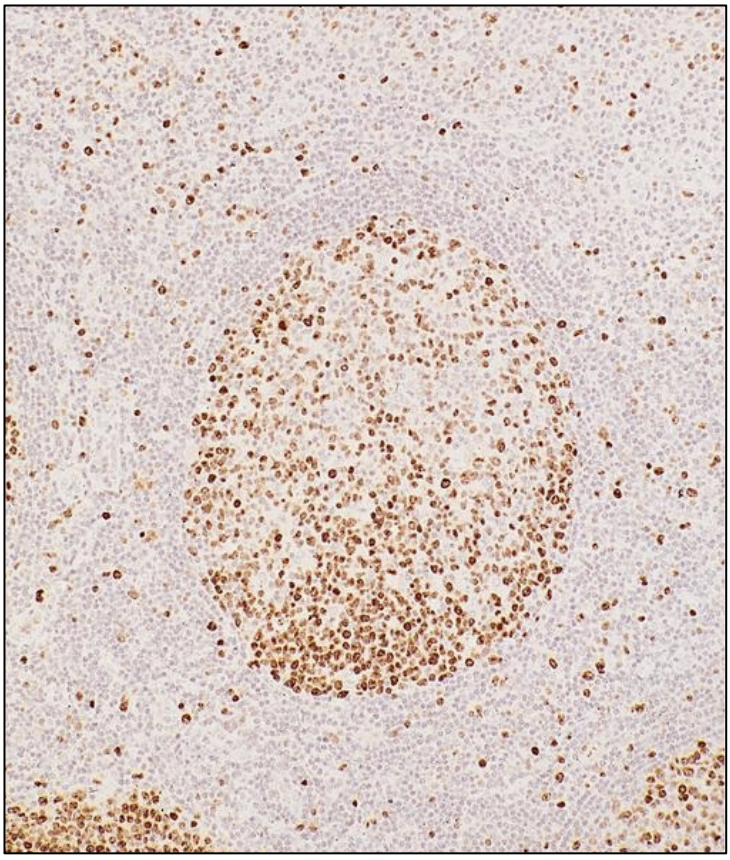

Figure 2.5 Secondary follicle in zoomed in cross section of tonsillar tissue stained with Ki67. Image reproduced from *Pathologyoutlines.com.*

The DZ is primarily occupied by the dividing B-cells known as centroblasts that are CXCR4^{hi}(Allen et al., 2004). The stroma of the DZ consists of CXCL12

(ligand for CXCR4) expressing reticular cells (CRCs). The CXCL12 gradient retains the centroblasts in the DZ, away from the LZ that is rich in FDCs (Bannard et al., 2013; Rodda, Bannard, Ludewig, Nagasawa, & Cyster, 2015). Centroblasts have higher levels of AID and therefore are believed to be the site of somatic hypermutation (SHM), through which clonal variants of different affinities for antigen are formed (Muramatsu et al., 2000). Variants with higher affinity for antigen are selected whereas the ones with lower affinities lose the selective competition and die out. The LZ is posited to be the site of this selection. The overall organization of the LZ is less compact but more diverse—in addition to the FDCs it also has T-follicular helper cells (T_{FH}-cells) and infiltrating naïve B-cells. The B-cells migrating from the DZ into the LZ are subsequently known as centrocytes. Extensive research has shown that affinity maturation is a result of an iterative process of SHM (in DZ) and selection (in LZ) over multiple cycles. B-cells with improving affinity for antigen can return to the DZ for another round of SHM to further improve their ability to recognize and neutralize an antigen (Allen, Okada, Tang, & Cyster, 2007; Gitlin, Shulman, & Nussenzweig, 2014; Schwickert et al., 2007; Victora et al., 2010). T_{FH}-cells in the LZ play a critical role in the positive selection process by providing proliferative signals and driving the fate of the GCB towards plasma cells (Allen et al., 2007; Meyer-Hermann, Maini, & Iber, 2006; Victora et al., 2010).

The fate of the GCB depends on the manner in which the affinity for antigen is modulated. Changes that potentially create affinity for self-antigens result in negative selection in addition to the ones where the affinity is decreased for antigen. Positively selected cells have two potential fates—they can either become antibody secreting plasma cells (PC) or long-lasting memory B-cells (memB). While the mechanisms that dictate the fate-decisions are not completely understood (and is currently somewhat

confusing), there are a few clues about the signals that correlate with one fate or another. A temporal hypothesis claims that the propensity of the B-cell to become a PC increases as the BCR affinity for the antigen increases, while the memB-cells arise from early GC phases (Weisel, Zuccarino-Catania, Chikina, & Shlomchik, 2016).

2.4 BCL6-the master regulator of Germinal Center B-cells.

A simplified version of the events that occur during the transition of an antigenically naïve B-cell (FOB) to GCB is shown in figure 2.6.

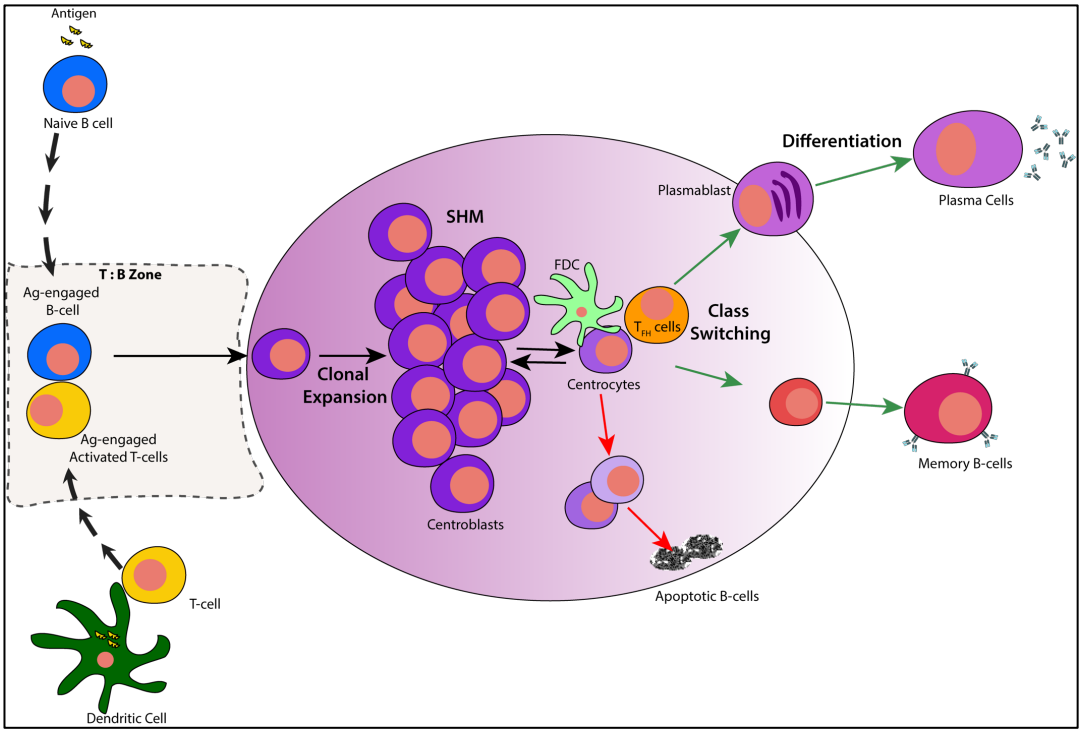

Figure 2.6 Schematic depicting transition from naïve B-cell to GCB-cells. The schematic also shows the T:B cell interaction priot to the formation of Germinal Centers and the interaction if GCBs with Follicular dendritic and Follicular T-helper cells.

A foundational concept in developmental biology is that differentiation is brought about through changes in gene expression. A cell transitioning from cell stage X to stage Y will exhibit a profound shift in the type and level of genes expressed. The

regulatory mechanisms involved in the transcriptional changes associated with such transitions have been a subject of interest for decades. With the advent of next-gen sequencing technologies, there has been an influx of information pertaining to the overall gene expression profiles that characterize different cells in eukaryotic organisms. A concept that emerged in in the late 70's provides insight into one of the key aspects of this regulation—it is the idea of the master regulator or master transcription factor. The existence of such a modality was first hypothesized to be involved in sex determination (Ohno, 1979). The concept was subsequently extended to cell specification in drosophila and plants. Chan and Kyba, noticing an upswing in the use of this term proposed the following criteria for the definition of a gene that would be classified as a master regulator, "a gene that is expressed at the inception of a developmental lineage… participates in the specification of that lineage by regulating multiple downstream genes … and critically, when misexpressed, has the ability to re-specify the fate of cells destined to form other lineages." (Chan & Kyba, 2013).

In line with this definition is the gene *BCL6*, which is now an accepted master transcription factor of GCBs. Basal level of *BCL6* transcripts and protein are present in the naïve B-cell stage, and the expression is upregulated many fold at the inception of the germinal center (Figure 3.3). *BCL6* was originally discovered in 1993 as the gene that was associated with the t(3;14)(q27;q32) and t(3;22)(q27;q11) chromosomal translocations frequently observed in B-cell lymphomas—primarily DLBCL (Baron et al., 1993; Ye BH, Lista F, Lo Coco F, Knowles DM, Offit K, Chaganti RS et al., 1993). This translocation is reported to be present in 20-35% DLBCL cases and is associated with the deregulated expression of *BCL6*.

BCL6 is a 95 KDa nuclear phosphoprotein primarily works as a transcriptional repressor. It belongs to the BTB/POZ/ZF family with the BTB/POZ domain at the N terminal, the Zinc fingers at the C terminal and PEST domains in between the two regions. The BTB domain dimerization is known to be a feature of proteins that possess these domains, and this implies that BCL6 itself must function as a dimer. Binding of BCL6 to DNA is via the ZF domains, whereas the BTB/POZ and PEST domains are involved in the actual repressive activities. The repression is achieved via direct or indirect recruitment of histone deacetylases (HDACs). The indirect recruitment is through corepressor complexes like NCOR2 (SMRT), NCOR1, BCOR, MTA3, and CTBP1. The BTB/POZ domains are known to recruit the NCORs, BCOR and CTBP1 whereas the central PEST domains recruit MTA3 (and CTBP1). The binding of BCL6 directly to the promoter DNA is usually a requirement for activity but recruiters of BCL6 like ZBTB17 (Miz1) have also been reported (Basso & Dalla-Favera, 2010)

The repressive function of BCL6 is essential for the formation of germinal centers, as the GCB cell experiencing genotoxic stress during the process of SHM would otherwise succumb to DNA-damage-induced apoptosis. Some of the genes repressed by BCL6 include TP53 (R. T. Phan & Dalla-Favera, 2004), CDKN1A (R. Phan, Saito, Basso, Niu, & Dalla-Favera, 2005), ATR (Stella Maris Ranuncolo et al., 2007) and CHEK1 (Stella M. Ranuncolo, Polo, & Melnick, 2008). In addition to the repression of the DNA-damage response genes, BCL6 also regulates the expression of genes involved in apoptosis. BCL2, an anti-apoptotic protein, is suppressed by the action of BCL6 (Ci et al., 2009; Saito et al., 2009). On one hand, the suppression of an anti-apoptotic molecule may seem counterintuitive, but it makes sense when the elimination of sub-par GCBs (the ones that need to be negatively selected due to

inefficient engagement of BCR to antigen or reactivity to self antigens) is of utmost importance. Furthermore, BCL6 targets also include genes that would otherwise regulate the differentiation of GCBs. A key gene involved in this is PRDM1 (gene encoding Blimp-1) which is itself a master regulator of plasmacytic differentiation (Tunyaplin et al., 2004).

Therefore, the actions of BCL6 represent a complex network of phenotypes maintained in a delicate balance. When this balance is disrupted through deregulation of BCL6, then as predicted by Chan and Kyba, there is a 'respecification of fate' in that they lead to various B-cell lymphomas (primarily DLBCL and occasionally FL).

2.5 Genomic remodeling during the NB to GCB transition.

As mentioned earlier, the differentiation of NB to GCB is accompanied by a profound shift in the type and level of the genes that are expressed. The underlying regulatory modalities that enact such transitions are not completely understood and are a subject of widespread research spanning different cell systems. Over the last decade, epigenetic regulatory mechanisms influencing coordinate and rapid gene expression changes have been shown to be critical for differentiation. This is especially important in the large scale changes seen in multicellular organisms (Cantone & Fisher, 2013; Natoli, 2010; Spitz & Furlong, 2012). This makes intuitive sense when we come to appreciate the complexity of the genome of higher organisms. To efficiently and consistently coordinate thousands of genes, spread across distinct chromosomes, so that they simultaneously undergo transcription at physiologically relevant levels requires a number of strategies that directly involve the genome to be spatially and qualitatively modified. While individual genes can be regulated through epigenetic mechanisms like DNA methylation or histone modifications (Zhou, Goren, &

Bernstein, 2011), another aspect of regulation involving the folding and looping of the genome is gaining significant attention.

Chromosomal conformation capture technologies and DNA-fluorescence in-situ hybridization (FISH) have given us a view into these 3D reorganizations that occur during different stages of differentiation (Bickmore & Van Steensel, 2013; Cavalli & Misteli, 2013; Fabre et al., 2015). A number of studies have also shown that the genome itself is compartmentalized in specific and recurrent ways to control gene expression in organisms (Baú et al., 2011; Dixon et al., 2012, 2015; Lieberman-aiden et al., 2009; Sanyal, Lajoie, Jain, & Dekker, 2012; Sexton et al., 2012; Sexton & Cavalli, 2015)

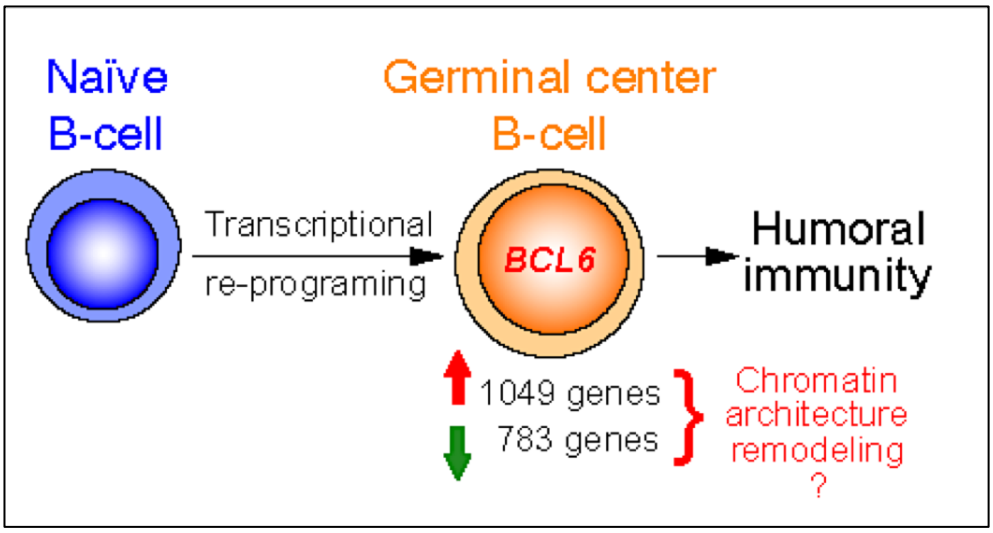

Figure 2.7 Transcriptional changes during germinal center B cell differentiation from RNA-seq on human tonsillar NB and GCB.

Published work from our group (Bunting et al., 2016) describes in immense detail the epigenetic and genetic changes that potentially regulate gene expression changes between NB and GCBs. In humans there are approximately 1800 genes that are differentially expressed (Figure 2.7). This change is accompanied by a

decompaction of the genome, increase in promoter-promoter interactions, reorganization of enhancer networks, 5' to 3' looping of actively transcribed genes, and the remodeling of gene neighborhoods which are small looping clusters of genes and their regulatory elements.

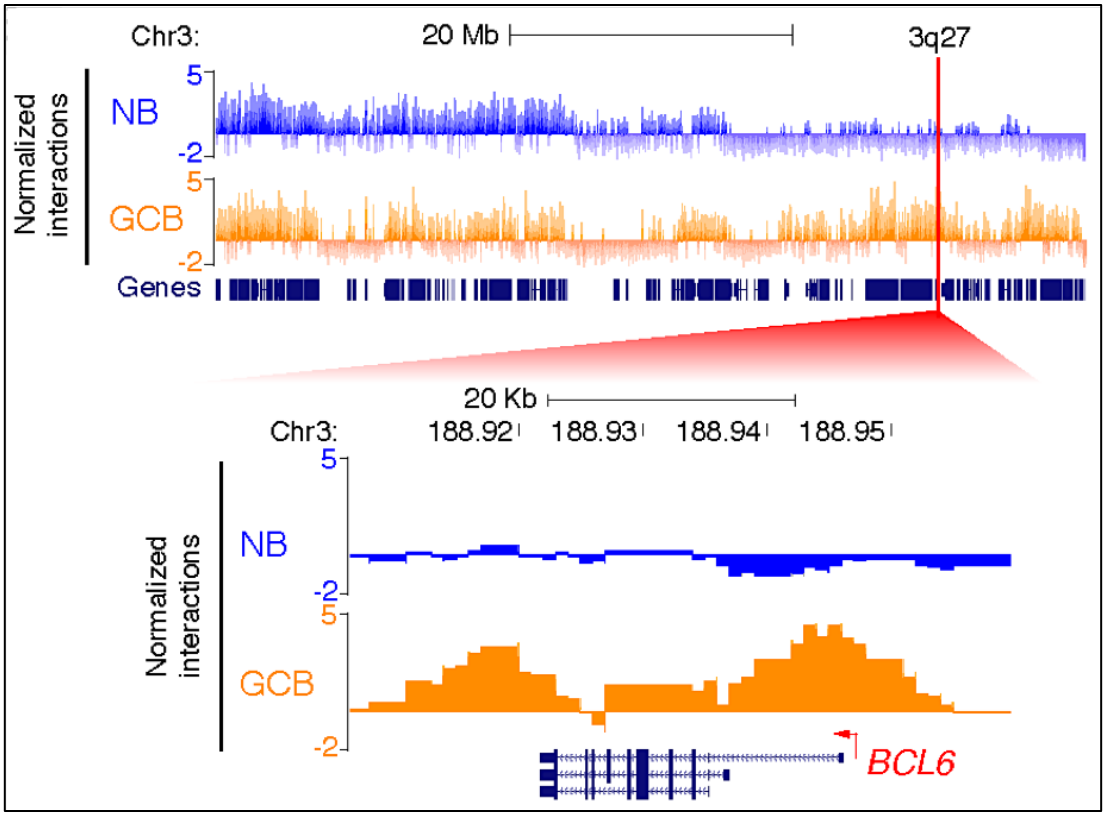

Figure 2.8 UCSC Browser view of normalized Hi-C counts in the 3q27 locus between human NB (blue) and GCB (orange). Significant enrichment of contacts is observed around the *BCL6* locus in GCBs compared to NB-cells.

The general decompaction of the genome can be thought of as an early step in the transition from NB to GCB. This decompaction has been captured through genome wide chromosomal conformation capture (Hi-C) studies in our lab on human tonsillar NBs (IgD+ CD38lo) and GCBs (CD77+ CD38hi). The loosening of the chromosomes is reflected in the Hi-C data as interactions between the p and q arm of chromosomes

are lost, and the nuclei become larger. Figure 2.8 is a browser view of the Hi-C data for the 3q27 locus in humans (which is the location *of BCL6*) where we can see a substantially higher level of chromatin interaction in GCBs as compared to NBs. This specific observation is an important clue in our subsequent studies as the locus coding for the GCB master regulator maybe doing much more than just coding for an influential transcriptional repressor.

An increase in promoter-promoter interactivity was observed on performing a gene centered analysis of the Hi-C data. Our understanding of active, poised and inactive regions of chromatin relies on the identification of associated histone modifications. To this extent, there are modifications of lysine-4 (K4) and lysine 27 (K27) of histone 3 (H3) which can be determined via ChIP-seq for these different marks. Active promoters are H3K4me3+, H3K27Ac+ and are bound to the histone acetyl-transferase P300 and RNA polymerase II (PolII) (spicuglia & Vanhille, 2012). These can also be H3K4me2+. Inactive chromatin is associated with H3K27me3 modifications. Our analysis showed that highly interactive promoters were associated with *BCL6*, *MTA3*, *LMO2*, *BCL7A*, BCR signaling pathway, *TEC*, *PIK3CG* and *CAM2KB*. The highly interactive promoters were enriched for active chromatin marks, had higher levels of transcription in GCBs vs NBs. The strongest promoters in GCB were bound by P300, PU.1, SpiB and IRF8. These promoters usually had significantly lower interactivity in NB-cells. Importantly, the genes with highly interactive promoters were also actively transcribing genes that drive the GCB-cell phenotype.

Cell type specific gene expression is coordinated in large part by the action of enhancers. Enhancers are H3K4me2+ and H3K4me3-. Active enhancers can be differentiated from poised enhancers through the presence of H3K27Ac marks

(Creyghton et al., 2010). It should be noted that P300 is bound to both Enhancers and promoters. H3K4me1 is associated more with enhancers than promoters. H3K4me2 is a mark that is more or less equitably laid down in enhancers and promoters whereas, H3K4me3 is a sign off active promoters more than it is of active enhancers (spicuglia & Vanhille, 2012). Another point that should be made is that the terms 'open' and closed' chromatin, while in common use, are less precise in their implications as open chromatin could be poised or active. The combinations of various histone modifications, transcription factor and chromatin modifier binding profiles create a somewhat complex network of chromatin states, therefore, here on the usage of 'open' and 'closed' chromatin in this text will be minimal.

As should be obvious, both NB and GCB have their specific and overlapping sets of enhancers. Our lab identified 5167 enhancers (<50Kb away from genes) of which 2818 were unique to NBs. Enhancers working in NB were largely involved in immune homeostasis functions. On the other hand, GCBs have 5339 enhancers (<50Kb away from genes) of which 2990 are unique. These contact GCB differentiation genes, cell proliferation genes, and GCB-type DLBCL genes including *BCL6*, *CKS2*, *MCM2*, *MCM5*, *RFC3*, *SPRED2*, *PRC1* and *TIAM2*. Generally, enhancer-enhancer and enhancer-promoter interactions were markedly increased in GCBs vs NBs. However, this increase was not random as interactions between non-regulatory loci did not increase as a by-product of looser chromatin. This brings home the point that the changes described thus far are relevant to the reprogramming of transcriptional networks specific to GCBs. When looking for genes that had the highest promoter-enhancer interactions we discovered a set of 32 genes, 90% of which are upregulated and relevant in GCBs. Some of these genes include *BCL6*, *CKS2*, *DGKG*, *ETV5*, *PVT1*, *SERPINA9*, and *SPP1*.

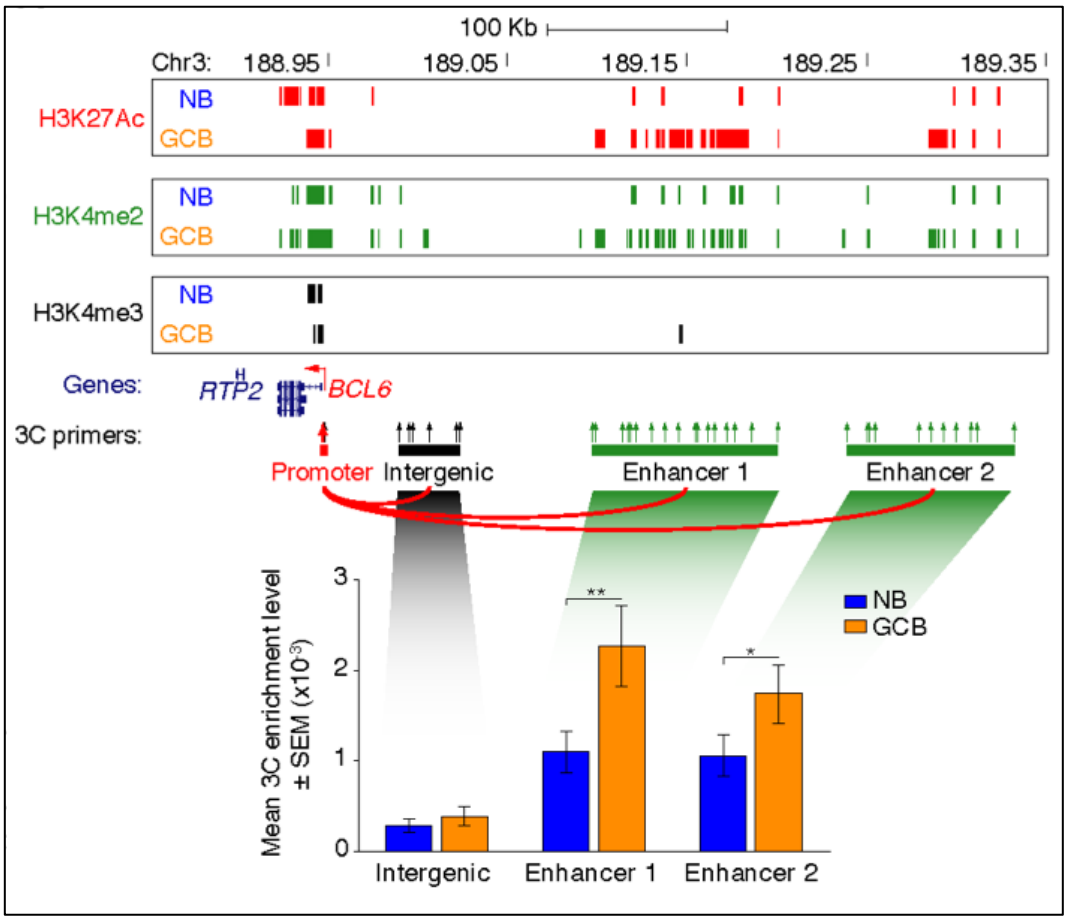

Figure 2.9 UCSC Genome Browser tracks in NB and GCB showing chromatin marks and locations of 3C primers (arrows) across a region upstream of BCL6. The red arrow denotes the anchor point for all 3C PCRs. Bar plots show the mean 3C enrichment in NB and GCB, 3C DNA templates (n = 3) at the regions indicated. Primer pairs were averaged across each region. Performed a one-tailed, unpaired t-test (**$p < 0.05$; *$p < 0.1$).

To validate the interactions between upstream enhancers and promoters for the set of 32 genes the *BCL6* locus was chosen for 3C studies. The browser image in figure 2.9 shows ChIP-seq tracks with called peaks for H3K27Ac, H3K4me2 and H3K4me3 to define the promoter and enhancer regions upstream of *BCL6*. The enhancers positioned ~100-400 Kb upstream showed significantly higher interactions with the BCL6 proximal promoter as compared to the inter and intragenic loci characterized by low levels of enhancer marks. Therefore, the data suggests an association of this reorganization of enhancer networks with the GCB transcriptional profile. Interestingly, this further promotes the idea that the chromatin around the BCL6 gene has enhancers that may be characterized as locus control regions as they might be involved in a critical control step for the overall transcriptional reprogramming and not just the nearby genes.

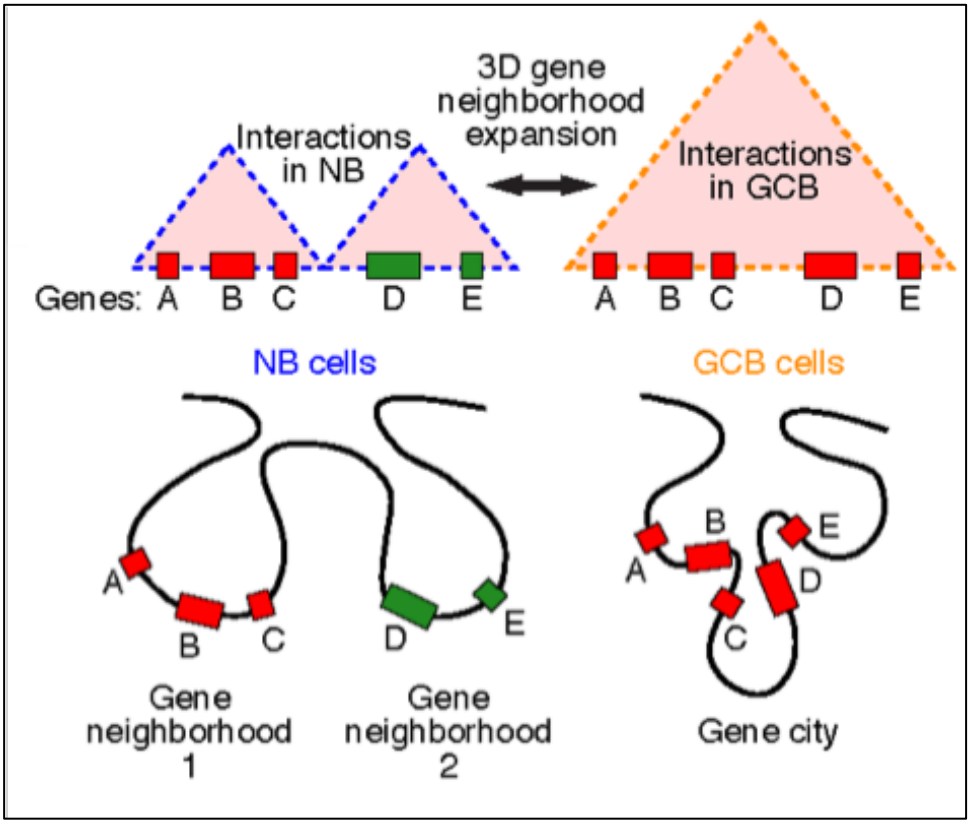

Figure 2.10 Schematic of merging gene neighborhoods into gene cities.

Further utilization of the Hi-C data also revealed groups of genes separated into boundary-delimited (or insulated) neighborhoods. These gene neighborhoods, previously described to be highly conserved between species which speaks to their potential role in gene regulation (Dixon et al., 2012; Vietri Rudan et al., 2015). Genes within such neighborhoods are usually expressed in a coordinated fashion and the boundaries are defined by CTCF binding. We noticed a similar pattern of expression, epigenetic marks, and significantly higher levels of chromatin interactions in the gene neighborhoods of GCB and NB cells. An interesting observation was the merging of these clusters into larger domains described as 'gene cities.'

This merging occurred from the NB to the GC stage and is accompanied by a coordination of expression of the genes from the original clusters. Furthermore, the de novo acquisition of the epigenetic mark H3K4me3 was also noticed between the groups of genes that were initially in distinct neighborhoods in NB. Again, the genes that fell into the category of merged gene cities were highly representative of gene sets involved in the GCB phenotype including proliferation, MHC Class II-mediated antigen presentation, and metabolic stress. They also have hypo-methylated promoters in GCBs compared to NBs.

The pattern emerging from the observations made thus far is that there is a deliberate attempt to modify the architecture of the genome that allows for coordination of gene expression relevant to the NB -GCB transition. Genes that are isolated and regulated independently in NB are brought physically closer together for better coordination and co-regulation of those genes in GCBs. The multiple levels of physical reorganization around BCL6 is interesting as it highlights an evolutionary pressure that results in clustering of genomic loci that are not only coding for critical

master regulators important for differentiation but also physically playing a role in the reorganization of other loci for regulatory purposes.

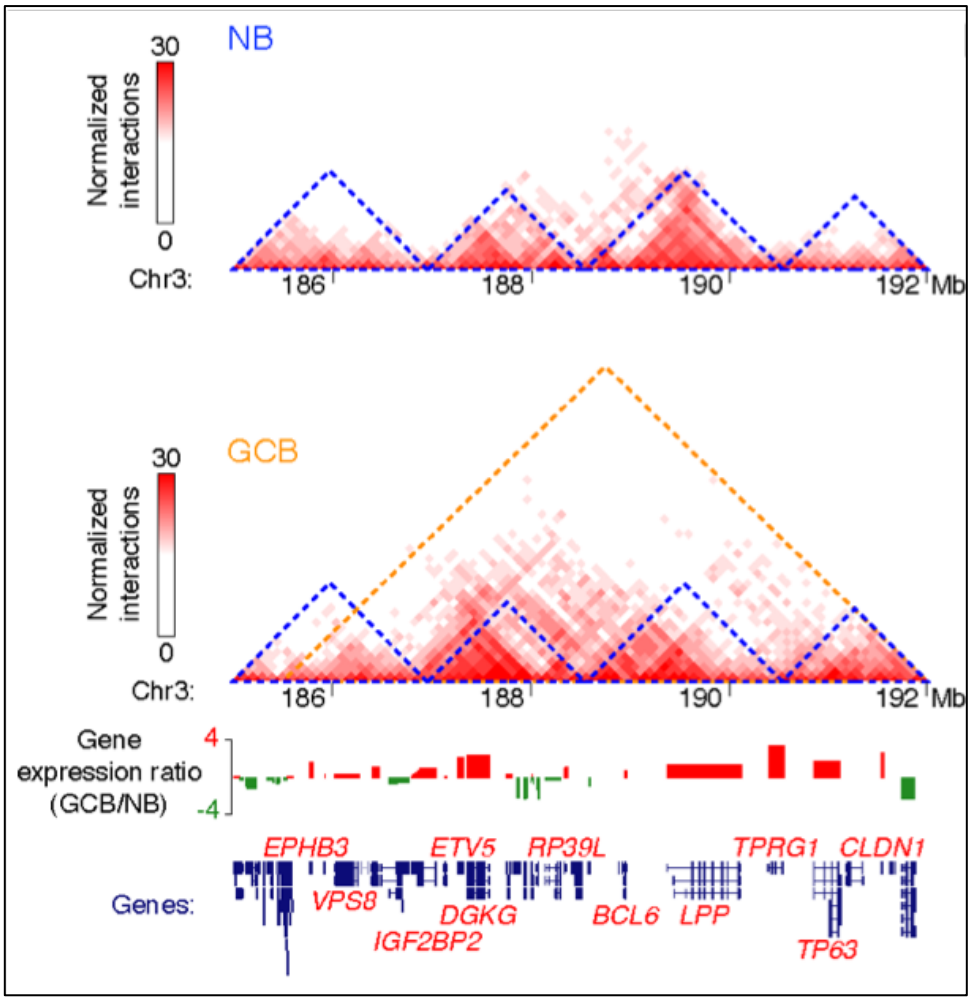

Figure 2.11 2D heat-maps of normalized interaction frequencies in NB and GCB cells and log2 gene expression ratio (GCB/NB) across a chromosome 3 region. 3D gene neighborhoods in NB and GCB cells are indicated (blue and orange triangles, respectively). Gene expression ratios between GCB versus NB cells determined by RNA-seq is shown below, along with location of each gene.

To further explore the interactome of *BCL6*, 4C-seq was performed in NB and GCBs. With 4C bait primers in the BCL6 promoter, approximately 3000 intra-chromosomal interactions were noted to be significantly gained in GCB vs NB (Figure

2.12). The majority of these gained interactions were within the merged gene city with *BCL6* (Figure 2.11). Another set of gained interactions that were of interest were again in the distal enhancers (two distinct enhancers) captured earlier via 3C, upstream of BCL6.

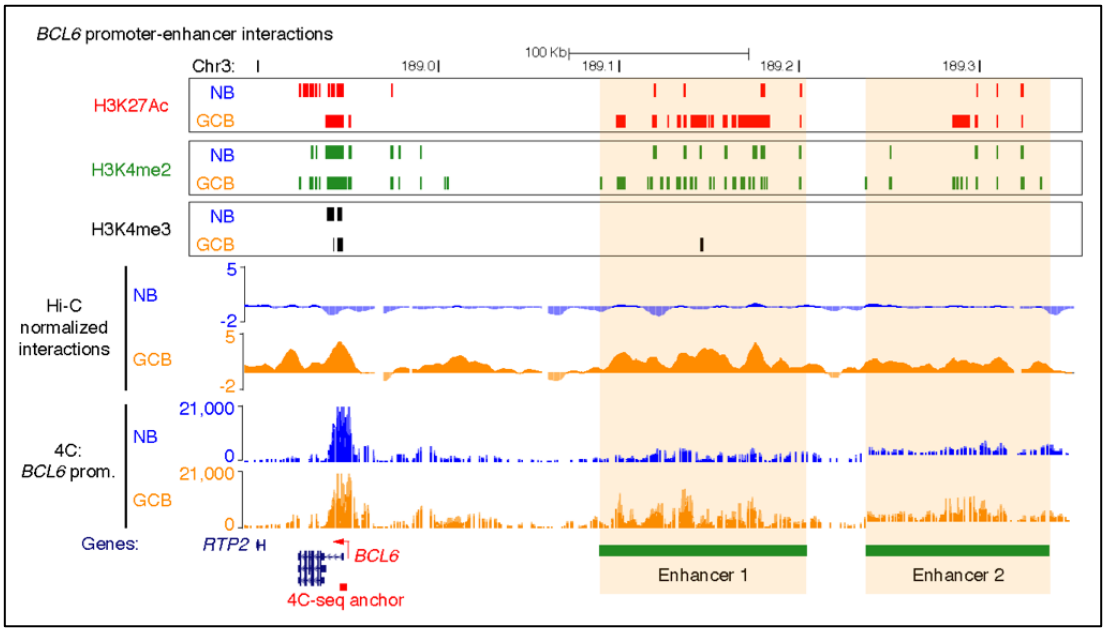

Figure 2.12 Genome visualization tracks showing H3K4me3, H3K4me2, and H3K27Ac histone modification peaks, normalized Hi-C interaction frequencies (merged), and normalized read counts of 4C contacts made with the BCL6 gene promoter in NB and GCB across the *BCL6* gene region on chromosome 3.

This cluster of enhancers—which gained interactions with the *BCL6* promoter in GCB/NB—was collectively categorized as one putative locus control region (LCR). We hypothesized that this LCR might play an important role in regulating *BCL6* and other GC specific genes, and thereby would be required for GC formation.

Furthermore, when the 4C bait was anchored within the putative LCR itself, we observed significant interactions with the BCL6 promoter (Figure 2.13). This further solidified our belief that the putative LCR was a regulatory hotspot involved in regulating GC physiology. This regulation could be due to direct contacts made with

both nearby and distant genes so as to pull them closer in proximity and thereby co-regulate their expression. Other potential mechanisms could involve a higher order function where the overall reorganization of the genome (centered around the *BCL6* locus) requires binding of multiple transcription factors and chromatin modifiers.

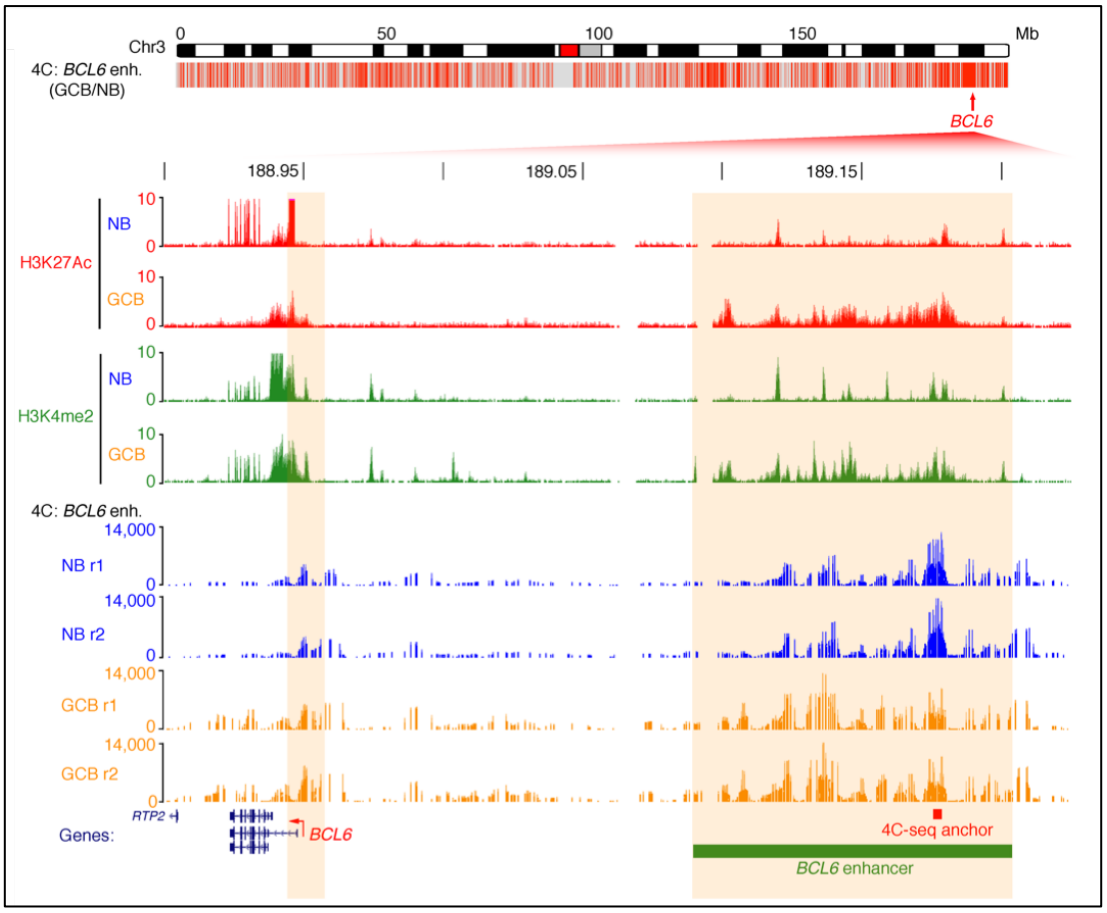

Figure 2.13 Top: plot showing locations of *BCL6* LCR contacts made in GCB vs NB detected by 4C-seq across chromosome 3 ($p < 0.05$, Fisher's exact test). Bottom: zoomed-in view of BCL6 and LCR showing histone modifications and normalized read counts of contacts made with the putative BCL6 LCR detected by 4C-seq in NB and GCB.

Analysis of the GCB specific enhancers defined by H3K27Ac and H3K4me2 enrichment in GCBs compared to NBs, we also found that a highly significant proportion of these enhancers also overlapped with the loci that increased contacts

with the putative LCR. A representation of this analysis is shown through a circus plot depicting the entire human chromosome 3, with H3K4me2 peaks in green, H3K27Ac peaks in red and the GCB specific enhancers overlapping 4C contacts with the putative LCR in blue (Figure 2.14). Additionally, an analysis of the genes most proximal to these enhancers, we discover that they include GC differentiation signature genes (lower panel of Figure 2.14).

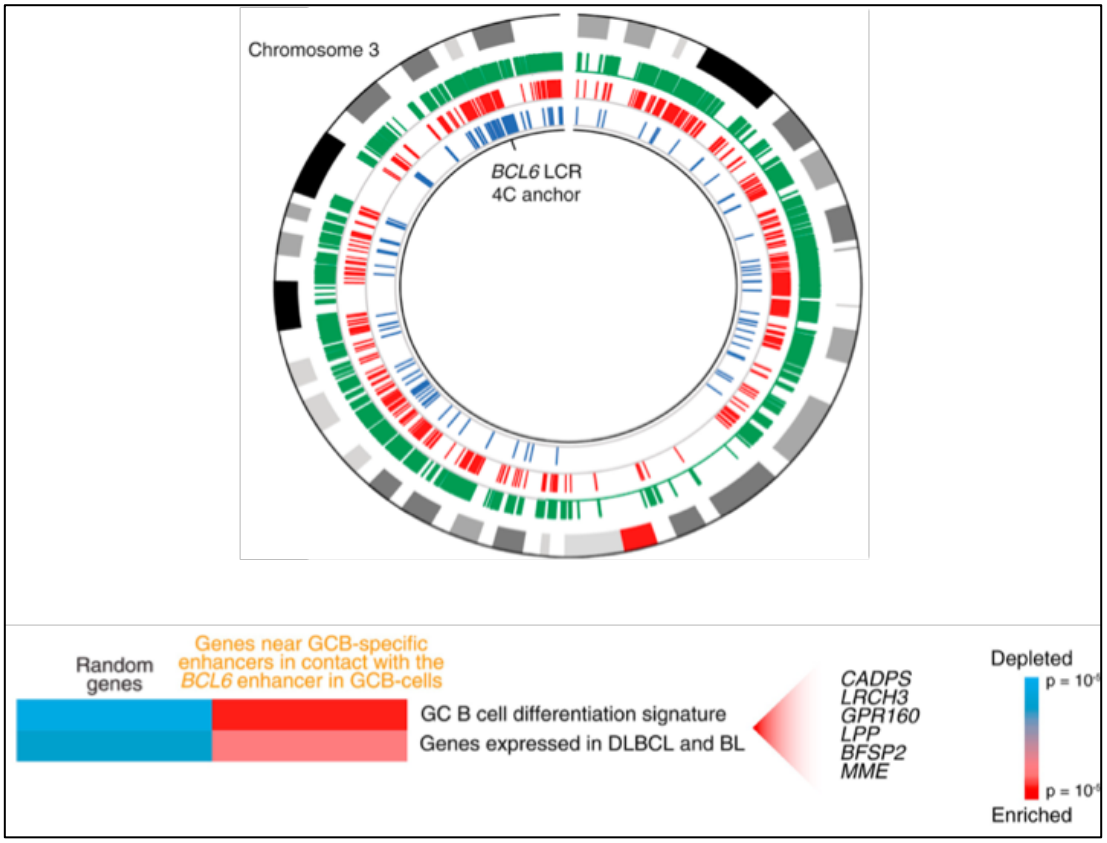

Figure 2.14 Top: Circos plot showing chromosomal locations of the enhancer-enhancer contacts made between the putative *BCL6* LCR (4C anchor in putative LCR) and other GCB specific enhancers in GCBs (but not in NB), as detected by 4C-seq across chromosome 3 ($p<0.05$, Fisher's exact test). The outermost ring of the plot is an ideogram of chromosome 3. The green and red peaks depict regions of enrichment in GCBs for H3K4me2 and H3K27Ac respectively. Bottom: Gene set enrichment and depletion among genes near GC B cell-specific enhancers that form contacts with the putative GC B cell-specific LCR upstream of BCL6 in GC B cells. Significant genes are listed ($p < 0.002$).

2.6 Locus Control Regions

Locus Control Regions are defined as genetic regulatory elements that control the expression of key genes involved in the specification of a cell fate. LCRs also confer tissue specificity and play an important role in the temporal upregulation of linked genes to physiologically relevant levels. In recent years, there has been a renewed focus on LCR biology as research into gene regulatory mechanisms made a giant leap in the era of genomics. The term, super-enhancers is now frequently used to describe LCRs and this rebranding in 2013 (Whyte et al., 2013) has been of some debate as there is yet to be a clear functional rationale to separate these modalities. However, trivial marketing ploys aside, the significance of such regulatory loci is becoming increasingly clear as more effort is poured into profiling the epigenetic landscape of various tissue types and cancer cells.

For clarity, it must be noted that there is a difference between an LCR and an enhancer. While functionally both enhancers and LCRs are gene regulatory loci, enhancers are known to exhibit a phenomenon known as 'position effect.' If a gene with an enhancer is introduced into the genome, the expression of that gene is not entirely dictated by the enhancer. Instead, the state of the chromatin in the region (accessibility) predicts the level of expression instead. While the enhancer is still critical for expression, it only influences the gene when permitted to do so by the preexisting nature of proximal chromatin. If the enhancer is coupled to a selectable marker, followed by the selection pressure then the cells that emerge are the ones where the insertion of the gene-enhancer locus was in a favorable region. When an enhancer is inserted into a region without any selection—for example when a transgene is inserted into a fertilized egg via microinjection—then the position effects

become clear as random insertion of the gene into the cells will result in 'patchy' expression. This is also known as position effect variegation or PEV.

On the other hand, LCRs have the ability to override PEV. They function as independent actors and do not rely on the chromatin state. Instead, the dictate the accessibility of the chromosome on their own terms through binding of master transcription factors, chromatin modifiers and other factors that can regulate these conditions. LCRs are also known to confer tissue specificity and the level of expression of linked genes is directly related to the copy number of the LCR. The DNA sequence of LCRs is obviously critical to their function and it has been shown that modification to LCRs (additions or deletions) have resulted in the emergence of PEV (Fraser & Grosveld, 1998).

The first LCR—also referred to as 'locus activating regions' or 'dominant control regions' (Felsenfeld, 1992)—to be discovered and extensively studied is the cluster of five-DNase Hypersensitive regions around the β-globin gene (Grosveld, van Assendelft, Greaves, & Kollias, 1987). The mechanisms that specifically enact LCR function are still not fully understood. It has been hypothesized that the one of the factors that influences LCR action is the distance of the genes from the LCR (Dillon, Trimbom, Strouboulis, Fraser, & Grosveld, 1997). Some models suggest that distal genes compete with proximal ones for LCR influence in a random contact dependent manner—more proximal genes therefore curry more favour i.e. are upregulated more frequently as they contact the LCR more frequently.

While these early studies shed light onto these vital regulatory elements. The studies over the last 5 years have expanded that knowledge many fold. With

the availability of ChIP-seq data for various transcription factors, histone modifications, chromatin modulators etc., groups across the world are identifying many more super enhancers that regulate differentiation of various tissues. Of note have been the LCR's/Super-enhancers identified in embryonic stem cells that are bound by the master transcription factors Oct4, Sox2, Nanog, Klf4 and Essrb (Whyte et al., 2013). It has also been shown that differential patterns of transcription factor binding in LCRs is related to the signalling pathways involved in the subsequent cell fate decisions. In many cases a master transcription factor, downstream of a signalling cascade, would bind an LCR proximal to a gene known to play a role in the response to that very specific signalling cascade (Chen et al., 2008; Mullen et al., 2011).

Another hallmark of LCRs/super-enhancers is the unusually high level of Mediator binding. Additionally, RNA PolII, cofactors and chromatin regulators like p300, CBP and BRD4 have been shown to bind these loci as well. The mediator complex has been of particular interest as it is responsible for stabilizing and facilitating long range enhancer looping interactions and the extremely high concentration of mediator subunits (identified via ChIP-seq) in LCRs speaks to their functional capability of bringing many loci in close proximity for co-regulation. A simplified depiction of the manner in which an LCR functions is shown in figure 2.15 (Maston, Landt, Snyder, & Green, 2012).

There are many known surrogate markers to establish the presence of an LCR. These include DNase hypersensitive sites, H3K27Ac, H3K4me2, presence of histone acetyltransferase p300 or H3K4me1 marks (Creyghton et al., 2010; Heintzman et al., 2009; Yue et al., 2014). Of these marks the best predictor thus

far has been the histone H3K27Ac modification and will be used as the main surrogate for LCR identity in this body of work as well.

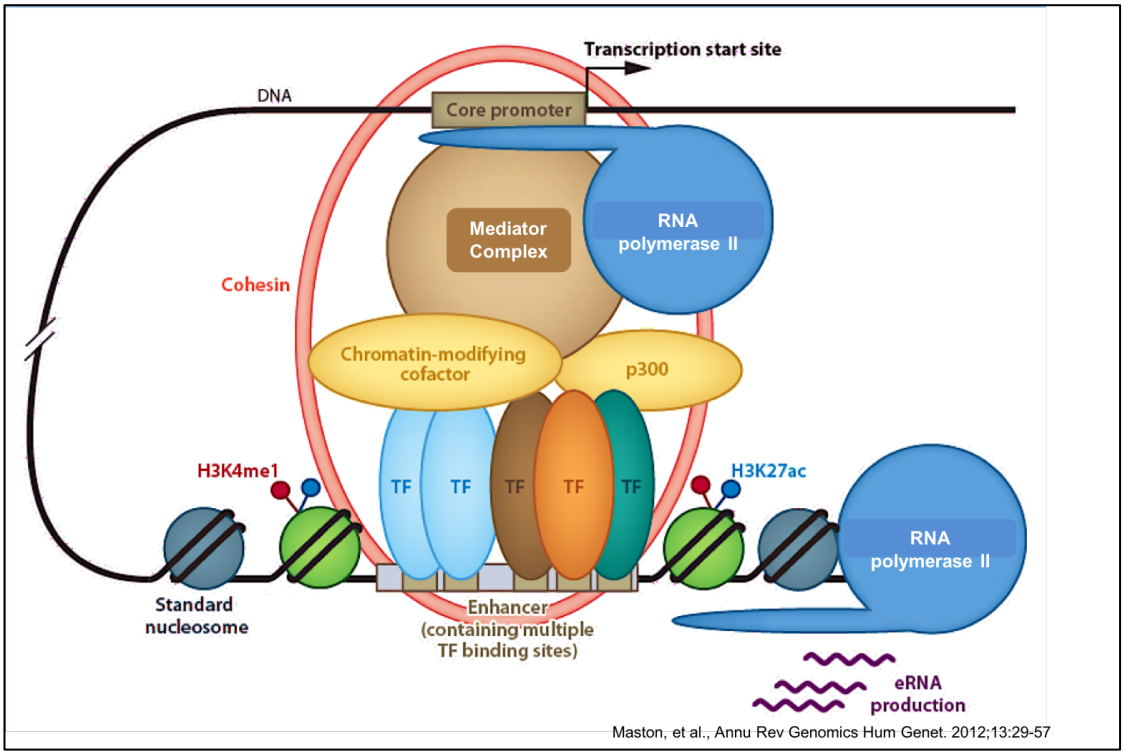

Figure 2.15 Schematic depicting a simplified view of a Locus Control Region bound by multiple transcription factors (TF), mediator, p300 and RNA polymerase II. *Figure from Maston et al. Annual Review of Genomics and Human Genetics (Vol. 13)*

2.7 Hypothesis

From the perspective of Germinal Center B-cells, the data shown in section 2.6. indicates that the enhancer clusters upstream of *BCL6* in human GCBs are most likely functioning collectively as an LCR. However, a set of criteria ought to be met to define them as such. To that extent, we decided to test the role this putative LCR might be playing in germinal center B-cells by deleting them in a mouse model. Based on our hypothesis, the constitutive deletion of a syntenic, functionally conserved LCR in mice should have a deleterious effect on GC

formation. However, such a phenotype should be specific to GC B-cells and a regulatory relationship between the genes contacted by the LCR ought to be established. Therefore, we predicted that GC formation upon immunization in a would be reduced in a knockout mouse model, and the homologous genes in mice that are contacted by the LCR in humans should also show lower expression levels.

The first step in this process is to come up with a strategy to identify and then delete the LCR in mice. The details of the strategy we devised are described in Chapter 3.

Chapter 2 References

Allen, C. D. C., Ansel, K. M., Low, C., Lesley, R., Tamamura, H., Fujii, N., & Cyster, J. G. (2004). Germinal center dark and light zone organization is mediated by CXCR4 and CXCR5. *Nature Immunology*, *5*(9), 943–952. http://doi.org/10.1038/ni1100

Allen, C. D. C., Okada, T., Tang, H. L., & Cyster, J. G. (2007). Imaging of germinal center selection events during affinity maturation. *Science*, *315*(5811), 528–531. http://doi.org/10.1126/science.1136736

Allman, D., Lindsley, R. C., DeMuth, W., Rudd, K., Shinton, S. A., & Hardy, R. R. (2001). Resolution of Three Nonproliferative Immature Splenic B Cell Subsets Reveals Multiple Selection Points During Peripheral B Cell Maturation. *The Journal of Immunology*, *167*(12), 6834–6840. http://doi.org/10.4049/jimmunol.167.12.6834

Ansel, K. M., Ngo, V. N., Hyman, P. L., Luther, S. A., Förster, R., Sedgwlck, J. D., … Cyster, J. G. (2000). A chemokine-driven positive feedback loop organizes lymphoid follicles. *Nature*, *406*(6793), 309–314. http://doi.org/10.1038/35018581

Balazs, M., Martin, F., Zhou, T., & Kearney, J. F. (2002). Blood dendritic cells interact with splenic marginal zone B cells to initiate T-independent immune responses. *Immunity*, *17*(3), 341–352. http://doi.org/10.1016/S1074-7613(02)00389-8

Bannard, O., Horton, R. M., Allen, C. D. C., An, J., Nagasawa, T., & Cyster, J. G. (2013). Germinal center centroblasts transition to a centrocyte phenotype according to a timed program and depend on the dark zone for effective selection. *Immunity*, *39*(5), 912–924. http://doi.org/10.1016/j.immuni.2013.08.038

Baron, B. W., Nucifora, G., McCabe, N., Espinosa, R., Le Beau, M. M., &

McKeithan, T. W. (1993). Identification of the gene associated with the recurring chromosomal translocations t(3;14)(q27;q32) and t(3;22)(q27;q11) in B-cell lymphomas. *Proceedings of the National Academy of Sciences of the United States of America*, *90*(11), 5262–6. http://doi.org/10.1073/pnas.90.11.5262

Basso, K., & Dalla-Favera, R. (2010). BCL6. master regulator of the germinal center reaction and key oncogene in B Cell lymphomagenesis. *Advances in Immunology*, *105*(C), 193–210. http://doi.org/10.1016/S0065-2776(10)05007-8

Baú, D., Sanyal, A., Lajoie, B. R., Capriotti, E., Byron, M., Lawrence, J. B., … Marti-Renom, M. A. (2011). The three-dimensional folding of the α-globin gene domain reveals formation of chromatin globules. *Nature Structural and Molecular Biology*, *18*(1), 107–115. http://doi.org/10.1038/nsmb.1936

Bernard, O., Hozumi, N., & Tonegawa, S. (1978). Sequences of mouse immunoglobulin light chain genes before and after somatic changes. *Cell*, *15*(4), 1133–1144. http://doi.org/10.1016/0092-8674(78)90041-7

Bickmore, W. A., & Van Steensel, B. (2013). Genome architecture: Domain organization of interphase chromosomes. *Cell*. http://doi.org/10.1016/j.cell.2013.02.001

Bretscher, P., & Cohn, M. (1970). A theory of self-nonself discrimination. *Science*, *169*(3950), 1042–9. http://doi.org/10.1126/SCIENCE.169.3950.1042

Bunting, K. L., Soong, T. D., Singh, R., Teater, M., Elemento, O., Melnick, A. M., & Poloway, D. W. (2016). Multi-tiered Reorganization of the Genome during B Cell Affinity Maturation Anchored by a Germinal Center-Specific Locus Control Region Article Multi-tiered Reorganization of the Genome during B Cell Affinity Maturation Anchored by a Germinal Center-Speci, *45*, 497–512. http://doi.org/10.1016/j.immuni.2016.08.012

Cantone, I., & Fisher, A. G. (2013). Epigenetic programming and reprogramming

during development. *Nature Structural and Molecular Biology*. http://doi.org/10.1038/nsmb.2489

Carsetti, R., Köhler, G., & Lamers, M. C. (1995). Transitional B cells are the target of negative selection in the B cell compartment. *The Journal of Experimental Medicine*, *181*(6), 2129–2140. http://doi.org/10.1084/jem.181.6.2129

Cavalli, G., & Misteli, T. (2013). Functional implications of genome topology. *Nature Structural and Molecular Biology*. http://doi.org/10.1038/nsmb.2474

Chan, S. S.-K., & Kyba, M. (2013, May). What is a Master Regulator? *Journal of Stem Cell Research & Therapy*. http://doi.org/10.4172/2157-7633.1000e114

Chen, X., Xu, H., Yuan, P., Fang, F., Huss, M., Vega, V. B., … Ng, H. H. (2008). Integration of External Signaling Pathways with the Core Transcriptional Network in Embryonic Stem Cells. *Cell*, *133*(6), 1106–1117. http://doi.org/10.1016/j.cell.2008.04.043

Ci, W., Polo, J. M., Cerchietti, L., Shaknovich, R., Wang, L., Shao, N. Y., … Melnick, A. (2009). The BCL6 transcriptional program features repression of multiple oncogenes in primary B cells and is deregulated in DLBCL. *Blood*, *113*(22), 5536–5548. http://doi.org/10.1182/blood-2008-12-193037

Coffey, F., Alabyev, B., & Manser, T. (2009). Initial Clonal Expansion of Germinal Center B Cells Takes Place at the Perimeter of Follicles. *Immunity*, *30*(4), 599–609. http://doi.org/10.1016/j.immuni.2009.01.011

Creyghton, M. P., Cheng, A. W., Welstead, G. G., Kooistra, T., Carey, B. W., Steine, E. J., … Jaenisch, R. (2010). Histone H3K27ac separates active from poised enhancers and predicts developmental state. *Proceedings of the National Academy of Sciences*, *107*(50), 21931–21936. http://doi.org/10.1073/pnas.1016071107

Dillon, N., Trimbom, T., Strouboulis, J., Fraser, P., & Grosveld, F. (1997). The effect

of distance on long-range chromatin interactions. *Molecular Cell*, *1*(1), 131–139. http://doi.org/10.1016/S1097-2765(00)80014-3

Dixon, J. R., Jung, I., Selvaraj, S., Shen, Y., Antosiewicz-Bourget, J. E., Lee, A. Y., … Ren, B. (2015). Chromatin architecture reorganization during stem cell differentiation. *Nature*, *518*(7539), 331–336. http://doi.org/10.1038/nature14222

Dixon, J. R., Selvaraj, S., Yue, F., Kim, A., Li, Y., Shen, Y., … Ren, B. (2012). Topological domains in mammalian genomes identified by analysis of chromatin interactions. *Nature*, *485*(7398), 376–380. http://doi.org/10.1038/nature11082

Early, P., Huang, H., Davis, M., Calame, K., & Hood, L. (1980). An immunoglobulin heavy chain variable region gene is generated from three segments of DNA: VH, D and JH. *Cell*, *19*(4), 981–992.

Eastman, Q., Leu, T., & Schatz, D. (1996). Initiation of V (D) J recombination in vitro obeying the 12/23 rule. Retrieved from http://www.nature.com/nature/journal/v380/n6569/abs/380085a0.html

Ebert, A., McManus, S., Tagoh, H., Medvedovic, J., Salvagiotto, G., Novatchkova, M., … Busslinger, M. (2011). The distal V(H) gene cluster of the Igh locus contains distinct regulatory elements with Pax5 transcription factor-dependent activity in pro-B cells. *Immunity*, *34*(2), 175–87. http://doi.org/10.1016/j.immuni.2011.02.005

Fabre, P. J., Benke, A., Joye, E., Nguyen Huynh, T. H., Manley, S., & Duboule, D. (2015). Nanoscale spatial organization of the HoxD gene cluster in distinct transcriptional states. *Proceedings of the National Academy of Sciences*, 201517972. http://doi.org/10.1073/pnas.1517972112

Felsenfeld, G. (1992). Chromatin as an essential part of the transcriptional mechanim. *Nature*, *355*(6357), 219–224. http://doi.org/10.1038/355219a0

Fraser, P., & Grosveld, F. (1998). Locus control regions, chromatin activation and

transcription. *Current Opinion in Cell Biology*, *10*(3), 361–5. http://doi.org/S0955-0674(98)80012-4 [pii]

Garside, P., Ingulli, E., Merica, R. R., Johnson, J. C., Noelle, R. J., & Jenkins, M. K. (1998). Visualization of Specific B and T Lymphocyte lnteracti ~ ns in the Lymph Node. *Science*, *281*, 96–99. http://doi.org/10.1126/science.281.5373.96

Gitlin, A. D., Shulman, Z., & Nussenzweig, M. C. (2014). Clonal selection in the germinal centre by regulated proliferation and hypermutation. *Nature*, *509*(7502), 637–640. http://doi.org/10.1038/nature13300

Grosveld, F., van Assendelft, G. B., Greaves, D. R., & Kollias, G. (1987). Position-independent, high-level expression of the human β-globin gene in transgenic mice. *Cell*, *51*(6), 975–985. http://doi.org/10.1016/0092-8674(87)90584-8

Hauser, J., Grundström, C., & Grundström, T. (2014). Allelic exclusion of IgH through inhibition of E2A in a VDJ recombination complex. *Journal of Immunology (Baltimore, Md. : 1950)*, *192*(5), 2460–70. http://doi.org/10.4049/jimmunol.1302216

Heintzman, N. D., Hon, G. C., Hawkins, R. D., Kheradpour, P., Stark, A., Harp, L. F., … Ren, B. (2009). Histone modifications at human enhancers reflect global cell-type-specific gene expression. *Nature*, *459*(7243), 108–112. http://doi.org/10.1038/nature07829

Jacob, J., Kassir, R., & Kelsoe, G. (1991). In situ studies of the primary immune response to (4-hydroxy-3-nitrophenyl)acetyl. I. The architecture and dynamics of responding cell populations. *The Journal of Experimental Medicine*, *173*(5), 1165–75. http://doi.org/10.1084/jem.176.3.679

Jung, D., & Alt, F. W. (2004). Unraveling V(D)J recombination: Insights into gene regulation. *Cell*, *116*, 299–311.

LeBien, T. (2000). Fates of human B-cell precursors. *Blood*, *96*(1), 9–23. Retrieved

from http://bloodjournal.hematologylibrary.org/content/96/1/9.short

Lieberman-aiden, E., Berkum, N. L. Van, Williams, L., Imakaev, M., Ragoczy, T., Telling, A., … Mirny, L. A. (2009). Comprehensive Mapping of Long-Range Interactions Revelas Folding Principles of the Human Genome. *Science (New York, N.Y.)*, *326*(October), 289–294. http://doi.org/10.1126/science.1181369

Loder, F., Mutschler, B., Ray, R. J., Paige, C. J., Sideras, P., Torres, R., … Carsetti, R. (1999). B cell development in the spleen takes place in discrete steps and is determined by the quality of B cell receptor-derived signals. *The Journal of Experimental Medicine*, *190*(1), 75–89. http://doi.org/10.1084/jem.190.1.75

Maston, G. a., Landt, S. G., Snyder, M., & Green, M. R. (2012). *Characterization of Enhancer Function from Genome-Wide Analyses*. *Annual Review of Genomics and Human Genetics* (Vol. 13). http://doi.org/10.1146/annurev-genom-090711-163723

Matsuda, F., Ishii, K., Bourvagnet, P., Kuma, K. I., Hayashida, H., Miyata, T., & Honjo, T. (1998). The complete nucleotide sequence of the human immunoglobulin heavy chain variable region locus. *The Journal of Experimental Medicine*, *188*(11), 2151–62. Retrieved from http://www.pubmedcentral.nih.gov/articlerender.fcgi?artid=2212390&tool=pmcentrez&rendertype=abstract

McBlane, J. F., van Gent, D. C., Ramsden, D. A., Romeo, C., Cuomo, C. A., Gellert, M., & Oettinger, M. A. (1995). Cleavage at a V(D)J recombination signal requires only RAG1 and RAG2 proteins and occurs in two steps. *Cell*, *83*(3), 387–395. http://doi.org/10.1016/0092-8674(95)90116-7

Meyer-Hermann, M. E., Maini, P. K., & Iber, D. (2006). An analysis of B cell selection mechanisms in germinal centers. *Mathematical Medicine and Biology : A Journal of the IMA*, *23*(3), 255–77. http://doi.org/10.1093/imammb/dql012

Mullen, A. C., Orlando, D. A., Newman, J. J., Lovén, J., Kumar, R. M., Bilodeau, S., … Young, R. A. (2011). Master transcription factors determine cell-type-specific responses to TGF-β signaling. *Cell*, *147*(3), 565–576. http://doi.org/10.1016/j.cell.2011.08.050

Muramatsu, M., Kinoshita, K., Fagarasan, S., Yamada, S., Shinkai, Y., & Honjo, T. (2000). Class Switch Recombination and Hypermutation Require Activation-Induced Cytidine Deaminase (AID), a Potential RNA Editing Enzyme. *Cell*, *102*(5), 553–563. http://doi.org/10.1016/S0092-8674(00)00078-7

Murphy, K. (2011). *Janeway's Immunobiology* (8th ed.). New York: Garland Science. Retrieved from http://books.google.com/books?hl=en&lr=&id=WDMmAgAAQBAJ&oi=fnd&pg=PP1&dq=Janeway's+Immunobiology&ots=xYtJOT9BHM&sig=MwJtmEAAz223F7u48cq9fppIcSQ

Namen, A. E., Lupton, S., Hjerrild, K., Wignall, J., Mochizuki, D. Y., Schmierer, A., … Goodwin, R. G. (1988). Stimulation of B-cell progenitors by cloned murine interleukin-7. *Nature*, *333*(6173), 571–573. http://doi.org/10.1038/333571a0

Natoli, G. (2010). Maintaining cell identity through global control of genomic organization. *Immunity*. http://doi.org/10.1016/j.immuni.2010.07.006

Nieuwenhuis, P., & Opstelten, D. (1984). Functional anatomy of germinal centers. *The American Journal of Anatomy*, *170*(3), 421–35. http://doi.org/10.1002/aja.1001700315

Noguchi, M., Yi, H., Rosenblatt, H. M., Filipovich, A. H., Adelstein, S., Modi, W. S., … Leonard, W. J. (1993). Interleukin-2 receptor γ chain mutation results in X-linked severe combined immunodeficiency in humans. *Cell*, *73*(1), 147–157. http://doi.org/10.1016/0092-8674(93)90167-O

Nuñez, C., Nishimoto, N., Gartland, G. L., Billips, L. G., Burrows, P. D., Kubagawa,

H., & Cooper, M. D. (1996). B cells are generated throughout life in humans. *Journal of Immunology (Baltimore, Md. : 1950)*, *156*(2), 866–872.

Ohno, S. (1979). *Major Sex-Determining Genes*. Berlin: Springer-Verlag.

Okada, T., Miller, M. J., Parker, I., Krummel, M. F., Neighbors, M., Hartley, S. B., … Cyster, J. G. (2005). Antigen-engaged B cells undergo chemotaxis toward the T zone and form motile conjugates with helper T cells. *PLoS Biology*, *3*(6), 1047–1061. http://doi.org/10.1371/journal.pbio.0030150

Pancer, Z., & Cooper, M. D. (2006). THE EVOLUTION OF ADAPTIVE IMMUNITY. *Annual Review of Immunology*, *24*(1), 497–518. http://doi.org/10.1146/annurev.immunol.24.021605.090542

Parra, D., Takizawa, F., & Sunyer, J. O. (2013). Evolution of B Cell Immunity. *Annual Review of Animal Biosciences*, *1*(1), 65–97. http://doi.org/10.1146/annurev-animal-031412-103651

Phan, R., Saito, M., Basso, K., Niu, H., & Dalla-Favera, R. (2005). BCL6 interacts with the transcription factor Miz-1 to suppress the cyclin-dependent kinase inhibitor {…}. *Nature Immunology*. Retrieved from http://www.nature.com/ni/journal/vaop/ncurrent/full/ni1245.html

Phan, R. T., & Dalla-Favera, R. (2004). The BCL6 proto-oncogene suppresses p53 expression in germinal-centre B cells. *Nature*, *432*(7017), 635–639. http://doi.org/10.1038/nature03147

Pillai, S., & Cariappa, A. (2009). The follicular versus marginal zone B lymphocyte cell fate decision. *Nature Reviews Immunology*. http://doi.org/10.1038/nri2656

Prieyl, J. a, & LeBien, T. W. (1996). Interleukin 7 independent development of human B cells. *Proceedings of the National Academy of Sciences of the United States of America*, *93*(19), 10348–53. http://doi.org/10.1073/pnas.93.19.10348

Puel, A., Ziegler, S. F., Buckley, R. H., & Leonard, W. J. (1998). Defective IL7R

expression in T-B+NK+ severe combined immunodeficiency. *Nature Genetics*, *20*(4), 394–397. http://doi.org/10.1038/3877

Ranuncolo, S. M., Polo, J. M., Dierov, J., Singer, M., Kuo, T., Greally, J., … Melnick, A. (2007). Bcl-6 mediates the germinal center B cell phenotype and lymphomagenesis through transcriptional repression of the DNA-damage sensor ATR. *Nature Immunology*, *8*(7), 705–714. http://doi.org/10.1038/ni1478

Ranuncolo, S. M., Polo, J. M., & Melnick, A. (2008). BCL6 represses CHEK1 and suppresses DNA damage pathways in normal and malignant B-cells. *Blood Cells, Molecules, and Diseases*, *41*(1), 95–99. http://doi.org/10.1016/j.bcmd.2008.02.003

Rodda, L. B., Bannard, O., Ludewig, B., Nagasawa, T., & Cyster, J. G. (2015). Phenotypic and Morphological Properties of Germinal Center Dark Zone *Cxcl12* -Expressing Reticular Cells. *The Journal of Immunology*, *195*(10), 4781–4791. http://doi.org/10.4049/jimmunol.1501191

Saito, M., Novak, U., Piovan, E., Basso, K., Sumazin, P., Schneider, C., … Dalla-Favera, R. (2009). BCL6 suppression of BCL2 via Miz1 and its disruption in diffuse large B cell lymphoma. *Proceedings of the National Academy of Sciences*, *106*(27), 11294–11299. http://doi.org/10.1073/pnas.0903854106

Sanyal, A., Lajoie, B. R., Jain, G., & Dekker, J. (2012). The long-range interaction landscape of gene promoters. *Nature*, *489*(7414), 109–113. http://doi.org/10.1038/nature11279

Schwickert, T. A., Lindquist, R. L., Shakhar, G., Livshits, G., Skokos, D., Kosco-Vilbois, M. H., … Nussenzweig, M. C. (2007). In vivo imaging of germinal centres reveals a dynamic open structure. *Nature*, *446*(7131), 83–87. http://doi.org/10.1038/nature05573

Sexton, T., & Cavalli, G. (2015). The role of chromosome domains in shaping the

functional genome. *Cell*, *160*(6), 1049–1059. http://doi.org/10.1016/j.cell.2015.02.040

Sexton, T., Yaffe, E., Kenigsberg, E., Bantignies, F., Leblanc, B., Hoichman, M., … Cavalli, G. (2012). Three-dimensional folding and functional organization principles of the Drosophila genome. *Cell*. http://doi.org/10.1016/j.cell.2012.01.010

spicuglia, salvatore, & Vanhille, L. (2012, March). Chromatin signatures of active enhancers. *Nucleus*. http://doi.org/10.4161/nucl.19232

Spitz, F., & Furlong, E. E. M. (2012). Transcription factors: from enhancer binding to developmental control. *Nature Reviews Genetics*, *13*(June), 613–626. http://doi.org/10.1038/nrg3207

Tonegawa, S. (1983). Somatic generation of antibody diversity. *Nature*. Retrieved from http://www.nature.com/nature/journal/v302/n5909/abs/302575a0.html

Tunyaplin, C., Shaffer, A. L., Angelin-Duclos, C. D., Yu, X., Staudt, L. M., & Calame, K. L. (2004). Direct Repression of prdm1 by Bcl-6 Inhibits Plasmacytic Differentiation. *The Journal of Immunology*, *173*(2), 1158–1165. http://doi.org/10.4049/jimmunol.173.2.1158

Van Gent, D. C., Ramsden, D. A., & Gellert, M. (1996). The RAG1 and RAG2 proteins establish the 12/23 rule in V(D)J recombination. *Cell*, *85*(1), 107–113. http://doi.org/10.1016/S0092-8674(00)81086-7

Vermi, W., Lonardi, S., Bosisio, D., Uguccioni, M., Danelon, G., Pileri, S., … Facchetti, F. (2008). Identification of CXCL13 as a new marker for follicular dendritic cell sarcoma. *J Pathol*. http://doi.org/10.1002/path.2420

Victora, G. D., Schwickert, T. A., Fooksman, D. R., Kamphorst, A. O., Meyer-Hermann, M., Dustin, M. L., & Nussenzweig, M. C. (2010). Germinal center dynamics revealed by multiphoton microscopy with a photoactivatable

fluorescent reporter. *Cell*, *143*(4), 592–605. http://doi.org/10.1016/j.cell.2010.10.032

Vietri Rudan, M., Barrington, C., Henderson, S., Ernst, C., Odom, D. T., Tanay, A., & Hadjur, S. (2015). Comparative Hi-C Reveals that CTCF Underlies Evolution of Chromosomal Domain Architecture. *Cell Reports*, *10*(8), 1297–1309. http://doi.org/10.1016/j.celrep.2015.02.004

Weisel, F. J., Zuccarino-Catania, G. V., Chikina, M., & Shlomchik, M. J. (2016). A Temporal Switch in the Germinal Center Determines Differential Output of Memory B and Plasma Cells. *Immunity*, *44*(1), 116–130. http://doi.org/10.1016/j.immuni.2015.12.004

Whyte, W. a., Orlando, D. a., Hnisz, D., Abraham, B. J., Lin, C. Y., Kagey, M. H., … Young, R. a. (2013). Master transcription factors and mediator establish super-enhancers at key cell identity genes. *Cell*, *153*(2), 307–319. http://doi.org/10.1016/j.cell.2013.03.035

Ye BH, Lista F, Lo Coco F, Knowles DM, Offit K, Chaganti RS, D.-F. R., Ye, B., Lista, F., Lo Coco, F., Knowles, D., Offit, K., … Dalla-Favera, R. (1993). Alterations of a zinc finger-encoding gene, BCL-6, in diffuse large-cell lymphoma. *Science*, *262*(5134), 747–750. http://doi.org/10.1126/science.8235596

Yue, F., Cheng, Y., Breschi, A., Vierstra, J., Wu, W., Ryba, T., … Consortium, T. M. E. (2014). A comparative encyclopedia of DNA elements in the mouse genome. *Nature*, *515*(7527), 355–364. Retrieved from http://dx.doi.org/10.1038/nature13992

Zhou, V. W., Goren, A., & Bernstein, B. E. (2011). Charting histone modifications and the functional organization of mammalian genomes. *Nature Reviews Genetics*. http://doi.org/10.1038/nrg2905

Chapter 3-Generation of the LCR KO Mice

3.1 Introduction

With an expanding trove of information about the state of enhancer clusters in human GCBs and DLBCL derived cell lines, we became curious about their role in GC physiology. Specifically, we hypothesized that the set of enhancers upstream of *Bcl6* making extensive physical interactions with the *Bcl6* promoter and other gene loci (*on chromosome 3 in human GCBs compared to NBs*) collectively qualify them as a putative Locus Control Region. By definition this implies that this putative LCR is involved in the regulation of Bcl6 expression and other genes vital for the formation of GCBs. We predicted that this LCR should be functionally conserved between human and murine GCBs i.e. while DNA sequence similarities may not be pronounced in a way that would permit straight forward elucidation of conserved regulatory mechanisms, the syntenic region should have open chromatin and enrichment of H3K27Ac marks in GCBs when compared to NBs. To assess the role of the LCR in GC formation, we decided to generate a knockout mouse model of the LCR. Coincidentally, the details of this endeavour were being discussed right around the time when the seminal papers on CRISPR-Cas9 system for genome editing had been published.

CRISPR, which refers to clustered regularly interspaced palindromic repeats, were first identified (though not named as such) by Japanese researchers in 1987 as short direct repeats in Escherichia coli (Ishino et al.). Over the next two decades, bioinformaticians and microbiologists determined that these sequences represent a the basis of an adaptive immune system in bacteria and the sequences themselves act as encoded memory of previous viral infections (Makarova et al.; Horvath and

Barrangou). In the mid 2000's, new information about CRISPR associated (Cas) genes encoding proteins that possessed DNA modifying—nuclease and helicase motifs (Pourcel et al.; Jansen et al.; Haft et al.). The advances in the field starting coming in fast and type II CRISPR-Cas was shown to cut targeted DNA (Garneau et al.), and in 2012 it was shown that Cas9 is an RNA directed endonuclease (Jinek, Chylinski, et al.). Within 6 months, a series of three papers showed that CRISPR-Cas9 can be utilized to edit DNA in human cells (Cong et al.; Jinek, East, et al.; Mali et al.). What has followed has been an incredible explosion of studies utilizing this system with far reaching possibilities for the future of biomedical research and gene therapies for personalized medicine.

Soon thereafter, The Zhang lab published a CRISPR method that could be utilized to alter multiple genes via sgRNA in 'one shot' (Wang et al.). We utilized the published method to target the LCR in mice after identifying a ~166 Kb locus syntenic to the previously described LCR in humans.

By definition, Locus Control Regions enhance the expression of linked genes in a tissue-specific fashion. The linked genes can be on the same or separate chromosomes, and it is hypothesized that the increased expression of these genes correlates with a the requirements of said tissue for development or differentiation purposes (Fraser and Grosveld; Li et al.). The putative murine *BCL6* LCR—chr16:24,119,037-24,285,604 *mm10*—is about 130 Kb upstream of the *Bcl6* transcription start site and is enriched for H3K27Ac marks (Figure 3.1) in GC derived B-cells (these cells are from tumors in the spleens from vavP-BCL2 mice which are GCB like cells. H3K27Ac called peaks from MINT ChIP in WT murine NB and GCB are shown in the UCSC browser tracks (Figure 3.2).

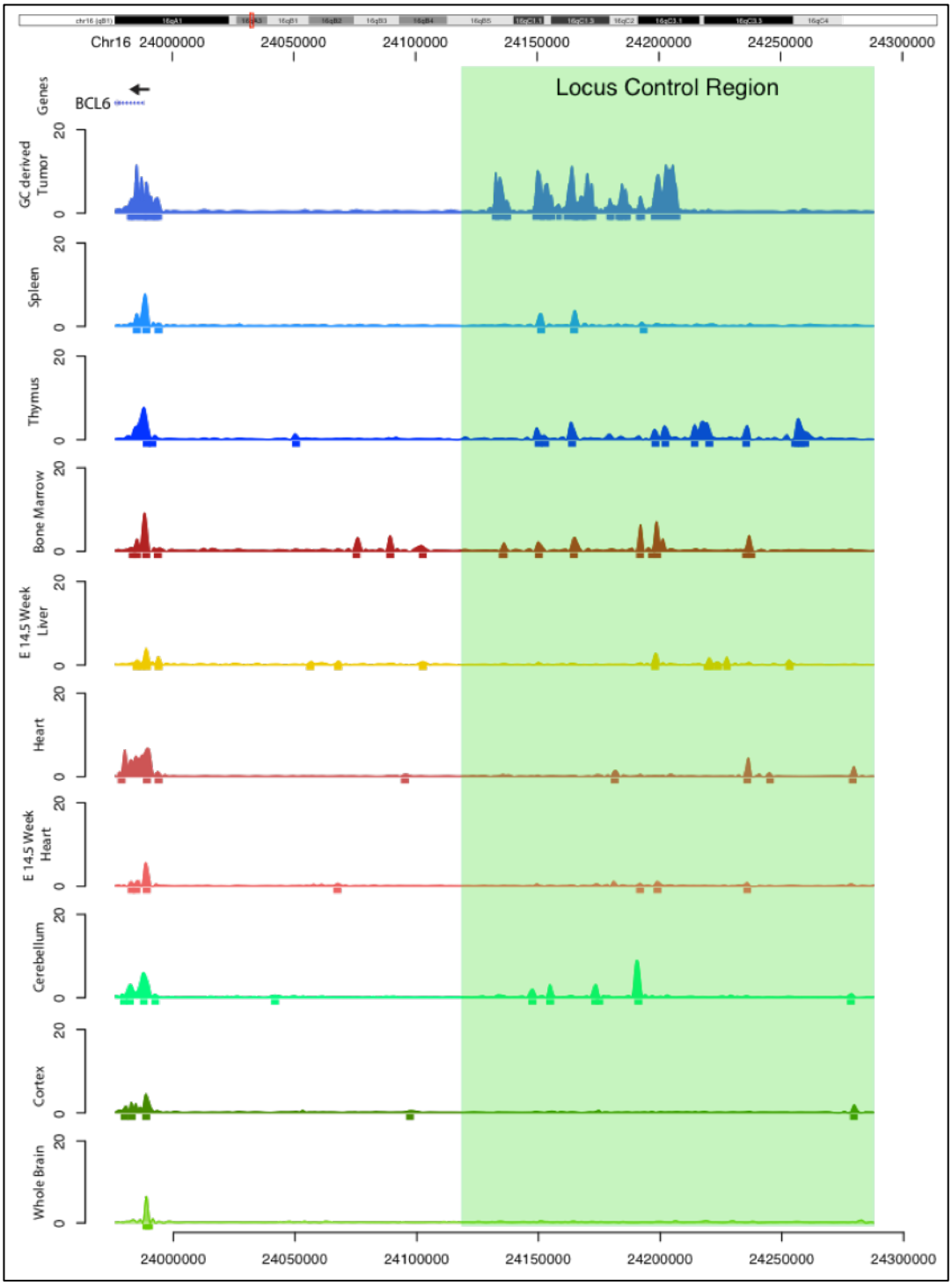

Figure 3.1 Tracks for H3K27Ac read densities (top) normalized to input for murine tissues including GC-derived malignant B-cells and other BCL6-expressing tissues. The region shaded in green represents the syntenic LCR targeted for CRISPR mediated deletion.

Figure 3.1 also shows tracks for H3K27Ac reads in various other murine tissues available through ENCODE (Yue et al.). These tissues include whole spleen, thymus, bone marrow, embryonic day 14.5 liver, adult heart, embryonic day 14.5 heart, cerebellum, cortex and whole brain. The region shaded in green denotes the LCR, and from the H3K27ac read densities, it was postulated that the LCR must be specifically involved in regulating the expression of genes in GCB as it is the cell type with the most enrichment. While there is some enrichment of the acetylation mark in other tissues—in the thymus, bone marrow and cerebellum—it is not as wide spread and the enrichment is not comparable to GCB.

Figure 3.2 shows H3K27Ac peaks along with read densities from ATAC-seq (Assay for Transposase-Accessible Chromatin using sequencing) in WT murine NB and GCB. ATAC-seq is a relatively recent technique that can reveal regions of open chromatin and can be used to reliably evaluate nucleosome repositioning at loci between stages of differentiation. A benefit of using this technique over other modalities like DNase hypersensitivity is that ATAC allows a view into chromatin accessibility with relatively few cells whereas other techniques require millions of cells for adequate processing material. When comparing murine NB (blue track) to GCB (black track), it becomes obvious that there is a profound increase in chromatin accessibility in GCBs which can be further studied to evaluate transcription factor and chromatin modifier binding sites.

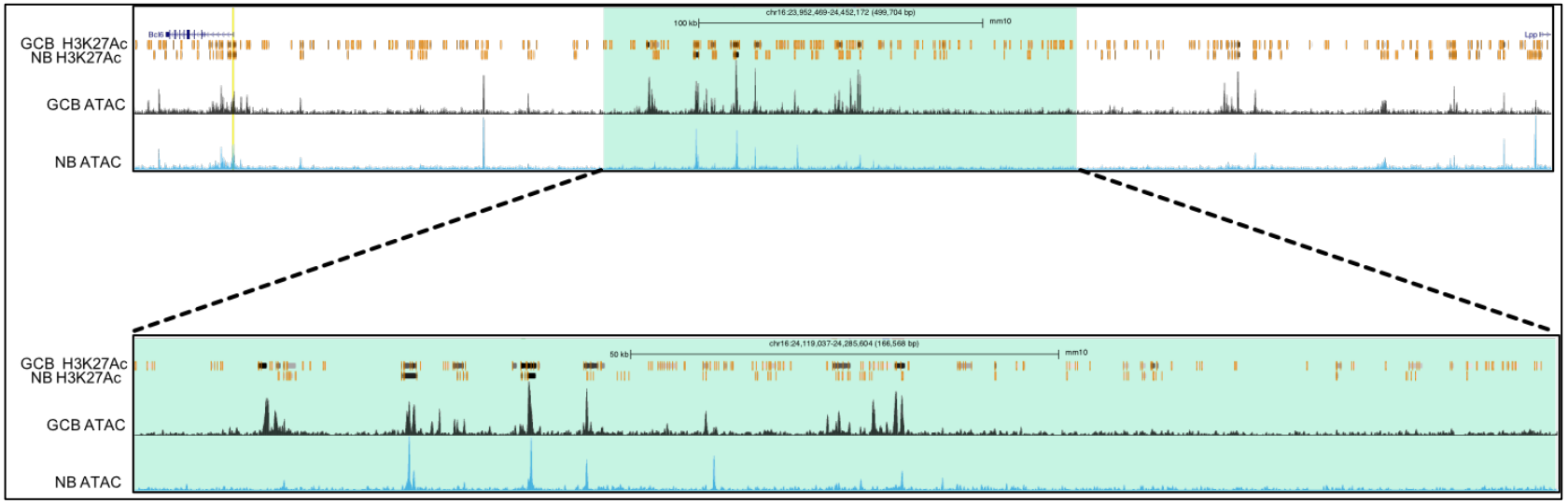

Figure 3.2 UCSC browser tracks from the mouse genome assembly mm10 depicting called peaks for H3K27Ac-MINT ChIP and read densities for ATAC-seq in murine NB and GCB.

A quick glance at ATAC tracks leads to a reasonable argument that specific transcription factor binding sites should be targeted via CRISPR to study their effect on gene regulation from within the LCR. While this is sound reasoning, we chose to target the entire enhancer cluster (LCR) as a preliminary step to determine if there was a physiological role for the region. If the deletion leads to a phenotype it would be a reasonable second step to proceed in that direction.

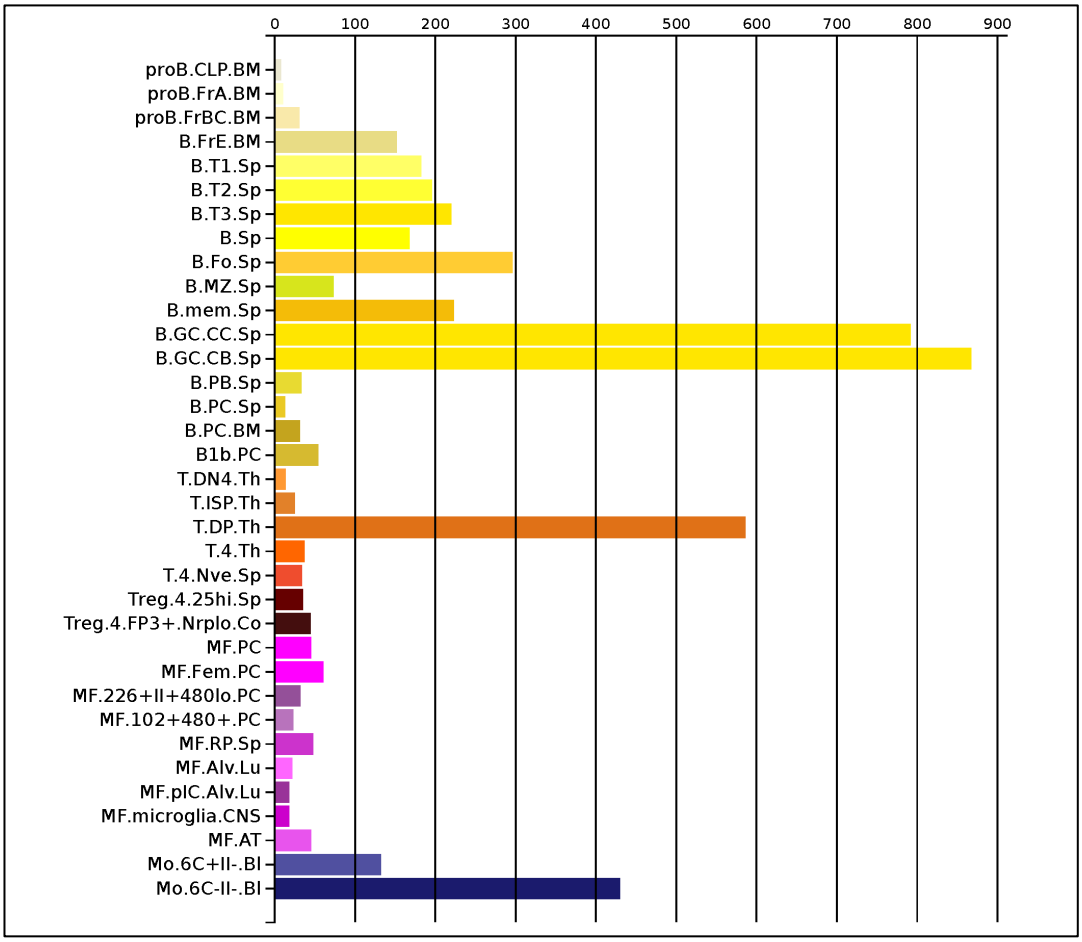

Figure 3.3 Bcl6 gene expression values in B-cell, T-Cell, Macrophage and Monocytes obtained through RNA-seq of sorted murine cells. Data from the Immunological Genome Project. Expression values are normalized by DESeq2.

As we hypothesized that the role of the LCR in primarily regulating BCL6 expression it is of pertinence to assess expression in other cells/tissues known to require BCL6. These include T-follicular helper cells, cortical neurons, monocytes, and other B-cells in early stages of differentiation (pro B-cells) (Tiberi et al.; Dent et al.). Publically available RNA-seq from the *Immunological Genome Project* shows some of the cell types of interest within immune compartments (Figure 3.3) (Heng and Painter).

3.2 Results

The schematic in figure 3.4 provides the stepwise workflow for the generation of the LCR KO mice once the sgRNAs required to target the LCR had been transcribed in-vivo. The guides were picked by utilizing the 'guide RNA design tool' available at crispr.mit.edu (Hsu et al.). Oligos encoding the sgRNA sequence are

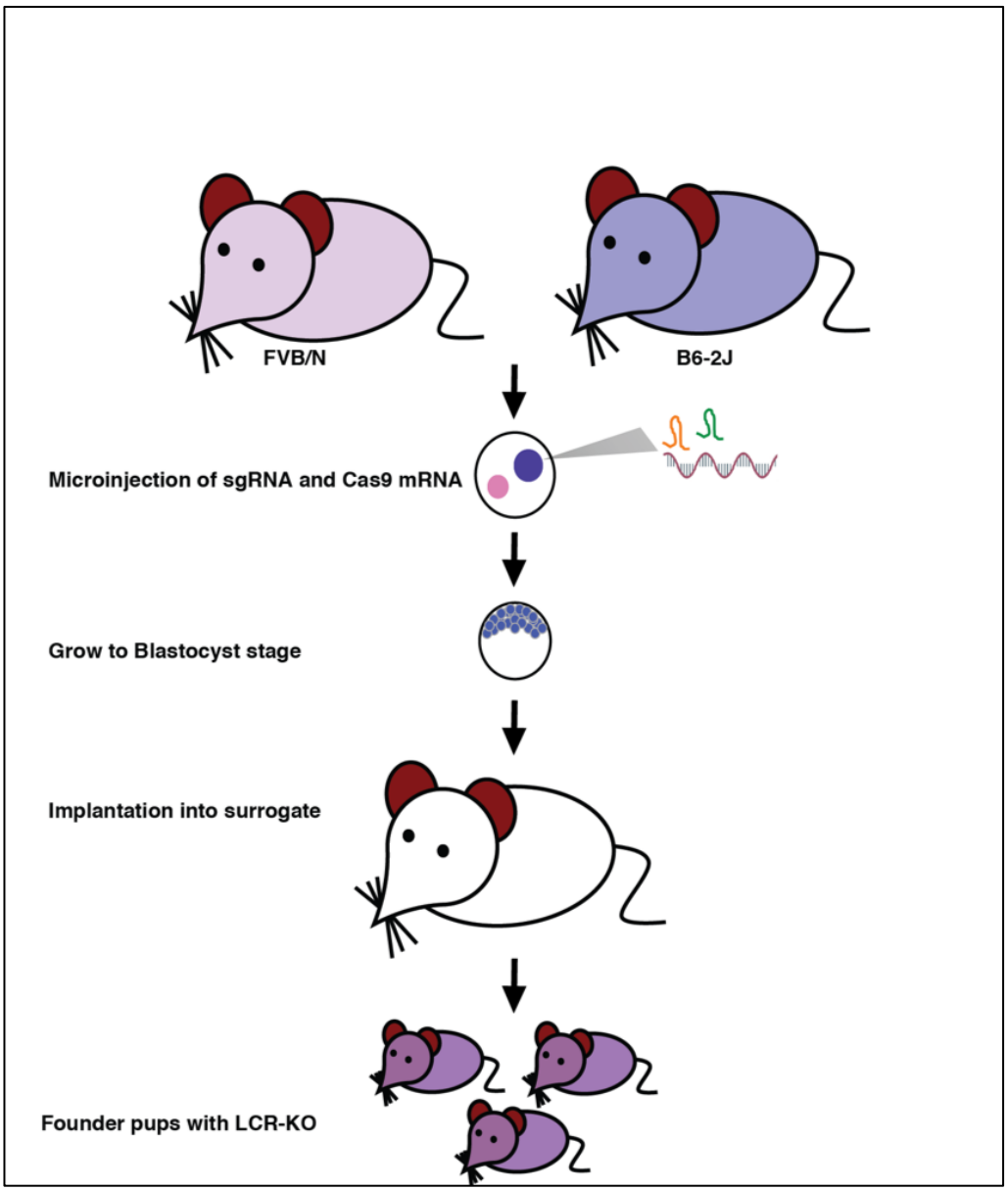

Figure 3.4 Schematic showing the steps involved in the generation of the LCR KO mouse.

annealed and then cloned into the pX330-U6-Chimeric_BB-CBh-hSpCas9 plasmid (Cong et al.) with the sgRNA backbone. The cloned plasmid was then used for a PCR amplification to introduce the T7 promoter at the 5' end of and sgRNA constructs. The PCR amplified product was subsequently used as template DNA for in-vitro transcription with the Ambion MEGAshortscript T7 transcription kit. Initial IVT attempts yielded extremely low RNA concentrations which was eventually attributed to low level of RNase contamination. When the IVT was performed with 'RNase-out', the RNA concentration was enough for embryonic microinjections. The concentrations obtained for each attempt are listed in table 3.1. RNA concentration was measured with the qubit.

Table 3.1 IVT sgRNA concentrations

Attempt #	mCr_BCL6enh_Tg1_1	mCr_BCL6enh_Tg3_2	Elution volume (ul)
Without RNase-out.			
1	20 ng/ul	18 ng/ul	25
2	26.8 ng/ul	19.1 ng/ul	25
3	23 ng/ul	1o ng/ul	20
With RNase-out.			
4	253 ng/ul	184 ng/ul	25

The RNA was shipped on dry-ice to the Stem Cell and Transgenics Core at Cornell University, Ithaca, NY. At the core, the two sgRNAs were combined with Cas9 mRNA and microinjected into mouse zygotes obtained from crosses between FVB/2J and C57BL/6 mice (of 10 donor mice, 6 had vaginal plugs within 24 hours when the zygotes were harvested). 117, one cell embryos were injected of which 81 reached the

two-cell stage. These 81 were eventually transplanted into four pseudo-pregnant mice. 20 days post implantation, 15 pups were born between the four pregnant mice. Clipped toe tissue from 7-day old pups were shipped back for genotyping.

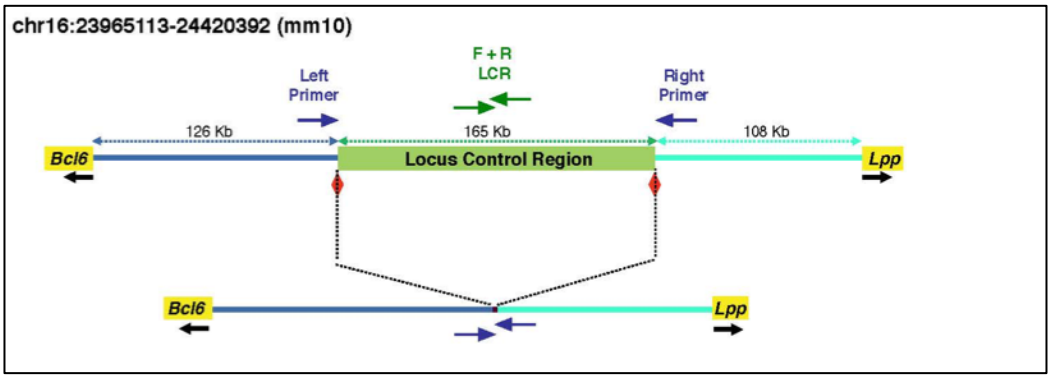

Figure 3.5 Schematic of the putative BCL6 LCR in mice before and after CRISPR mediated deletion. Dotted lines show approximate distances between gene loci. The blue and green arrows represent primer pair used to genotype the founder mice.

The genotyping strategy employed for the mice is described in the schematic in figure 3.5. A deletion of the LCR would result in a PCR product of 70bp (For_Tg1_1 + Rev_Tg3_2 primer pairs) as shown in the gel image (Figure 3.6). An intact LCR acts as a template for a 172bp PCR product (For_LCR1_1 + Rev_LCR1_1). On genotyping the 15 tails, we discovered that four of the pups had the deletion product and therefore would be candidates for further breeding. To confirm the deletion, we gel purified the deletion product and cloned it into a TOPO vector and sanger sequenced the product. Indeed, the product was not only the expected size but the sequence analysis matched that of the flanking loci at the 5' and 3' of the sgRNA binding sites (Figure 3.7)

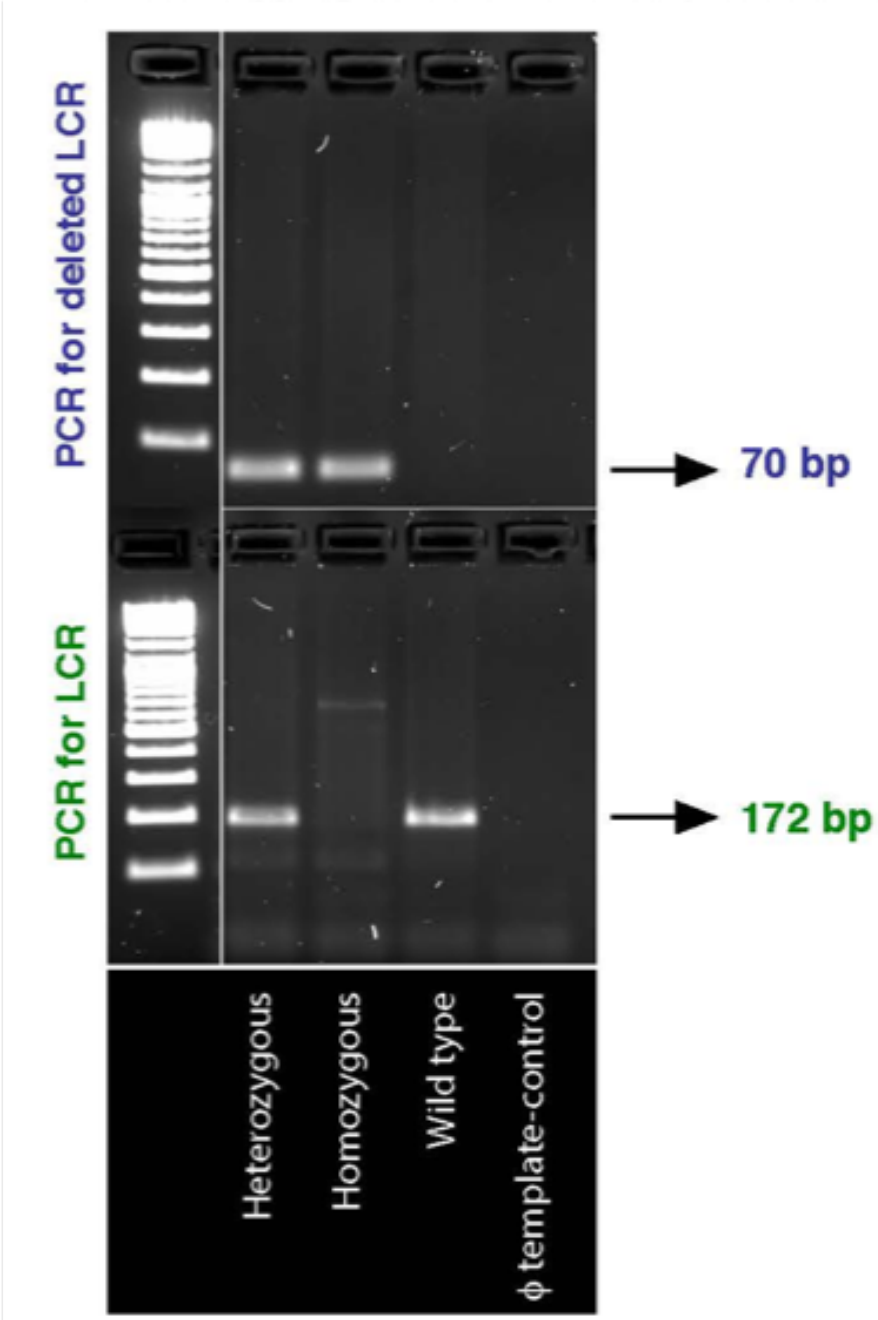

Figure 3.6 Agarose gel with PCR product bands for the two genotyping primer pairs: Primer pair for For_Tg1_1 + Rev_Tg3_2 → 70bp product if LCR is deleted. For_LCR1_1 + Rev_LCR1_1 → 172bp product even if one copy of the LCR is present in the genome.

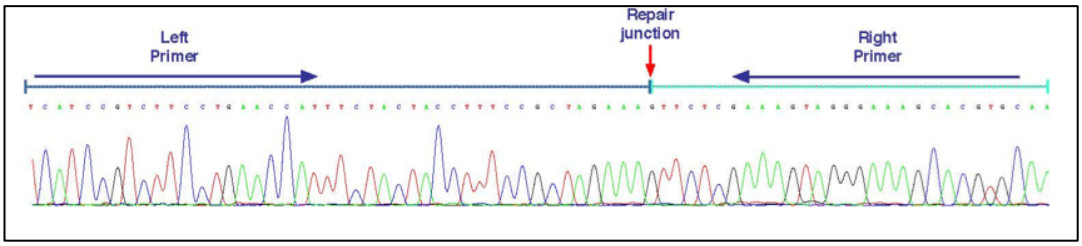

Figure 3.7 Sequencing results from repair junction in LCR KO mouse.

The blue arrows in figure 3.7 denote the loci where the PCR primers bind whereas the red vertical arrow points at the junction where the post deletion repair occurred. While indel formations are frequently reported when non-homologous-end-joining mechanisms repair DNA breaks post CRISPR-Cas9 mediated deletion. However, in the mice, remarkably, there was no indels formed. This observation led to some skepticism. While the sequencing results were definitive, I decided to perform another test to confirm if the deletion of the LCR was complete and proper. This was achieved through a TaqMan Assay which is a qPCR based genotyping method. Taqman probes were ordered and the loci tey bound are depicted in figure 3.8.

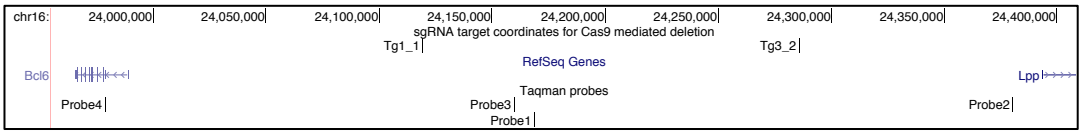

Figure 3.8 Loci where the 4 different TaqMan probes bind in the mouse genome. Probe#1 and Probe#3 bind within the LCR. Probe#2 binds outside the LCR proximal to *Lpp*. Probe#4 binds within the gene body of *Bcl6*.

The assay results are shown in figure 3.9, and they confirmed an interesting and predictable outcome. While the deletion was true, it was chimeric, i.e. not every cell in the mouse had the deletion. The purported reason for this is that the deletion process mediated via CRISPR does not occur at the one cell stage (zygote). Instead, as the cells grow ex-vivo into a blastocyst pre-impantation. Some of the cells may escape the deletion due to a number of reasons including insufficient distribution of the Cas9

mRNA or the sgRNA itself. When the embryos with the deletion continue to develop the distribution of the deletion becomes patchy and leads to a chimera. This is reflected in figure 3.9 as the copy number for the LCR is a non-integer. This meant that for a constitutive homozygous deletion of the LCR in the mouse, we would have to back cross the pups to WT C57BL/6 and monitor litter genotypes to select the pups with first, a heterozygous deletion and subsequently after crossing the heterozygous mice, monitor for homozygous deletions. This is exactly the strategy we employed to obtain mice for phenotyping purposes.

Another notable observation is that not all four pups seemed to have the deletion. Only three of the four were chimeras whereas 'founder pup #7' had no copy-number alteration compared to the WT control mouse. The appearance of a deletion product in the PCR performed for founder pup #7 was most likely due to contamination. This further highlighted the importance of employing orthogonal techniques to confirm deletions when utilizing CRISPR-Cas9 for genome editing. The three founders were maintained as separate LCR KO lines in the animal facility. This proved to be an important step as each line could be treated as an independent biological control and any observed phenotype would be considered valid if all three lines exhibited the same defect. The backcrossing of the mice to WT C57BL/6 was important to obtain constitutive heterozygous mice that could be used for further breeding but it also proved important to dilute out any off-target effects that might have resulted from non-specific binding of the sgRNA. Every successive generation bred with a WT mouse would theoretically remove 50% of the off-target effects and therefore mice separated by 6 generations from the founder can be assumed to exhibit phenotypes that are attributable to the deletion and no other genomic lesion.

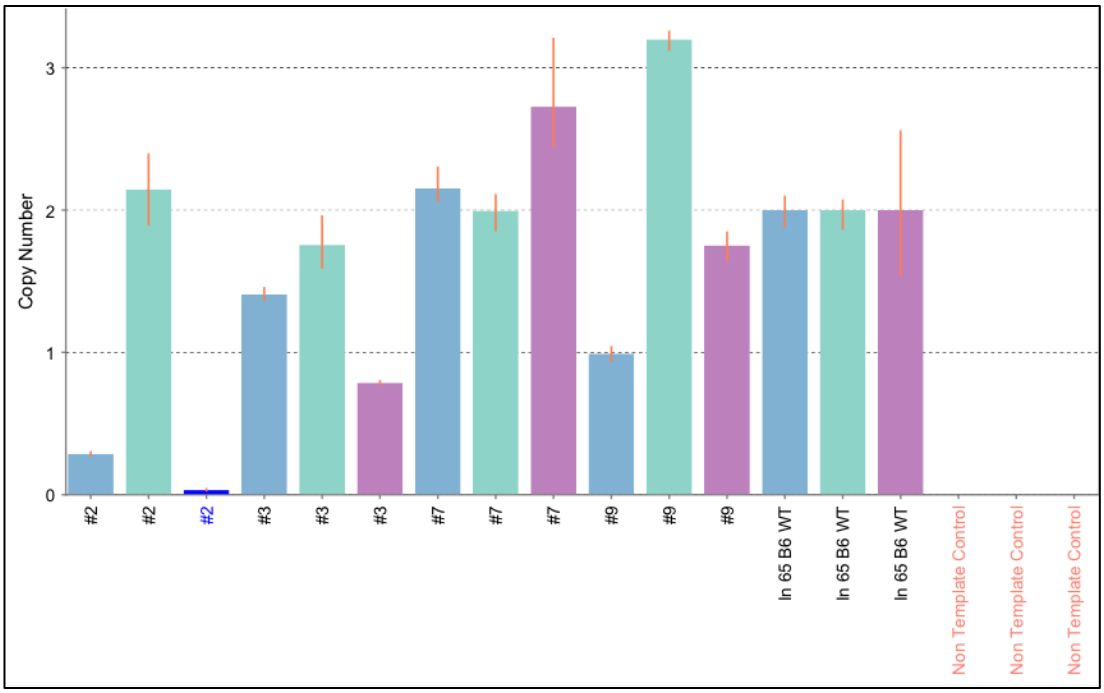

Figure 3.9 Analysis of the TaqMan Copy number qPCR performed on the founder mice using the Applied Biosystems CopyCaller® software v2.0. Error bars represent technical replicates. Pink is Probe#1 (for LCR), Blue is Probe#3 (for LCR) and Green is Probe#4 (for Bcl6). The analysis shows that founder#7 was most likely WT. The other three founders (#2, #3 and #9) were chimeras for the LCR deletion. The third bar from the left for founder pup #2 is highlighted and is therefore labeled dark blue.

While the mice were eventually utilized to assess GC formation post SRBC immunization, the original mouse line for the founders created a problem that needed to be addressed for the purpose of mixed bone marrow chimera experiments. Usually, such experiments utilize two variants of CD45—CD45.1 and CD45.2. However, the embryos utilized for the microinjection of sgRNAs and Cas9 mRNA were from FVB/NJ and B6(Cg)-Tyr$^{c\text{-}26}$/J mice. The crossing of these two mice provides zygotes which are larger than C57BL/6 zygotes and makes microinjections easier. However, the cross also results in the mixing of the two CD45 variants. This limited our ability to use these markers to differentiate mixed bone marrows. However, once we became

of this problem we utilized GFP expressing mice for those experiments. The phenotyping of the mice and the subsequent experiments based on the new observations are described in detail in chapter 4.

3.3 Materials and Methods

3.3.1 Generation of LCR KO mouse via CRISPR

3.3.1-1 *Designing and Cloning guides into pX330-U6-Chimeric_BB-CBh-hSpCas9 plasmid*

Guide RNA sequences targeting the regions flanking the 166Kb LCR in mice were selected with the CRISPR design tool at http://crispr.mit.edu/. Complementary oligos were ordered from integrated DNA technologies, annealed and cloned into the BbsI restriction enzyme digestion site of the pX330-U6-Chimeric_BB-CBh-hSpCas9 plasmid. The steps are described in further detail below.

Annealing oligos

2 µL oligo 1 (100µM) , 2 µL oligo 2 (100µM) , 4 µL 5X T4 Ligation Buffer (NEB), and 12 µL ddH_2O are added per tube. The tubes are incubated at 95 degree C for 3 minutes and subsequently cooled down at room temperature for 1 hour.

BbsI digestion of pX330

2µL (1 µg) of pX330, 1 µL of NEB BbsI enzyme, 5 µL of 10X NE buffer 2.1, and 42 µL of ddH_2O for a total of 50µL per reaction. Plasmid is digested at 37 degree C for 30 minutes. The digested plasmid is gel purified using the QIAquick gel extraction kit.

Ligation

50 ng of digested pX330, 1 μL of *annealed* oligo duplex (diluted 1:250), 5μL of 2X Quick ligation Buffer (NEB), and x μL of ddH_2O are added (x is the volume to bring the reaction to 10 μL. Then add 1 μL of Quick Ligase for a final total volume of 11ul. Ligation is performed at room temperature for 15 minutes.

Transformation

Competent DH5-α cells are used for transformation with the ligated pX330 plasmids. 150ul of 0.1M Calcium Chloride (sterile conditions, use flame) is added to a tube of DH5-α cells. The competent cells are split into four 1.5 ml eppendorf tubes kept on ice. 2.5μl of ligation reaction (~12.5ng of DNA) is added to 50ul of competent cells. Tubes are gently flicked and incubated on ice for 30 minutes. The cells are then heat shocked at 42 degree C for 30 seconds. Tubes are placed back on ice for 10 minutes. Transfer the competent cells to 250ul of S.O.C. media (without antibiotics). Incubate with shaking at 37 degree C for 1 hour. After incubation plate the cells on a carbenicillin plate, and incubate overnight at 37 degree C.

PCR amplification (and addition of T7 promoter)

The two primers ordered for each amplification are as follows:

Primer 1 (T7-target R#_For): This is specific to our sgRNA but has the T7 promoter sequence (TTAATACGACTCACTATAG) at the 5' end followed by the CACC (for the BbsI site) followed the by the sequence for the guide RNA target (GN_{20}). The sequences of these oligos are listed in table 3.2

Primer 2: A universal primer (T7-sgR Rev) specific for the pX330 plasmid: AAAAGCACCGACTCGGTGCC.

Setup multiple PCR reactions (~5) for sufficient amount of amplified product.

PCR conditions:

Component	**Per reaction**	**Volume for 5 reactions (X 6)**
Water	22.6 μL	135.6 μL
~20ng plasmid DNA	1 μL	6 μL
10X buffer	3 μL	18 μL
25mM dNTP	0.3 μL	1.8 μL
Primer 1 (10 μM)	1.5 μL	9 μL
Primer 2 (10 μM)	1.5 μL	9 μL
Taq polymerase	0.1 μL	0.6 μL
Total Volume	30 μL	180 μL

Thermocycler setup:

Step 1-1 Cycle at 95 degree C for 1 minute.

Step 2-30 cycles of [95 degree C for 30 seconds, (Primer Tm-5 degree C) for 30 seconds, 72 degree C for 1 minute]

Step 3-1 Cycle at 72 degree C for 10 minutes.

Qiagen PCR cleanup kit is used to purify the amplified product.

Table 3.2 Single guide RNA sequences, and primer sequences used for cloning into the pX330 plasmid.

Name	**Sequence (5' to 3')**	**Purpose**
mCr_BCL6enh_Tg1_1F	CACCGATTTTTGTGAGTACGGATT	CRISPR oligo for cloning in pX330
mCr_BCL6enh_Tg1_1R	AAACAATCCGTACTCACAAAAATC	CRISPR oligo for cloning in pX330
mCr_BCL6enh_Tg3_2F	CACCGTGTCAGCGACTCATAAGTTA	CRISPR oligo for cloning in pX330
mCr_BCL6enh_Tg3_2R	AAACTAACTTATGAGTCGCTGACAC	CRISPR oligo for cloning in pX330
TgSpBCL6enh_Tg1_1	TTAATACGACTCACTATAGCACCGATTTTTGTGAGTACGGATT	Forward primer for amplification of template for IVT of left sgRNA
TgSpBCL6enh_Tg3_2	TTAATACGACTCACTATAGCACCGTGTCAGCGACTCATAAGTTA	Forward primer for amplification of template for IVT of left sgRNA
T7-sgR_Rev	AAAAGCACCGACTCGGTGCC	Reverse primer for amplification of template for IVT of both sgRNA

3.3.1-2 *In Vitro transcription and purification of short guiding chimeric RNA*

The kit used for IVT is the Ambion MEGAshortscript T7 Transcription kit (Life Technologies). The T7 10X Reaction Buffer, the four ribonucleotide solutions, and Water are thawed at room temperature. Briefly vortex the T7 10X Reaction Buffer and ribonucleotide solutions. Microfuge all reagents briefly before opening to prevent loss and/or contamination of material that may be present around the rim of the tube. Keep the T7 Enzyme Mix on ice during assembly of the reaction.

Use an RNase-free microfuge tube at room temperature in the order below. For convenience, all four nucleotides are premixed; added 8 μL of the mixture to a standard 20 μL reaction instead of adding the ribonucleotides separately.

Component	**Amount**
Water (Nuclease Free)	To bring final volume to 20 μL
T7 UTP solution	2 μL
T7 ATP solution	2 μL
T7 CTP solution	2 μL
T7 GTP solution	2 μL
T7 10X reaction Buffer	2 μL
Template DNA	1 μg in less than or equal to 8 μL
T7 Enzyme mix	2 μL

The volumes above are for a single 20 μL reaction. Reactions maybe scaled as needed. Components in the transcription buffer can lead to precipitation of the template DNA if the reaction is assembled on ice.

The reaction contents are mixed thoroughly by gently flicking the tube, and then microfuged briefly to collect the reaction mixture at the bottom of the tube. Samples are incubated at 37°C for 4 hours. Once IVT is complete, added1 μL of TURBO DNase and incubate at 37°C for 15 min

Termination of the Reaction and RNA Recovery

The degree of purification required after the transcription reaction depends on the downstream application of the transcribed RNA. We used the Ambion MEGAclear kit (Life Technologies) for purity compatible with zygotic injections.

The MEGAclear™ Kit (Ambion P/N AM1908) is a glass filter-based system for purification RNA transcripts (>100 nt) from salts, free nucleotides, and enzymes in an easy 15-minute procedure that requires no organic solvents. The steps involved in purification were as follows: We brought the RNA sample to 100 μL with elution solution. Mixed gently but thoroughly. Added 350 μL of binding solution concentrate to the sample. Mixed gently by pipetting. Then added 250 μL of 100% ethanol to the sample. Mixed gently with pipette. Applied the sample to the filter. The filter cartridge is inserted into one of the collection and elution tubes supplied. Pipetted the RNA mixture onto the filter cartridge. Centrifuged for ~15 seconds to 1 min, or until the mixture has passed through the filter at 10,000–15,000 × g. The flow through is discarded, and the collection and elution tube is reused for the washing steps. Washed with 2 × 500 μL wash solution (with added ethanol) and centrifuging again at 10,000g for 30 seconds each time. Centrifuge one last time after discarding the wash solution

after the second wash. Elute RNA as follows: First pre-heated 110 μL of elution solution per sample to 95° C. Apply 50 μL of the pre-heated elution solution to the center of the filter cartridge, close the cap of the tube and centrifuge for 1 min at room temperature (RCF 10,000–15,000 x g) to elute the RNA.

3.3.1-3 *Embryonic microinjections of sgRNA*

The embryonic microinjection of the sgRNA pair flanking the LCR along with Cas9 mRNA was in F1 hybrid zygotes from FVB/NJ and B6(Cg)-Tyr^{c-26}/J mice. The microinjections were performed as described by Singh et al (1) at the Cornell core facility in Ithaca, NY. 81 of the 117 one-cell embryos progressed to the two-cell stage and were transferred into 4 pseudo-pregnant mice (Figure 3.4). A total of 15 pups were born from the resulting pregnancy.

3.3.2 Genotyping mice

Genomic DNA was isolated from the 15 pups (and all subsequent pups from breeding LCR +/- and -/- mice) using the method described here. Proteinase K (10mg/ml) is added to the reagent (Viagen directPCR (tail) lysis reagent Cat#102-T) to a final conc. Of 0.5 mg/ml. Added 275ul of reagent (with 0.5mg/ml of Proteinase K) to each tube with tail tissue. Placed tube on thermo-mixer set at 700rpm and 55 degree C. Incubate tubes 4-16 hours. Next day, raise the temperature of the thermo-mixer to 95 degree C and incubate the tubes for an additional 45 minutes with shaking at 300rpm. Centrifuge tubes at 5000 rpm for 3 minutes. Transfer 200 μl of the supernatant (hair and other debris will be in the pellet) to new 1.5 ml eppendorf tubes Add 12.5 μl of 4M NaCl to bring the final concentration of the sample to 250 mM NaCl. Then add 0.7 volumes of Isopropanol to each tube and centrifuge the sample on bench-top centrifuge for 1 hour at 16000g (16 degree C). Carefully remove supernatant. Wash the DNA pellet by adding 1 ml of 70% ethanol to each tube and

then centrifuging for 30 minutes at 16000g. Again, carefully remove the supernatant. Allow the samples air-dry for 5 minutes and then add 50uL of nuclease free water to each sample. Gently tap the tubes to mix the sample and measure the DNA concentration on a nanodrop.

Deletion of the LCR was confirmed by the presence of a PCR product from a primer pair that flanked the LCR (Forward primer: For_Tg1_1_q: CATCCGTCTTCCTGAACCAT; Reverse primer: Rev_Tg3_2_q: GCACGTGCTTTCCCTACTTT) (Figure 3.5). Additionally, the deletion of LCR was confirmed with a primer pair complementary to a region within the deleted LCR (Forward primer: For_LCR1_1_q: GCTTGTGGACTTGCATCTCA; Reverse primer: Rev_LCR1_1_q: TGTGGGTCTGTGTGTGAACAT). PCR with these primers revealed 3 of the 15 pups to have a deletion (Figure 3.6).

The LCR deletion was further confirmed with a TaqMan copy number assay using probes for the deleted region (*Assay ID: Mm00451576_Cn, Chr16: 24159427-*Probe#3 and *Assay ID: Mm00451574_Cn, Chr16:24168442*-Probe#1). Another probe (Probe#4) specific for the BCL6 locus (*Assay ID: Mm00445402_Cn, Chr16: 23978604*) was used as a control. Copy number assay results revealed the founders to be chimeras for the deletion instead of pure knockouts. (Figure 3.8 and 3.9).

The founder mice were crossed with wildtype C57BL/6 mice. PCR products from the resulting pups along with that from the founder mice were cloned into the pcr Blunt-II TOPO vector and sequenced using the M13R primer (CAGGAAACAGCTATGAC) by Genewiz DNA sequencing services. The sequencing confirmed the presence of the deletion (Figure 3.7).

Chapter 3 References

Cong, Le, et al. "Multiplex Genome Engineering Using CRISPR/Cas Systems." *Science (New York, N.Y.)*, vol. 339, no. 6121, Feb. 2013, pp. 819–23, doi:10.1126/science.1231143.

Dent, A. L., et al. "Control of Inflammation, Cytokine Expression, and Germinal Center Formation by BCL-6." *Science*, vol. 276, no. 5312, 1997, pp. 589–92, doi:10.1126/science.276.5312.589.

Fraser, P., and F. Grosveld. "Locus Control Regions, Chromatin Activation and Transcription." *Current Opinion in Cell Biology*, vol. 10, no. 3, 1998, pp. 361–65, doi:S0955-0674(98)80012-4 [pii].

Garneau, Josiane E., et al. "The CRISPR/cas Bacterial Immune System Cleaves Bacteriophage and Plasmid DNA." *Nature*, vol. 468, no. 7320, 2010, pp. 67–71, doi:10.1038/nature09523.

Haft, Daniel H., et al. "A Guild of 45 CRISPR-Associated (Cas) Protein Families and Multiple CRISPR/cas Subtypes Exist in Prokaryotic Genomes." *PLoS Computational Biology*, vol. 1, no. 6, 2005, pp. 0474–83, doi:10.1371 /journal.pcbi.0010060.

Heng, T. S., and M. W. Painter. "The Immunological Genome Project: Networks of Gene Expression in Immune Cells." *Nature Immunology*, vol. 9, no. 10, 2008, pp. 1091–94, doi:10.1038/ni1008-1091.

Horvath, Philippe, and Rodolphe Barrangou. "CRISPR/Cas, the Immune System of Bacteria and Archaea." *Science (New York, N.Y.)*, vol. 327, no. 5962, Jan. 2010, pp. 167–70, doi:10.1126/science.1179555.

Hsu, Patrick D., et al. "DNA Targeting Specificity of RNA-Guided Cas9 Nucleases." *Nature Biotechnology*, vol. 31, no. 9, 2013, pp. 827–32, doi:10.1038/nbt.2647.

Ishino, Y., et al. "Nucleotide Sequence of the Iap Gene, Responsible for Alkaline

Phosphatase Isozyme Conversion in Escherichia Coli, and Identification of the Gene Product." *Journal of Bacteriology*, vol. 169, no. 12, 1987, pp. 5429–33, doi:10.1128/jb.169.12.5429-5433.1987.

Jansen, Ruud., et al. "Identification of Genes That Are Associated with DNA Repeats in Prokaryotes." *Molecular Microbiology*, vol. 43, no. 6, 2002, pp. 1565–75, doi:10.1046/j.1365-2958.2002.02839.x.

Jinek, Martin, Krzysztof Chylinski, et al. "A Programmable Dual-RNA-Guided DNA Endonuclease in Adaptive Bacterial Immunity." *Science*, vol. 337, no. 6096, 2012, pp. 816–21, doi:10.1126/science.1225829.

Jinek, Martin, Alexandra East, et al. "RNA-Programmed Genome Editing in Human Cells." *eLife*, vol. 2013, no. 2, 2013, doi:10.7554/eLife.00471.

Li, Qiliang, et al. "Locus Control Regions." *Blood*, vol. 100, no. 9, 2002, pp. 3077–86, doi:10.1182/blood-2002-04-1104.

Makarova, KS Kira S., et al. "A Putative RNA-Interference-Based Immune System in Prokaryotes: Computational Analysis of the Predicted Enzymatic Machinery, Functional Analogies with Eukaryotic RNAi, and Hypothetical Mechanisms of Action." *Biology Direct*, vol. 1, no. 1, 2006, p. 7, doi:10.1186/1745-6150-1-7.

Mali, Prashant, et al. "RNA-Guided Human Genome Engineering via Cas9." *Science*, vol. 339, no. 6121, 2013, pp. 823–26, doi:10.1126/science.1232033.

Pourcel, C., et al. "CRISPR Elements in Yersinia Pestis Acquire New Repeats by Preferential Uptake of Bacteriophage DNA, and Provide Additional Tools for Evolutionary Studies." *Microbiology*, vol. 151, no. 3, 2005, pp. 653–63, doi:10.1099/mic.0.27437-0.

Tiberi, Luca, et al. "BCL6 Controls Neurogenesis through Sirt1-Dependent Epigenetic Repression of Selective Notch Targets." *Nature Neuroscience*, vol. 15, no. 12, 2012, pp. 1627–35, doi:10.1038/nn.3264.

Wang, Haoyi, et al. “One-Step Generation of Mice Carrying Mutations in Multiple Genes by CRISPR/Cas-Mediated Genome Engineering.” *Cell*, vol. 153, no. 4, Elsevier Inc., May 2013, pp. 910–18, doi:10.1016/j.cell.2013.04.025.

Yue, Feng, et al. “A Comparative Encyclopedia of DNA Elements in the Mouse Genome.” *Nature*, vol. 515, no. 7527, Nature Publishing Group, a division of Macmillan Publishers Limited. All Rights Reserved., Nov. 2014, pp. 355–64, http://dx.doi.org/10.1038/nature13992.

Chapter 4-Phenotypic Characterization of the LCR KO mice

4.1 Introduction

Previous studies on $Bcl6^{-/-}$ mice have revealed a number of pathologies in mice (Dent et al.). In these mice, SRBC immunization—which is a gold standard method to assess T-cell dependent immune responses (Luster, Munson, et al.; Luster, Portier, et al.)—results in a complete loss of GC formation. Spleen sections also reveal eosinophilic infiltrations, the reason for which is not entirely clear. Hematoxylin and Eosin (H&E) staining of lung and heart reveals widespread inflammation (pulmonary vasculitis) and myocarditis. The knockout mice also have cellular infiltrates in these tissues which are composed of mononuclear cells and eosinophils. At approximately 3-weeks after birth, the $Bcl6^{-/-}$ mice start showing growth retardation compared to WT mice. Other studies have also revealed a critical role for BCL6 in neurogenesis (Tiberi et al.; Leamey et al.), and cortical neurons have been shown to express BCL6 at high levels in mice.

Since we hypothesized the LCR to be regulating BCL6 expression, we used the phenotype of $BCL6^{-/-}$ mice to guide our initial assessment of the LCR KO mice. Additionally, as the deletion is germline, it warranted analysis of all tissues where BCL6 might play a role.

After establishing three separate founder mice for the LCR deletion, we maintained the mice bred from each founder as separate colonies. This set up provided an opportunity to replicate the results of our analysis in a truly independent fashion. After back crossing the chimeric founders with WT C57BL/6 mice, we obtained mice with a single copy of the LCR (LCR hets), which were subsequently crossed to obtain

the $LCR^{-/-}$ mice. We obtained these mice at expected mendelian rations and no significant male:female bias was observed in any of the breedings in the three colonies. For controls, we used the WT littermates of the $LCR^{-/-}$ animals.

4.2 Results

4.2.1 LCR KO (-/-) mice have a specific and complete GC formation defect

For the pilot experiment, we used mice from founder #9. We immunized 10-11-week-old mice with SRBC (via intraperitoneal injections) and sacrificed them 10 days later to collect the spleens. We used 5 WT and 4 $LCR^{-/-}$ mice for this experiment. The processed splenocytes were stained with fluorophore conjugated antibodies to assess GCB, NB, centroblasts and centrocytes. The mice (pre-euthanasia) and the spleens (post-euthanasia) were also weighed. Flow cytometry revealed an almost complete loss of GCBs (B220+, FAS+, CD38**-,** DAPI-) in LCR deficient mice compared to WT mice (P value = 0.002, two tailed unpaired t-test) (Figure 4.1b). There were no statistically significant differences between WT and LCR KO when assessing total B-cell (B220+, DAPI-), marginal zone B-cell (B220+, CD21hi, CD23lo DAPI-), or follicular B-cell (B220+, CD21lo, CD23hi DAPI-) proportions (Figure 4.1a & c). Furthermore, there were no differences observed in overall mouse or spleen weights between the two groups (Figure 4.1d). This exciting result confirmed our hypothesis that the LCR was critical for GC physiology. However, the pilot experiment did not assess a number of other cellular compartments that might be of interest from an immunological perspective. To address those questions, we repeated the experiment with another founder colony (founder#3).

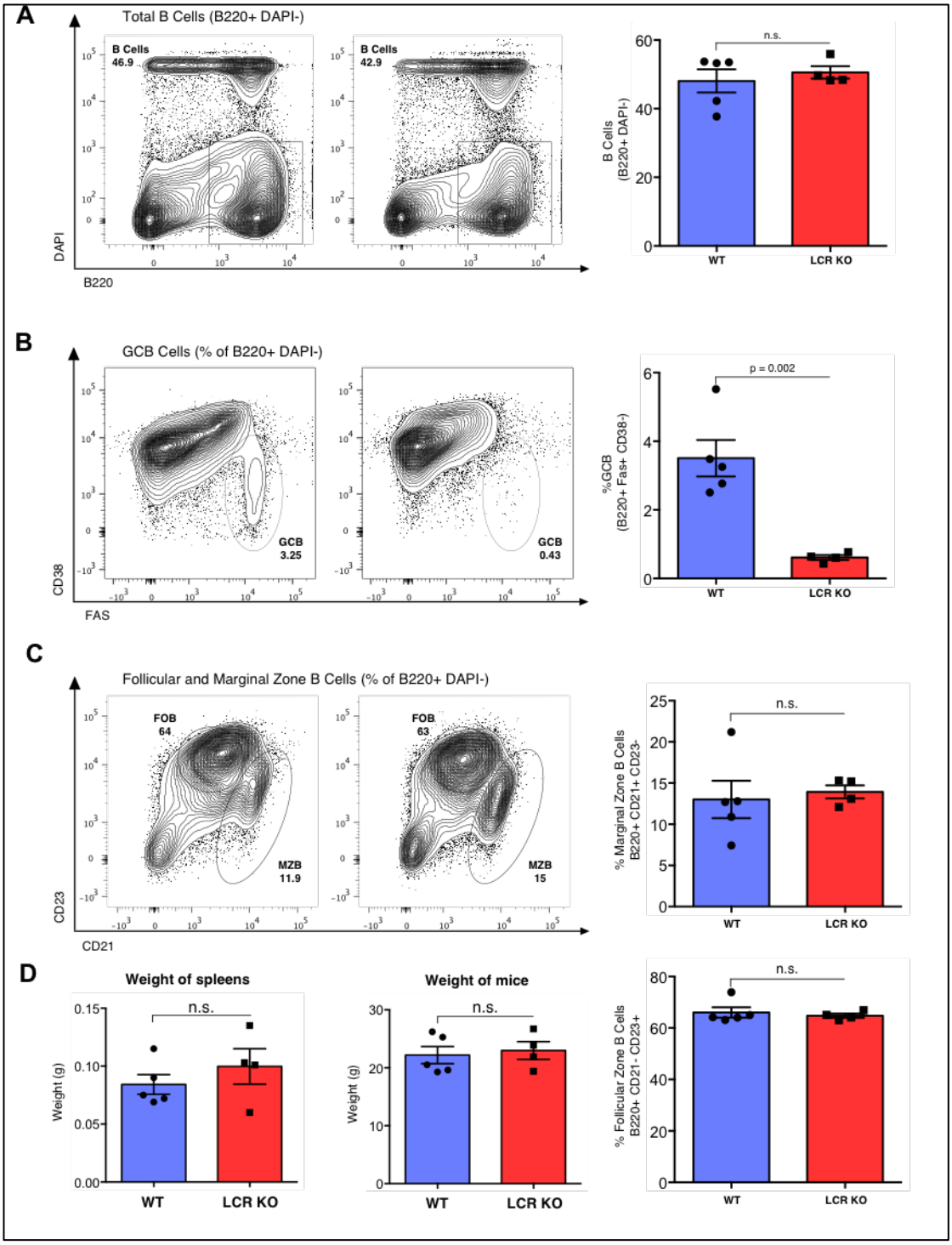

Figure 4.1 (A-C) Representative flow-cytometry plots along with bar plots quantifying splenic B-cells, splenic GCB and Follicular and Marginal Zone B-cells. (D) Bar plots representing the weights of the mice and the spleen.

The experiment was repeated with 5 LCR KO and 4 WT littermate control mice. The experiment was setup in the exact same manner as the pilot, with the animals being sacrificed 10 days post immunization with SRBC. All of the observations reported from the pilot experiment were successfully replicated. Flow cytometry again revealed the complete loss of GCBs (B220+, Fas+, CD38-, and DAPI-) in LCR deficient mice compared to WT mice (P value= 0.0254, two tailed unpaired t-test) (Figure 4.2b & f). We also stained the splenocytes with another antibody mix for GCBs (B220+, Fas+, GL7+ and DAPI-) and reached the same conclusion (P value = 0.0056, two tailed unpaired t-test) (Figure 4.3a & d). As observed earlier, there were no statistically significant differences between WT and LCR KO when assessing total B-cell (B220+, DAPI-), marginal zone B-cell (B220+, CD21hi, CD23lo DAPI-), or follicular B-cell (B220+, CD21lo, CD23hi DAPI-) proportions (Figure 4.2a, c, e, g & h). There were no differences observed in the overall mouse or spleen weights between the two groups (Figure 4.2d).

The additional stains for flow cytometry in the second experiment include those for T-cells and Monocytes. As was originally hypothesized, the LCR defect should be specific to GCBs, and in line with this idea, there were no differences observed in overall NB, Monocyte (Figure 4.3b, c, e & f) or T-cell proportions (n.d., two tailed unpaired t-test) (Figure 4.4).

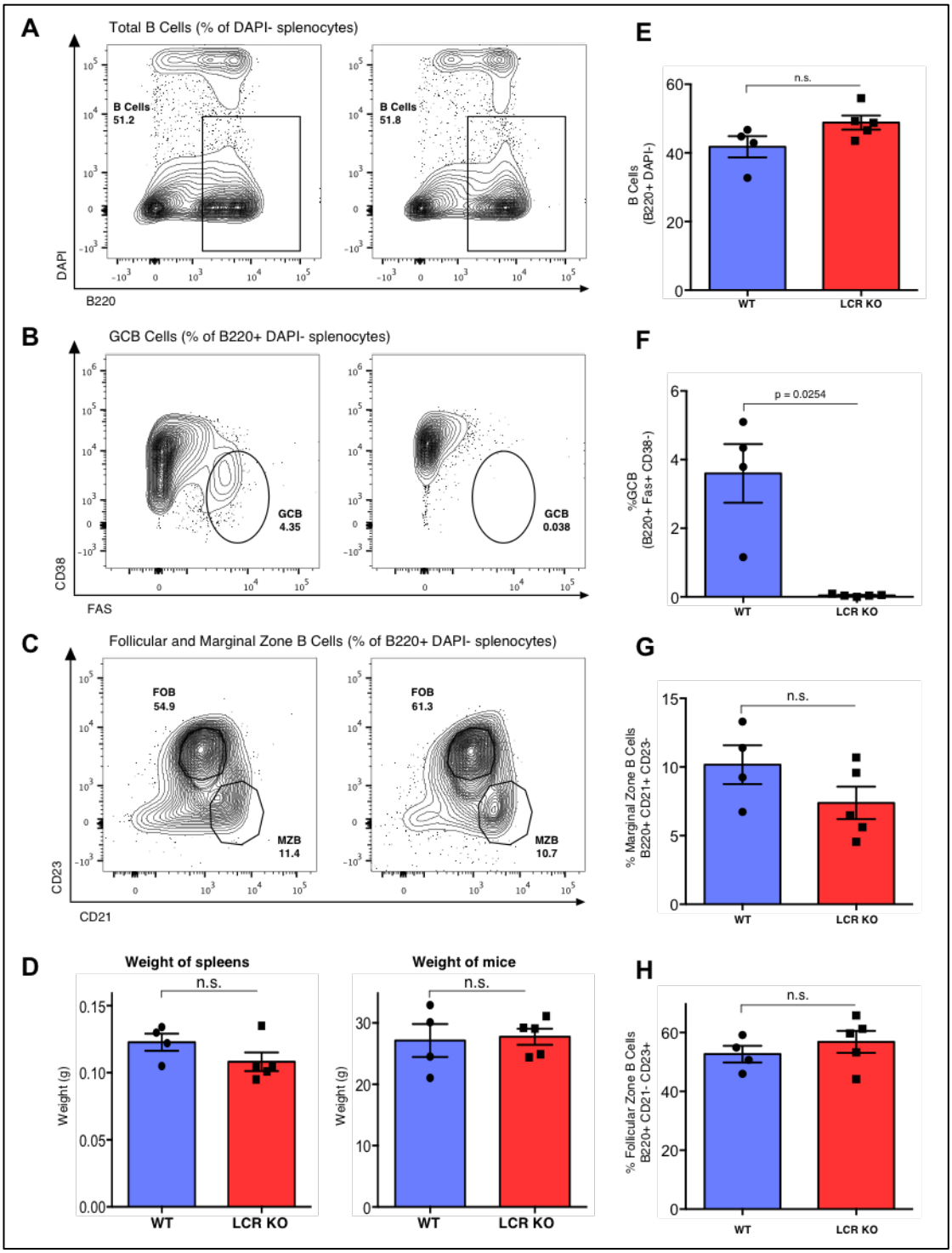

Figure 4.2 (A-C) Representative flow-cytometry plots for splenic B-cells, splenic GCBs and Follicular and Marginal Zone B-cells. (D) Bar plots representing the weights of the mice and the spleen. (E-H) Bar plots quantifying the splenic B-cells, GCBs, Marginal Zone B-cells and Follicular B-cells.

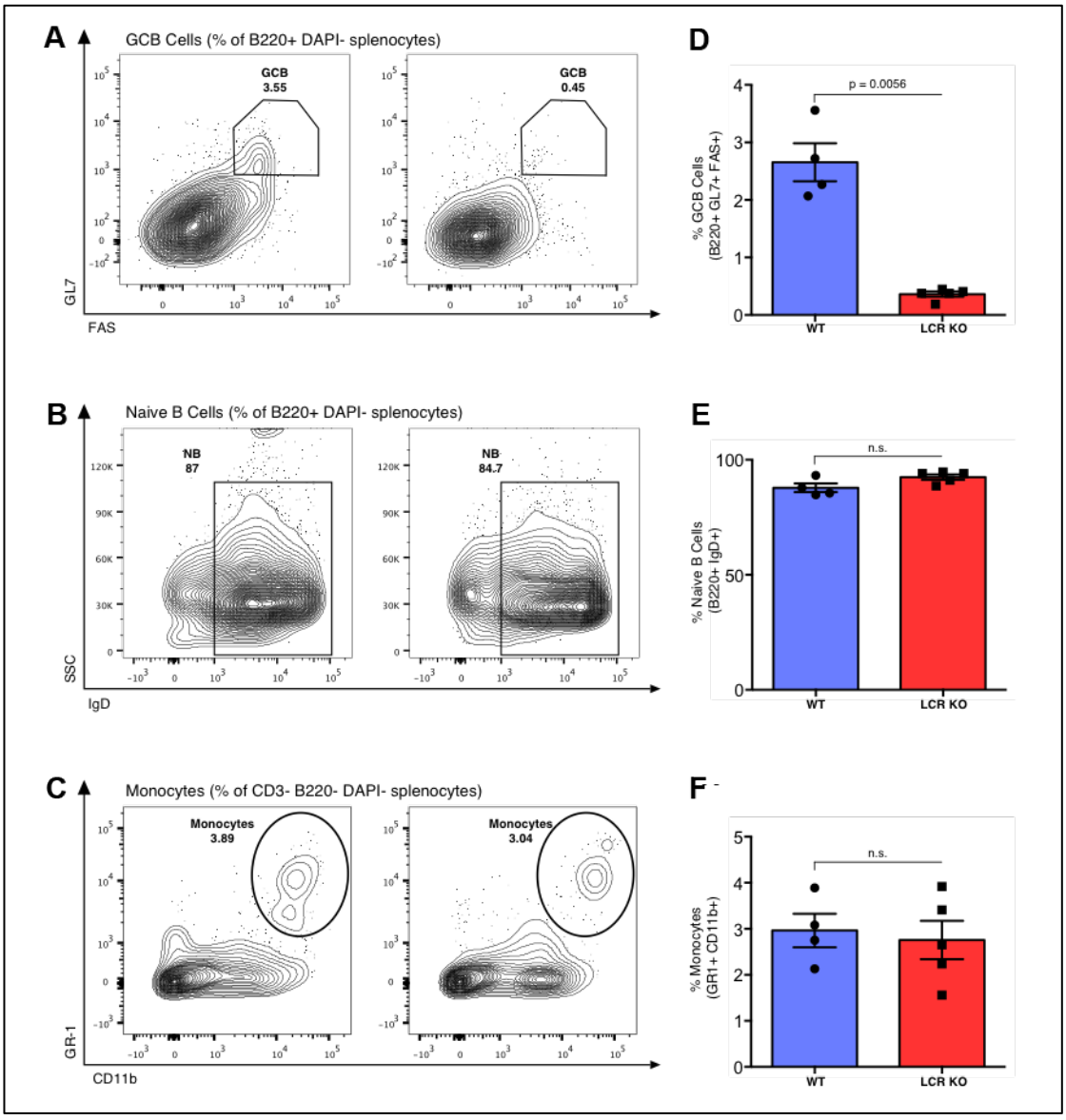

Figure 4.3 (A-C) Representative flow-cytometry plots for splenic GCBs (B220+, Fas+, GL7+ and DAPI-), Naïve B-cells and Monocytes. (D-F) Bar plots quantifying the splenic GCBs, Naive B-cells and Monocytes.

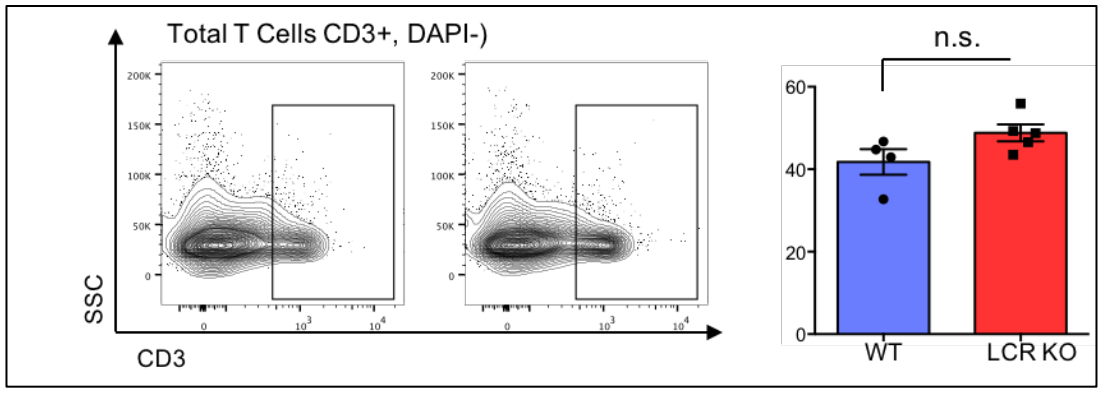

Figure 4.4 Representative flow-cytometry plot for total splenic T-cells along with bar plot quantifying the T-cells between the two groups. No significant difference is observed between LCR KO and WT mice.

In addition to the analysis of cell populations in the spleen via flow cytometry, we also analysed tissue sections via immunohistochemistry. Spleen sections were stained using peanut agglutinin (a GCB marker), BCL6, B220, H&E, Ki-67 and CD3 (Figure 4.6 & 4.7). Analysis of the PNA stained sections revealed the profound defect in the formation of GCs in the LCR deficient spleens compared to WT. We quantified the germinal centers in the PNA stained images and plotted the total area of GCs per unit area of the spleen, which reflected the differences seen in the flow cytometry data (P value = 0.0013, two-tailed, unpaired t test) (Figure 4.5).

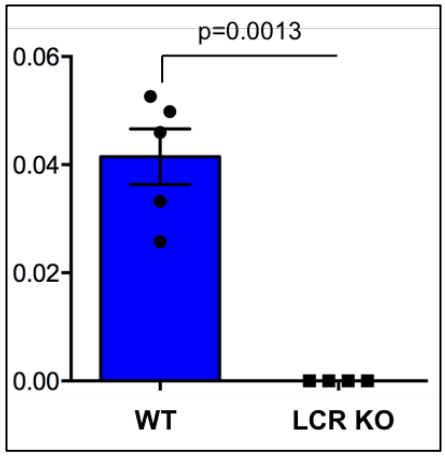

Figure 4.5 Bar plot representing the splenic area occupied by GCs based on PNA-IHC in WT versus LCR-deficient mice.

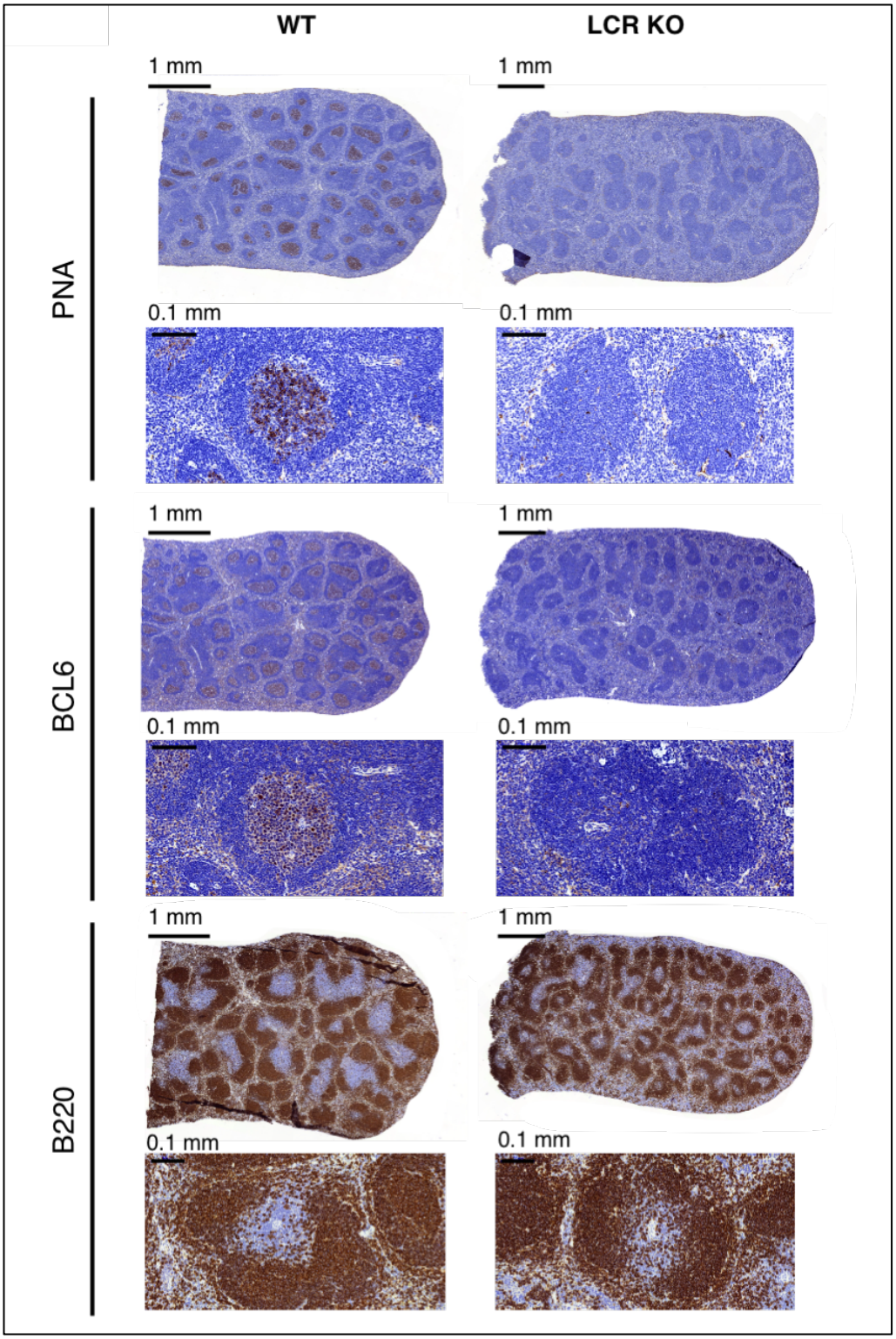

Figure 4.6 Immunohistochemistry images of WT and LCR KO mouse spleens stained for PNA, BCL6, and B220.

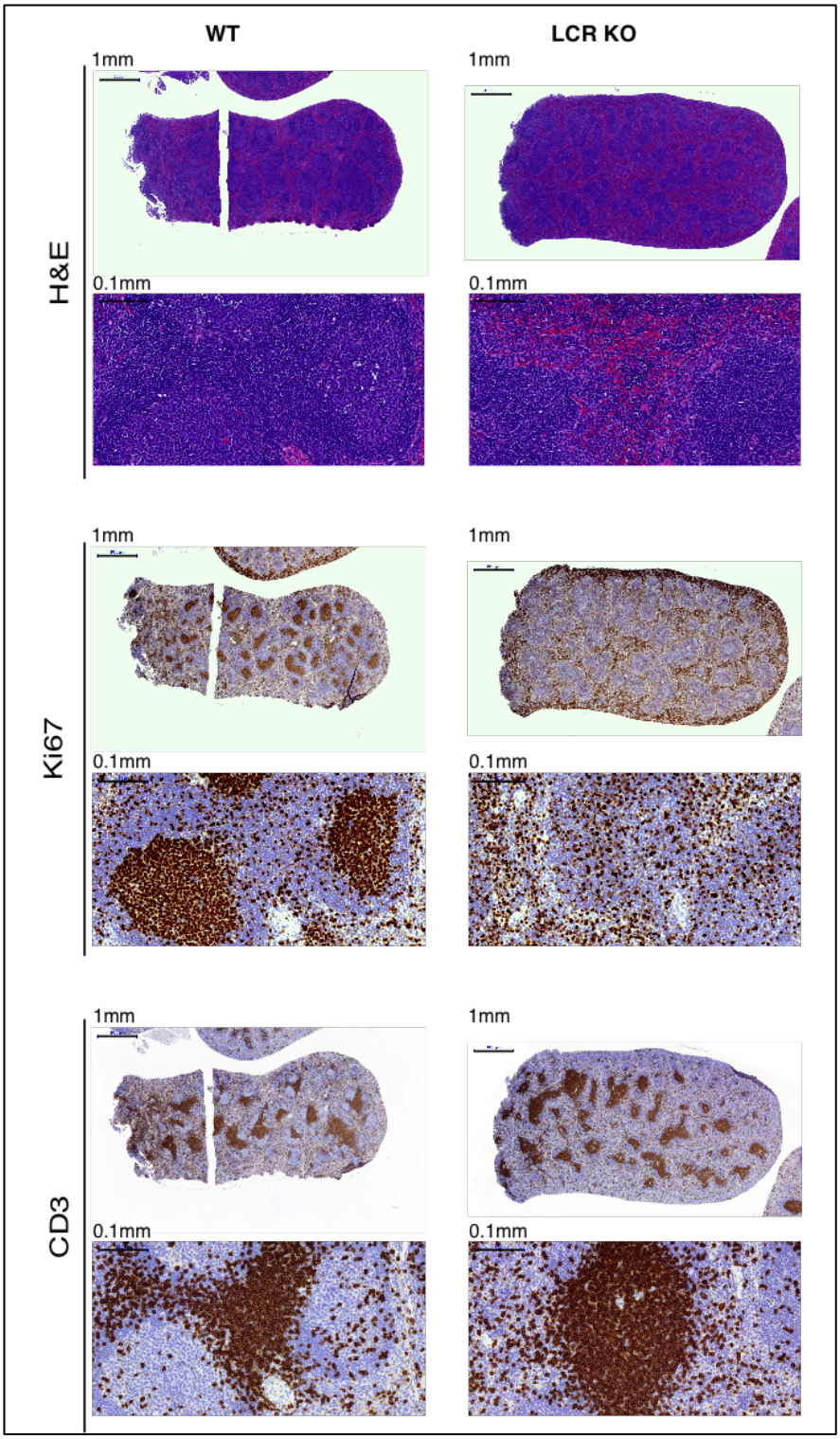

Figure 4.7 Immunohistochemistry images of WT and LCR KO mouse spleens stained with H&E, and for Ki67 and CD3.

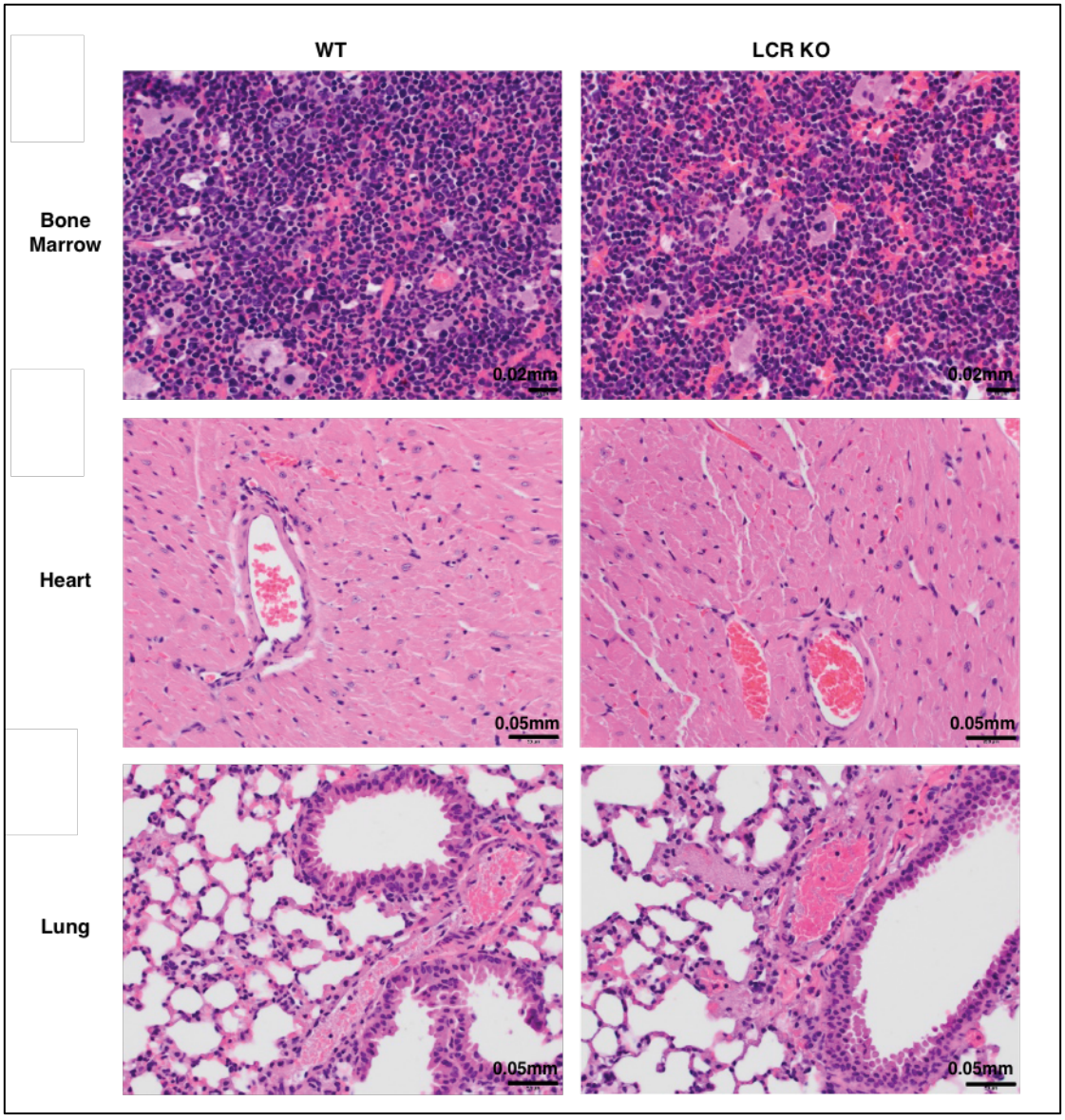

Figure 4.8 Representative images of H&E-stained bone marrow, heart and lung sections from the WT and LCR-deficient mice. No differences observed between the two groups.

Unlike the phenotype of BCL6$^{-/-}$ mice, the LCR KO mice do not have any apparent inflammatory pathologies in lung or cardiac tissue (Figure 4.8). The analysis of the images was performed by Dr. Sebastien Monette from the WCMC and MSKCC lab of comparative pathology.

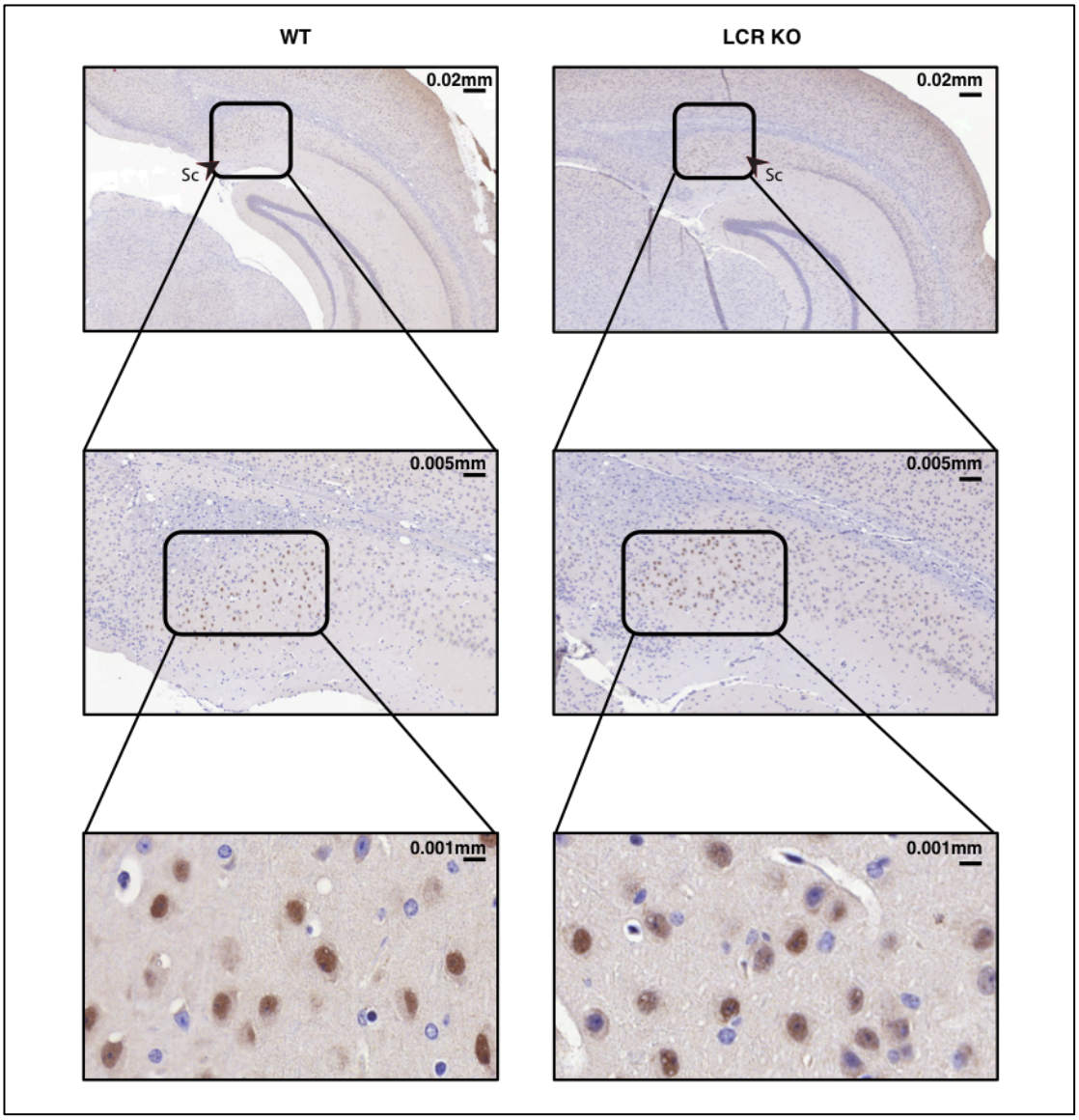

Figure 4.9 Representative images of BCL6 stained brain sections from WT (left) and LCR-deficient (right) mice. Sc is the subiculum (a region inferior to the hippocampus). Top to bottom, sequentially zoomed in images of the subiculum with normal BCL6 staining in both WT and LCR KO mice.

An interesting and relevant observation was made when analysing the BCL6 stained brain sections from the WT and LCR KO mice (Figure 4.9). While the assertion that the LCR regulates expression of *Bcl6* may be true—though not definitively proven at this point—it is interesting to observe that another tissue that has

been known to require BCL6 for development and differentiation remains unaffected. As mentioned earlier, cortical neurons are known to require BCL6 for development during early stages of brain development in mice. The lack of the LCR in the mice is clearly a critical deficiency with regards to the humoral immune response, but has no apparent effect on the neurons. This observation further supports the idea that the region of the genome identified as the putative *Bcl6* LCR is indeed an LCR as it seems to have a tissue specific phenotype.

We also performed a survival study for the LCR KO, LCR het and WT (littermate) mice. No significant differences were observed in the survival curves of the three groups (Figure 4.10).

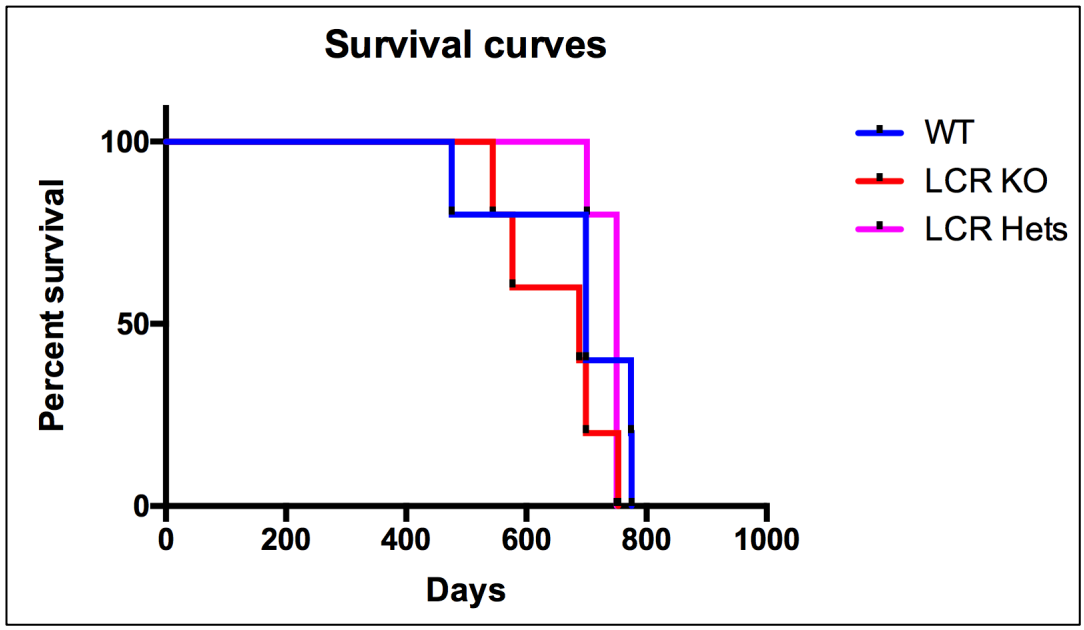

Figure 4.10 Kaplan-Meier plot for WT, LCR KO (-/-) and LCR het (+/-) mice. Log-rank (Mantel-Cox) tests reveals no significant differences between any of the survival curves.

4.2.2 The GC defect in LCR KO mice is GC intrinsic, and not related to T_{FH}.

An unaddressed yet extremely important question with respect to the defect in GC formation in the LCR KO mice was whether the origin of the defect was GCBs or T_{FH}. These specialized T-helper cells are touted to provide at least seven different types of 'help' to B-cells. These include survival, proliferation and hypermutation signals via BAFF, IL-4, IL-21 and CD40 ligand stimulation, adhesion and attraction ligands via SLAM associated proteins (SAP) and CXCL13, and immunoglobulin class switching, and plasma cell differentiation signals via IL-4, IL-17, TGFβ and IL-21 (Crotty). Therefore, the origin of a defect in GC formation could potentially be a defect in the T_{FH} compartment.

To determine if the GC defect is cell intrinsic, we decided to perform a mixed bone marrow chimera experiment. For this we would normally utilize the CD45.1-CD45.2 system to differentiate between the lymphocytes originating from different mice. However, the LCR KO mice were both CD45.1 and CD45.2 positive. To overcome this problem, we decided to use GFP as a marker to differentiate the WT and LCR-KO cells. We purchased C57BL/6-Tg (CAG-EGFP)131Osb/LeySopJ (Stock no. 006567) mice from Jackson labs. A robust level of GFP expression is reported in both bone marrow and splenocytes of these mice, as shown in the Jackson labs data sheet (Figure 4.11) (Okabe et al.).

GFP Expressing Lymphocyte Populations

Stock Number	Strain	Cell population:	Relative Proportions of GFP Expressing Cells: B cells	CD4 T cells	CD8 T cells	Dendritic Cells	Eosinophils	Neutrophils	Monocytes	Number of animals tested
		Tissue	% of B220 +	% of CD4+	% of CD8+	% of CD11c+	% of High SSC/Gr-1 low/CD11b+	% of High SSC/Gr-1 high/CD11b+	% of Low SSC/CD11b+ Gr-1+	
003291	C57BL/6-Tg(CAG-EGFP)1Osb/J	Bone Marrow	72.03+/-5.25	78.43+/-4.84	79.97+/-2.66	86.97+/-2.29	41.10+/-8.21	39.00+/-4.71	86.53 +/-3.26	3
006567	C57BL/6-Tg(CAG-EGFP)131Osb/LeySopJ		98.83+/-1.27	99.20+/-0.46	99.70+/-.10	97.63+/-1.67	99.23+/-0.72	98.97+/-1.04	97.80+/-1.92	3
007075	CByJ.B6-Tg(CAG-EGFP)1Osb/J		36.20+/-3.96	42.85+/-7.28	34.40+/-6.79	54.95+/-2.62	11.78+/-5.27	17.40+/-5.80	74.75+/-3.32	2
003291	C57BL/6-Tg(CAG-EGFP)1Osb/J	Spleen	82.33+/-3.18	82.53+/-3.61	81.87+/-3.91	98.83+/-0.21	49.43+/-6.17	50.73+/-6.48	95.83+/-0.06	3
006567	C57BL/6-Tg(CAG-EGFP)131Osb/LeySopJ		99.07+/-1.10	99.70+/-0.44	99.63+/-0.47	99.77+/-0.25	99.83+/-0.29	99.03+/-1.06	99.33+/-0.90	3
007075	CByJ.B6-Tg(CAG-EGFP)1Osb/J		62.30+/-3.25	40.10+/-7.21	39.60+/-5.94	93.10+/-2.40	20.85+/-18.03	26.40+/-8.91	78.30+/-1.70	2

Figure 4.11 Relative proportions of GFP expressing cells in the three different stocks of the C57BL/6-Tg (CAG-EGFP)131Osb/LeySopJ mice.

The GFP mice were deemed suitable to provide WT bone marrow. However, before performing the experiment we decided to test engraftment of the GFP bone marrow when mixed with regular WT bone marrow (from C57BL/6 mice not expressing GFP). The layout of the test is shown in figure 4.12. The results (Figure 4.13) show that the splenic GCBs post-immunization approximate the GFP proportions in the transplanted mixed bone marrow. The mouse that received only GFP positive bone marrow has 89% of the GCBs in the GFP positive window. The mouse that received a 1:1 mix of GFP: non-GFP bone marrow has a 42:58 ratio in the GC compartment. This was deemed a promising result as minor deviations from the original ratio were to be expected. We therefore proceeded to determine the role of T_{FH} in the LCR KO related GC defect by performing an experiment where the LCR KO bone marrow would be mixed with the WT GFP positive bone marrow.

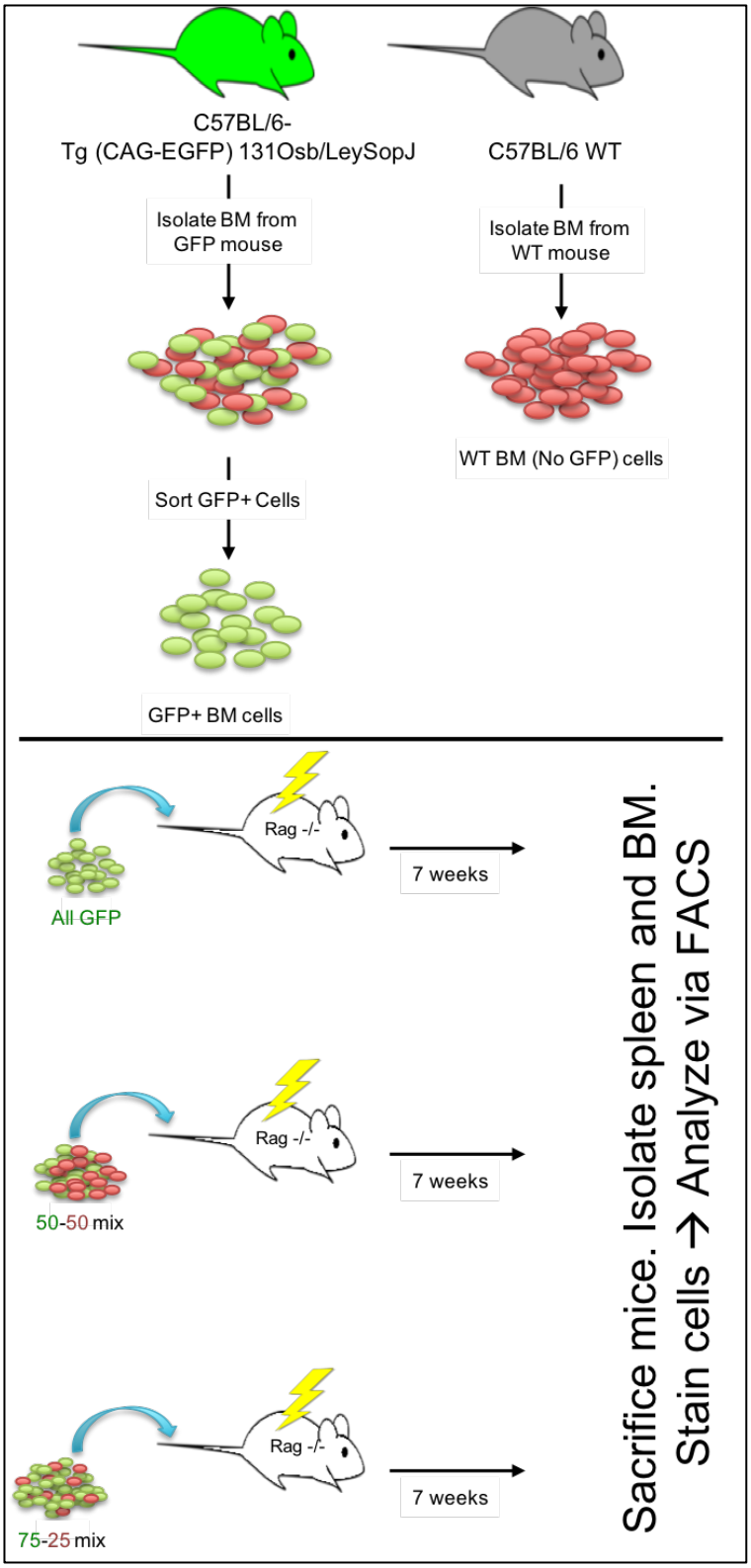

Figure 4.12 Schematic of the mixed bone marrow transplant experiment performed to evaluate engraftment of GFP positive bone marrow with non-GFP bone marrow.

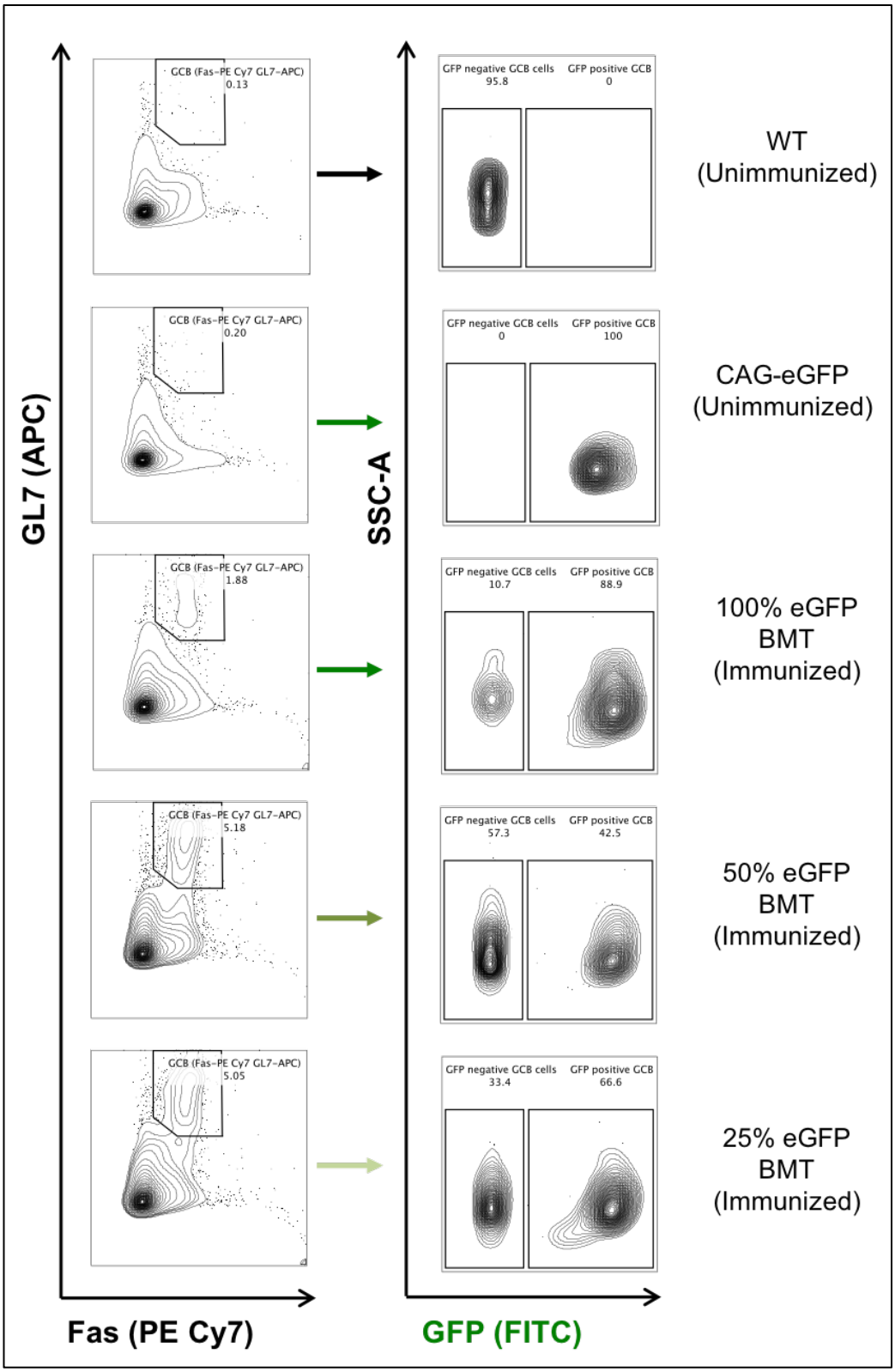

Figure 4.13 Representative flow plots showing relative proportions of GFP positive cells in the GC compartment post mixed BMT.

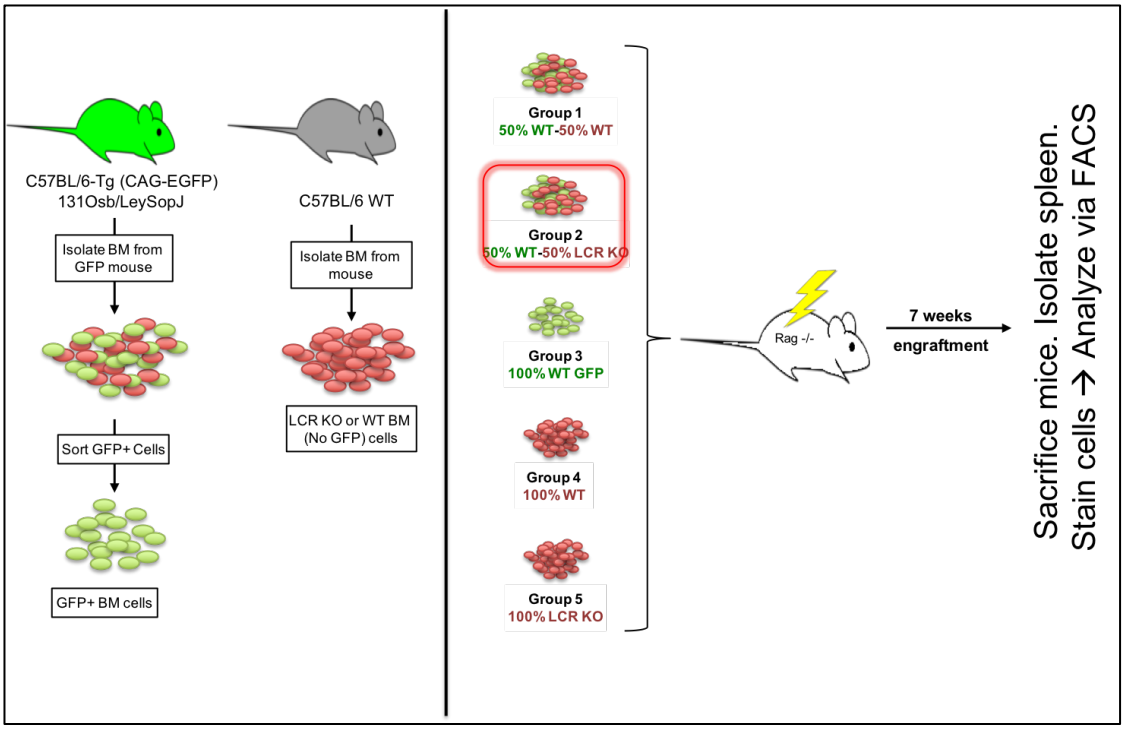

Figure 4.14 Schematic of the mixed bone marrow experiment to evaluate if the LCR KO mice have a GCB intrinsic defect or a T_{FH} intrinsic defect. The groups on the right side of the figure depict the ratio and type of cells mixed together.

We performed the transplant with 5 groups. Group 1: 50% GFP (WT) + 50% WT C57BL/6: 6 recipient mice; Group 2: 50% GFP (WT) + 50% LCR KO Homo: 6 recipient mice; Group 3: 100% GFP mice: 4 recipient mice; Group 4: 100% WT C57BL/6 mice (non GFP): 3 recipient mice; and Group 5: 100% LCR KO mice: 3 recipient mice (Figure 4.14). After the transplant, the mice were allowed 4 weeks for engraftment and subsequently immunized with SRBC to evaluate the cells of interest. The gating strategy for both GCB and T_{FH}-cells are shown in figures 4.15 and 4.16.

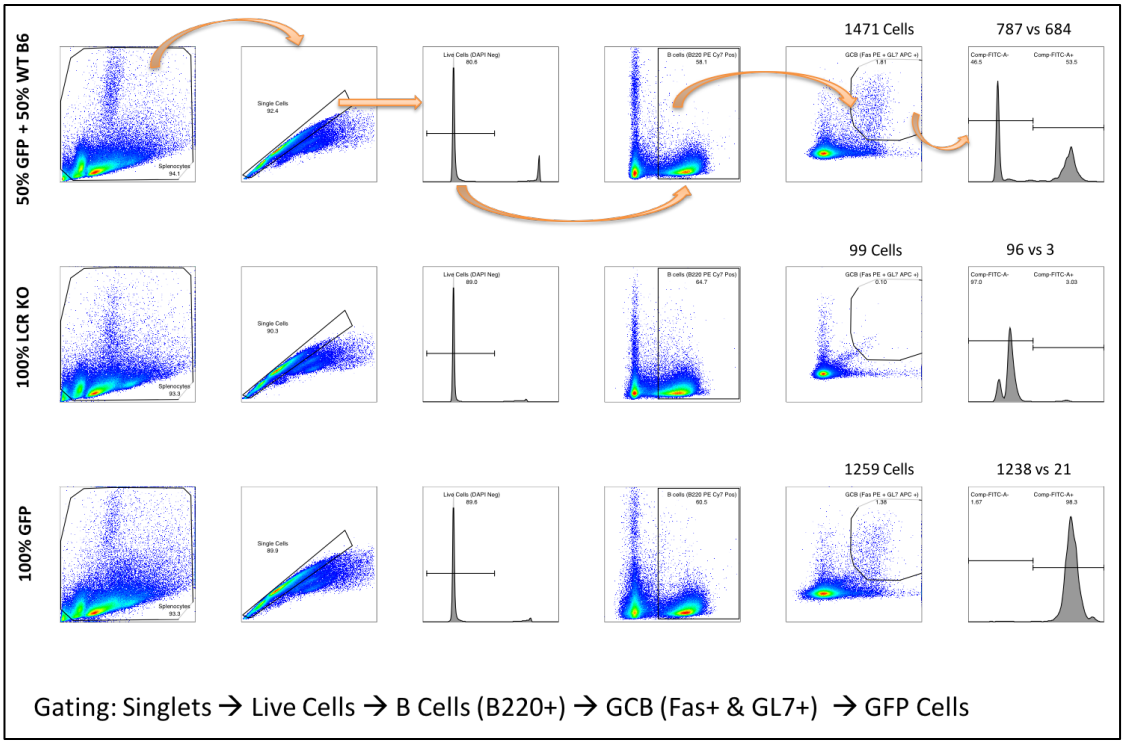

Figure 4.15 Gating strategy for evaluation of relative proportions of GFP positive cells in stained splenic GCBs.

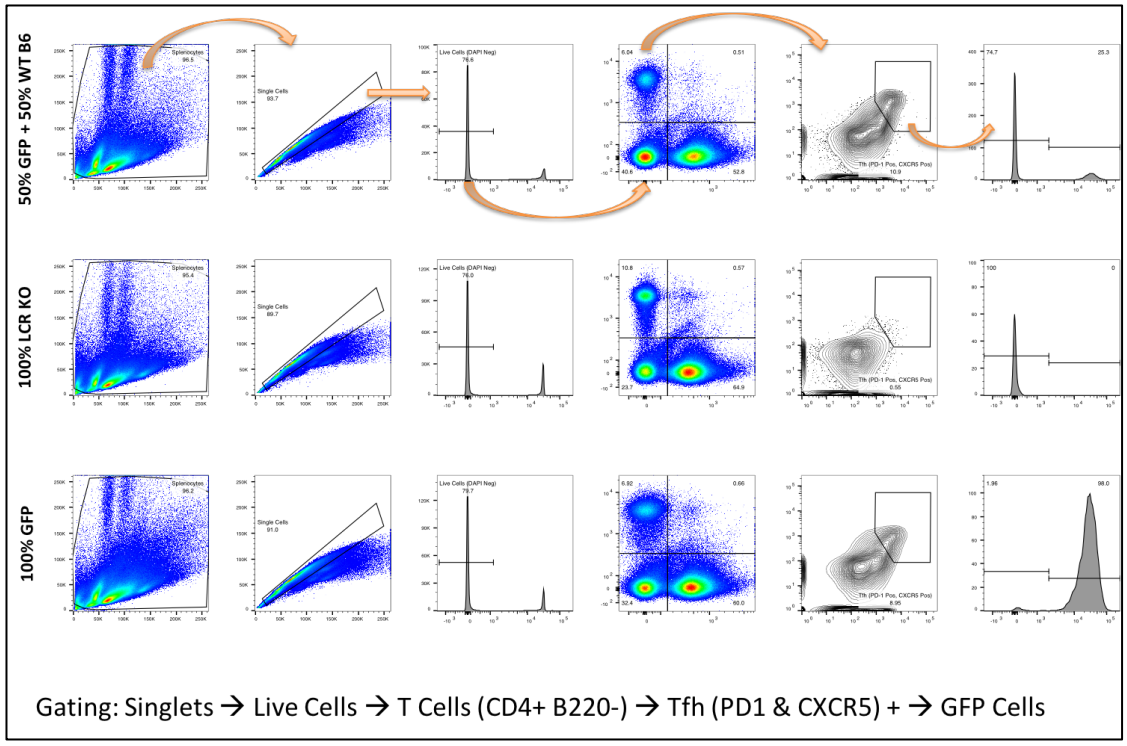

Figure 4.16 Gating strategy for evaluation of relative proportions of GFP positive cells in stained splenic T_{FH} cells.

GC formation was evaluated 10 days post immunization and, as expected, groups 1-4 formed germinal centers (as evident from the GCB and T_{FH} proportions observed through flow cytometry) (Figure 4.17). Group 5 (which only received LCR KO bone marrow) did not form any GCs. However, each group had comparable levels of B and T cells (Figure 4.17).

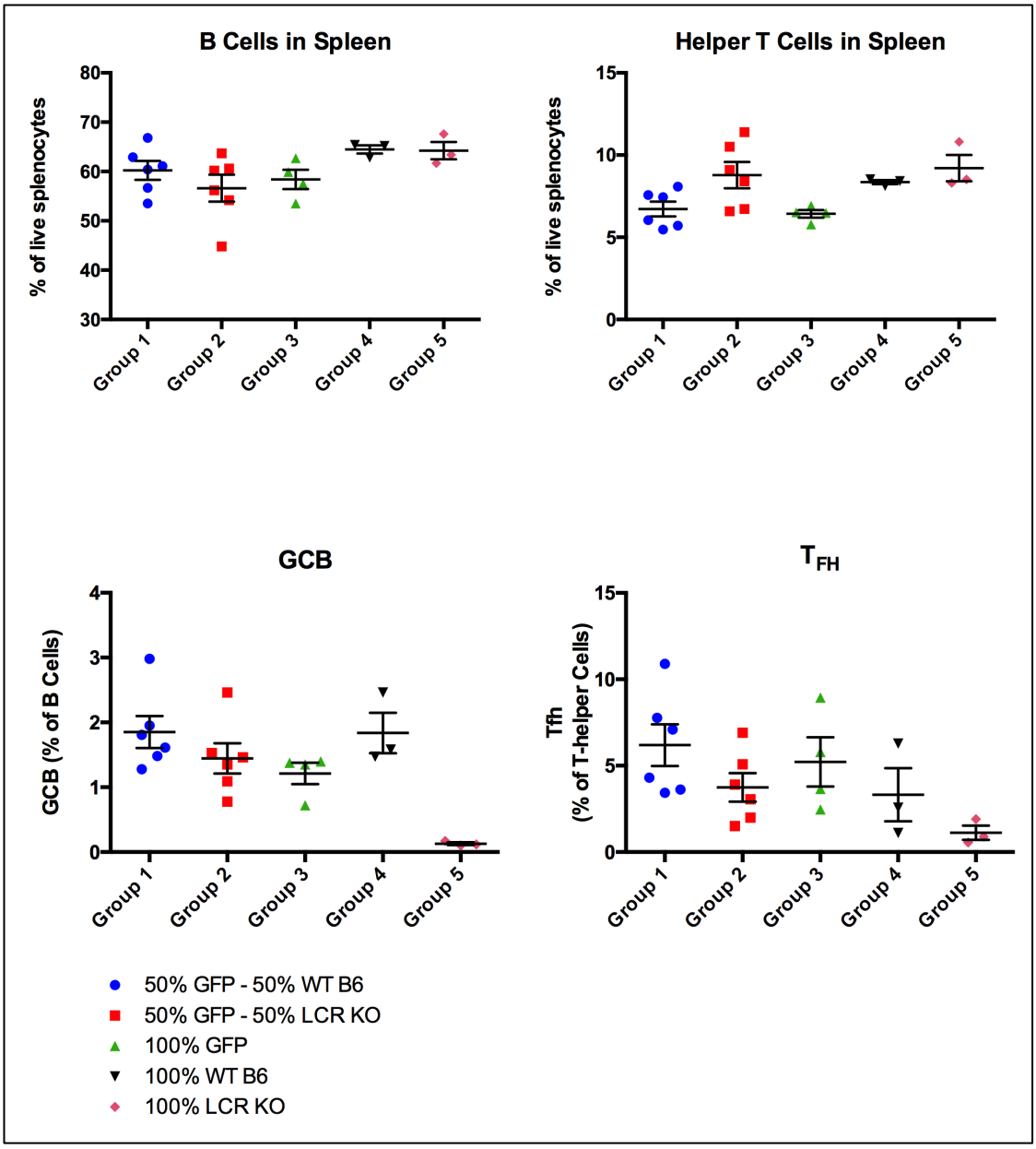

Figure 4.17 Plots representing total B-Cells (top left), total T-Cells (top right), GCB (bottom left) and T_{FH} (bottom right) proportions in splenocytes from mice in the mixed bone marrow chimera experiment.

Upon analysis of the relative proportion of GFP positive cells in each cell compartment, interesting observations were made (Figure 4.18). In group 1 (1:1 ratio of WT-GFP and WT-non-GFP bone marrow), both the GCB and T_{FH} compartments had GFP and non-GFP cells. The higher proportion of non-GFP cells in both the total

T-cell and T_{FH} compartments had been noted and interpreted to be a result of slightly lower level of GFP being expressed in the T-cells. The fact that the T_{FH} compartment displayed the same bias as the total T-cell compartment assuaged our concerns as reasonable conclusions from the experiment could still be made.

In group 2 (1:1 ration of WT-GFP and LCR KO bone marrow), the GFP proportions in GCB and T_{FH} compartments had a story to tell (Figure 4.18). In the GCB compartment, 93.62 ± 0.6052% (mean ± SEM), of the cells were GFP positive and 6.387 ± 0.6081% (mean ± SEM) were non-GFP cells (n=6), indicating that only the WT-GFP cells had contributed to this cell population and the LCR deficient non-GFP cells were incapable of forming GCBs. The difference in the mean was -87.23 ± 0.8579% with a 95% confidence interval of -89.14 to -85.32. (two tailed t-test with welch's correction). The T_{FH} compartment on the other hand, had a more equitable distribution of GFP positive and negative cells. Here, the GFP positive cells were 60.75 ± 7.163% (mean ± SEM) and the non-GFP LCR KO cells represented 39.25 ± 7.163% (mean ± SEM) of the T_{FH} cells. The difference between the means of GFP positive and negative in the T_{FH} compartment was -21.50 ± 10.13%. This difference is statistically non-significant with a 95% confidence interval from -44.07 to 1.070 (two tailed t-test with welch's correction). These results conclusively proved that the LCR deficient mice had a GC formation defect that was directly tied to a defect within the GCB and not T_{FH} cells.

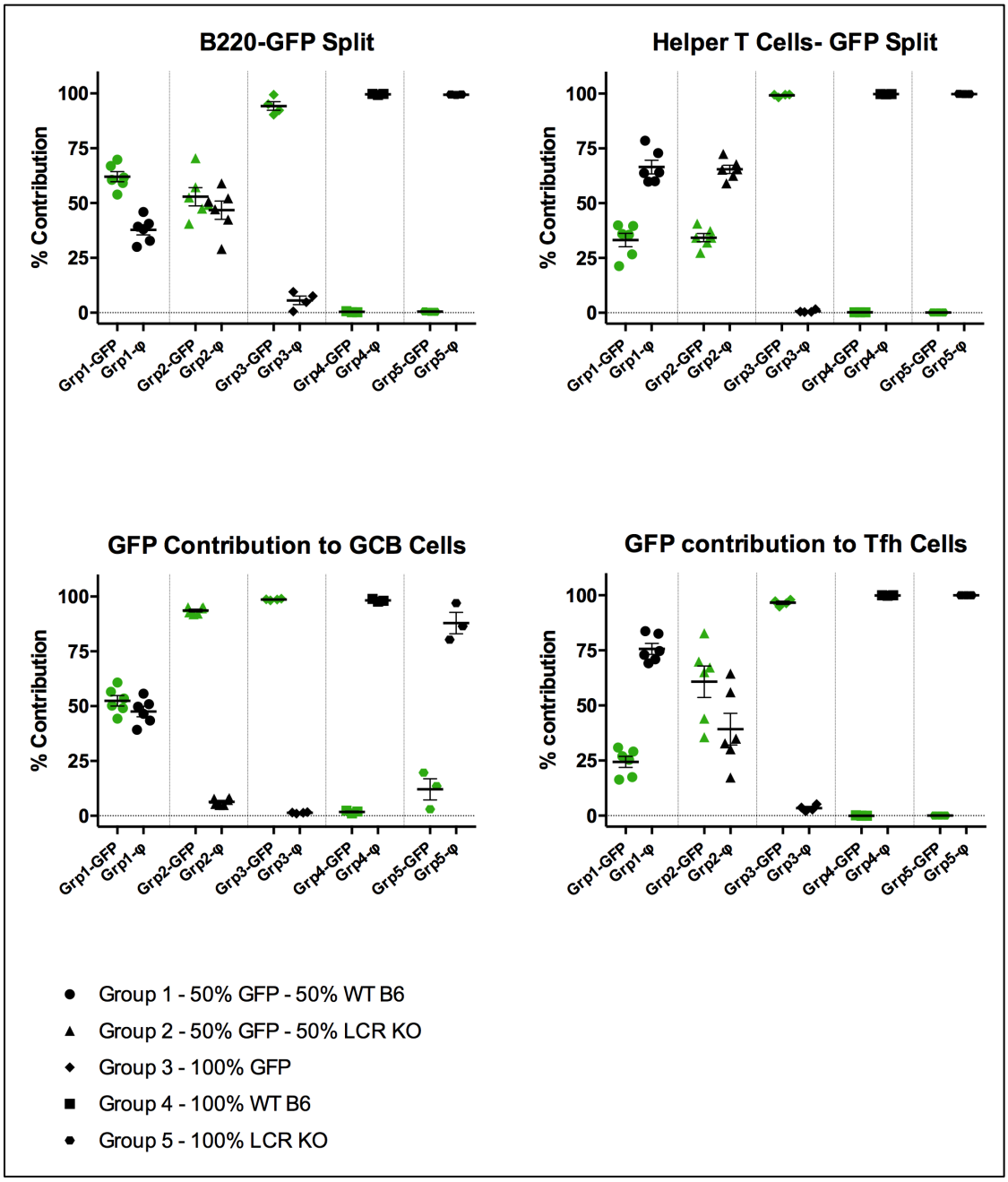

Figure 4.18 Relative proportions of GFP positive cells in groups that received mixed bone marrow transplants. Total B-Cells (top left), total T-Cells (top right), GCB (bottom left) and T_{FH} (bottom right). Error bars are SEM. Statistics in text.

4.2.3 The LCR ought to be in cis with Bcl6 to allow GCB formation

While the $LCR^{-/-}$ mice display a severe GC defect, mice with one copy of the LCR consistenly form germinal centers, albeit to a lesser extent when compared to WT mice. At first glance, this observation led us to believe that there might be a dose response. This explanation is not completely without reason. One of the earliest observations pertaining to LCR biology includes the copy number dependent increased expression of genes linked in *cis* to LCRs (Grosveld et al.). However, in a number of experiments, the deviation from the mean would often be large, to the extent that differences between WT and heterozygous LCR KO mice became difficult to establish and explain. We hypothesized a relatively complex idea as an explanation for this observation (the hypothesis is contingent upon another unproven hypothesis that BCL6 expression is monoallelic). We proposed that the *Bcl6* gene—which is undergoing transcription at low levels , as observed in NB-cells (Figure 3.3)—requires an early 'boost' from the LCR in *cis* during the NB to GCB transition. If the LCR is not in *cis, then* the level of expression required by the transitioning cells would not be sufficent for GCB formation.

To test a part of this hypothesis, we came up with a breeding strategy with $Bcl6^{+/-}$ mice and the $LCR^{-/-}$ mice that would result in $Bcl6^{+/-}LCR^{+/-}$ (double het) mice. These mice (without any crossover between the two loci) would result in the loci being in single copies and in *trans* (Figure 4.19). According to our hypothesis, these mice should not be able to make any GCBs.

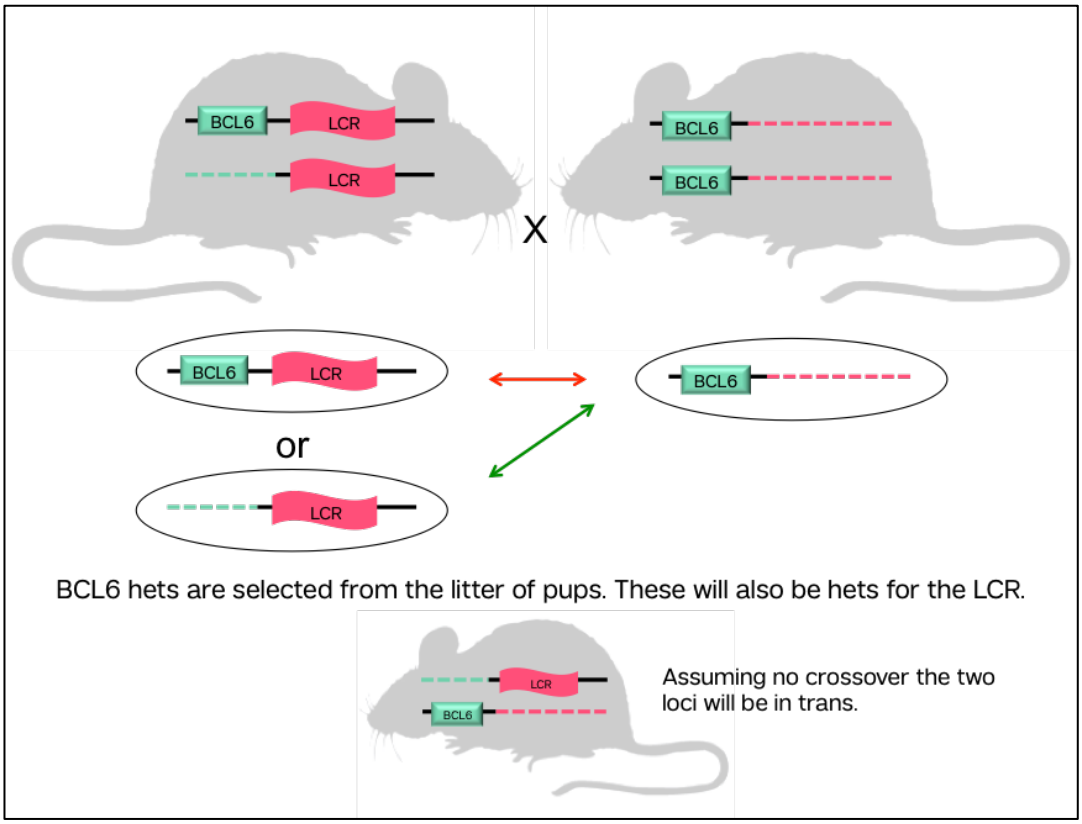

Figure 4.19 Schematic for breeding straegy employed to obtain BCL6$^{+/-}$;LCR$^{+/-}$ mice.

A pilot experiment was performed with the following groups of mice. WT (n=3), LCR KO (n=3), double hets (n=6), BCL6 hets (n=3) and LCR hets (n=2). Mice were between 8-10 weeks at the time if SRBC immunization. The results show that the double heterozygous phenocopy the LCR KO mice—the ability to form GCBs is completely abrogated (Figure 4.20). Even with relatively smaller numbers of mice in the LCR het and *Bcl6* het groups, the difference between the double hets and these two groups is staistically significant (compared to LCR hets P value < 0.001, compared to BCL6 hets P value < 0.0001, two tailed t-test with welch's correction). The gating strategy is depicted in figure 4.21. To validate these results we repeated the experiment with more mice in each group (Figure 4.22).

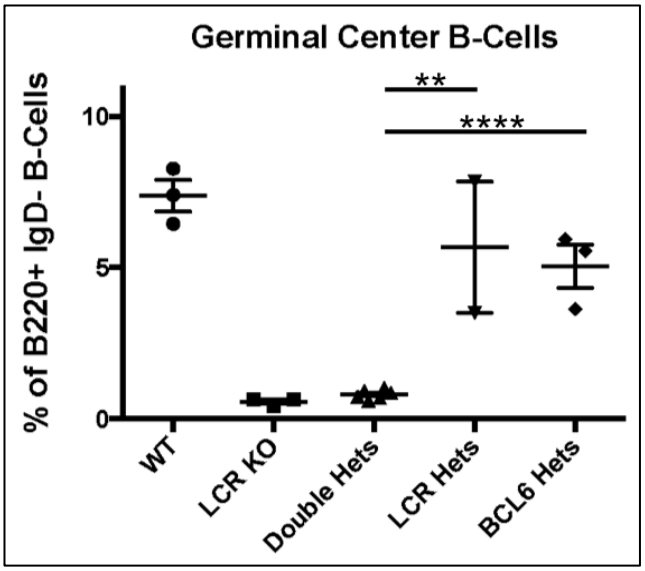

Figure 4.20 Plot quantifying live GCB (% of B220+, IgD-) in spleen from flow cytometry data. Error bars are SEM. Performed a two-tailed t-test with welch's correction**.**

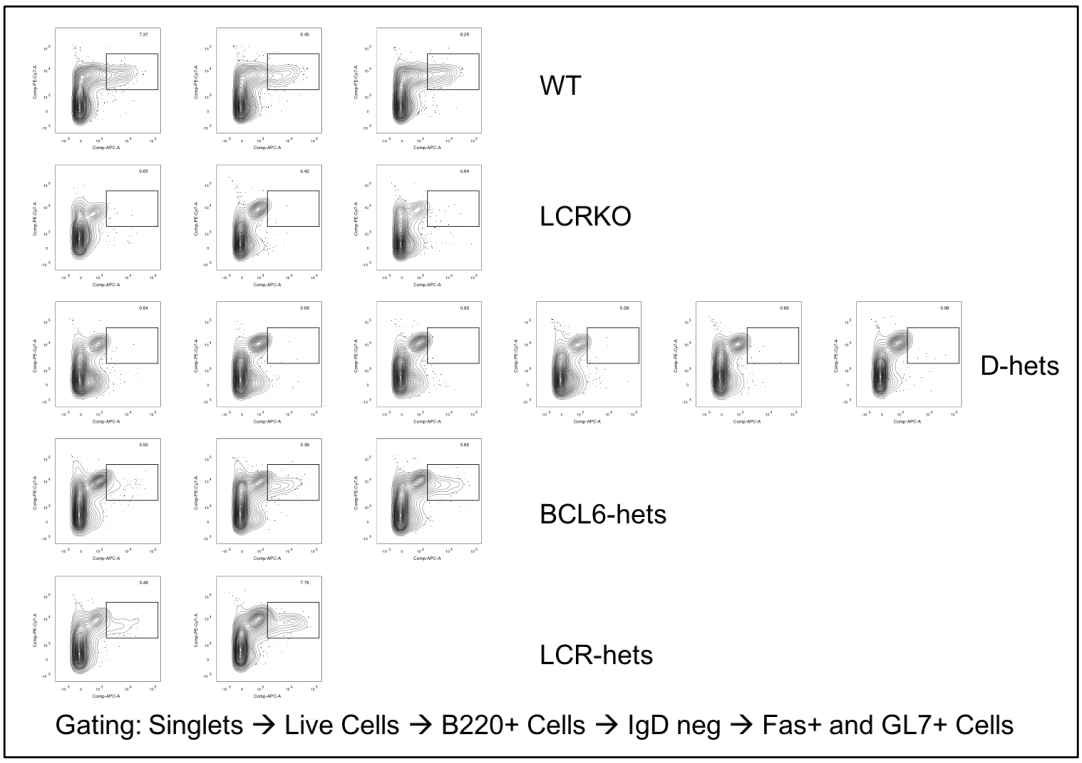

Figure 4.21 Flow cytometry plots showing GC proportions from pilot experiment with double heterozygous Bcl6$^{+/-}$; LCR$^{+/-}$ mice.

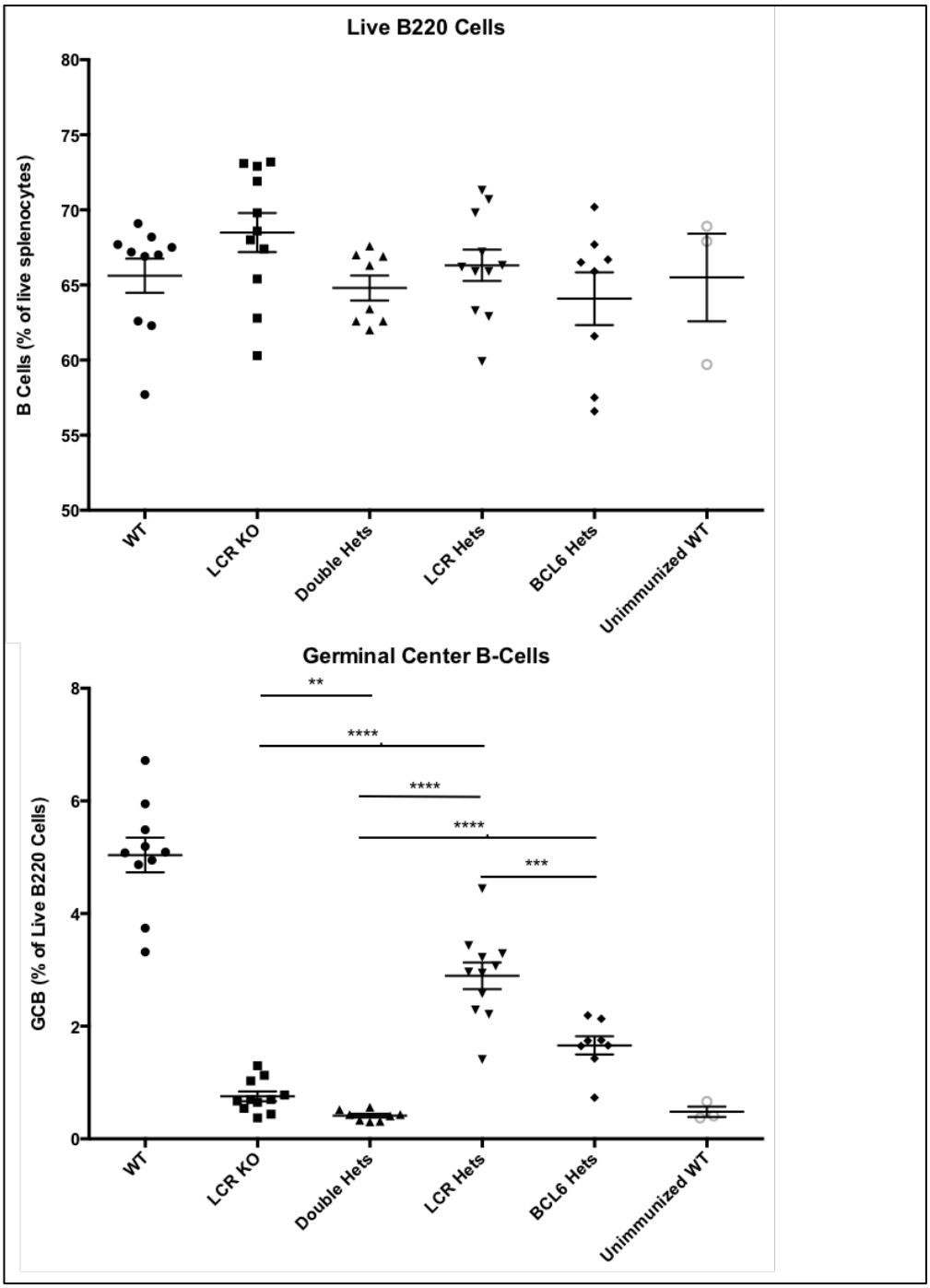

Figure 4.22 Plot quantifying live, total B-cells proportions in spleen (top) and GCB (bottom) % of live B220+ cells in spleen, from flow cytometry data. Error bars are SEM. Performed a two-tailed t-test with welch's correction**.** *** means P value < 0.001, **** means P value < 0.0001.

When the experiment was repeated, we had WT (n=10), LCR KO (n=11), double hets (n=8), BCL6 hets (n=8), LCR hets (n=11) and unimmunized WT (n=3) mice. Mice were between 8-10 weeks at the time of SRBC immunization. There were no significant differences between any of the groups when comparing total B-cell proportions in the splenocytes (Figure 4.22). The analysis of the GCB proportions in the splenocytes comfirmed our earlier observations (Figure 4.22). While the LCR hets and *Bcl6* hets form GCB (fewer than WT), GC formation in the double hets is completely abrogated. The statistics for the differences between the groups are mentioned in the figure.

4.3 Materials and Methods

4.3.1 Germinal Center Formation Assay-Flow Cytometry Analysis

For assessment of germinal center formation defects, the mice were intra-peritonealy injected with 500ul of 1:10 diluted (in D-PBS) sheep red blood cells. On day 10 post-immunization the mice were euthanized with CO_2 and the spleens were collected. One half of the spleen was crushed on a 70-micron filter and the splenocytes were suspended in RPMI, 10% FBS and 5mM EDTA. The splenic mononuclear cells are separated from the cell suspension using Fico/Lite-LM (Atlanta Biologicals). The cells were then stained with antibody mixes specific for germinal center B cells(B220+, IgD-, Fas+, CD38- or B220+, IgD-, Fas+, GL7+), naïve B cells (B22, centroblasts, centrocytes, follicular zone B cells (B220+, CD23hi, CD21lo), marginal zone B cells (B220+, CD23lo, CD21hi), and monocytes (B220-, CD3-, CD11b+, GR1+). DAPI was used for live//dead cell staining. The cells were analysed in a BD FACS Canto II flow cytometer.

4.3.2 Staining splenocytes for T-follicular helper cell analysis via flow cytometry

Antigens used for T_{FH} cell staining include, CD3, CD4, CXCR-5 and PD-1 (fixed cells can be stained with Foxp3 to different regulatory T_{FH} cells after fixing and permeabilizing). However, due to the lack of a functional fluorophore conjugated anti-CXCR-5 antibody, we utilized a biotin-streptavidin based system to stain splenocytes for analysis. The splenocytes were processed with RBC lysis solution for 10 minutes (or with mouse-Ficol), washed with FACS buffer (PBS + 0.5% BSA + 0.1% Sodium Azide) and subsequently centrifuged at 300 X g for 5 minutes. Primary ab (Rat anti-mouse CXCR5 purified 2G8 from BD) was diluted 1:100 in FACS stain buffer.

CXCR5 staining was performed before adding any of the other fluorophore-antibodies. Staining was performed in 96-well v-bottom plates for flow cytometry. 50ul of the Fc-block diluted 1:500 in FACS buffer was added to the wells with splenocytes and incubated for 30 minutes. Cells were then washed once with FACS buffer. Removed buffer and added 50ul of 1:100 primary rat-anti-mouse CXCR5 per 10^6 cells. Incubated for at least 60 minutes at 4-degree C, and then washed twice with FACS buffer. Added secondary antibody (conjugated to biotin), diluted 1:1000 in FACS buffer with serum (PBS + 0.5% BSA + 0.1% Sodium Azide + 2% NMS + 2% FCS). Incubated for 30 minutes at 4-degree C. Cells were washed twice with FACS buffer. Stained with SA-Fluorophore (SA-PECy7/SA-APC) at 1:100 dilution in FACS buffer with serum. Incubated for another 30 minutes at 4-degree C.
Added remaining surface stains (CD4, PD-1, B220) and incubated for another 60 minutes. Washed thrice with FACS buffer and immediately analyze the samples on the flow cytometer.

4.3.3 Immunohistochemistry

Spleen, Bone marrow, Heart, Lung and Brain tissue are fixed in formalin for 24 hours and then transferred to 70% ethanol. Spleens and were fixed in 4% paraformaldehyde and embedded in paraffin. Sections of each sample 6 μm in thickness were prepared, cleared in xylene and hydrated through a descending alcohol series to distilled water. Slides were boiled for 20 mi in citrate antigen retrieval buffer, followed by washes under running water. Endogenous peroxidase activity was blocked by treatment of the sections for 20 min with 3% hydrogen peroxide in methanol. Tissue sections were then incubated overnight at 4-degree C with biotin-conjugated peanut agglutinin (Vector Laboratories). After a further wash in TBS, streptavidin–horseradish peroxidase was added, followed by incubation for 30 min. Horseradish peroxidase activity was detected with a DAB kit (Vector Laboratories). Finally, sections were counterstained with hematoxylin if necessary. For double staining, sections were incubated overnight at 4-degree C with anti-Bcl-6 (N3; Santa Cruz), followed incubation for 1 h with biotin-conjugated secondary antibody (sc-2030; Santa Cruz). Streptavidin–alkaline phosphatase was added after a further wash in TBS followed by incubation for 30 min. Alkaline phosphatase activity was detected with an Alkaline Phosphatase Substrate Kit III (Vector Laboratories). Sections were boiled for 10 min followed by incubation with biotin-conjugated anti-B220 (RA3-6B2; Caltag Metsystems), then incubation with streptavidin–horseradish peroxidase. Horseradish peroxidase activity was detected with a DAB kit (Vector Laboratories).

4.3.4 Bone marrow transplant

6-7-week-old WT-GFP (2 mice), WT C57BL/6-non GFP (2 mice), and LCR KO (1 mouse) were sacrificed under CO_2. The tibia and fibula bones were immediately removed from the sacrificed mice and placed in cold RPMI media. After removing muscle and connective tissue from the bones, we isolated the bone marrow and counted the cells using a hemocytometer. The cells were resuspended in cold sterile D-PBS. The bone marrows were subsequently mixed in ratios required for the experiment. The mixed suspensions were centrifuged for 5 minutes at 400 X g at 4 degree C. The supernatant was removed and the suspension was resuspended in cold D-PBS to a final concentration of 10 million per ml. A total of 22, 10-week old, female $Rag^{-/-}$ mice were irradiated with 900 cy (450 X 2 over a course of 24 hours) prior to transplant. 4 hours after the second dose of radiation, the transplant was performed via tail I.V. injection (100ul of suspension per mouse). Mice were observed for morbidity post-transplant every week. Mice were immunized with SRBC for assessment of GC formation response 4-weeks post-transplant.

Chapter 4 References

Crotty, Shane. "A Brief History of T Cell Help to B Cells." *Nature Reviews Immunology* 15.3 (2015): 185–189. Web.

Dent, A L et al. "Control of Inflammation, Cytokine Expression, and Germinal Center Formation by BCL-6." *Science* 276.5312 (1997): 589–592. Web.

Grosveld, Frank et al. "Position-Independent, High-Level Expression of the Human β-Globin Gene in Transgenic Mice." *Cell* 51.6 (1987): 975–985. Web.

Leamey, Catherine A. et al. "Differential Gene Expression between Sensory Neocortical Areas: Potential Roles for Ten_m3 and Bcl6 in Patterning Visual and Somatosensory Pathways." *Cerebral Cortex* 18.1 (2008): 53–66. Web.

Luster, Michael I., Albert E. Munson, et al. "Development of a Testing Battery to Assess Chemical-Induced Immunotoxicity: National Toxicology Program's Guidelines for Immunotoxicity Evaluation in Mice." *Toxicological Sciences* 10.1 (1988): 2–19. Web.

Luster, Michael I., Christopher Portier, et al. "Risk Assessment in Immunotoxicology: I. Sensitivity and Predictability of Immune Tests." *Toxicological Sciences* 18.2 (1992): 200–210. Web.

Okabe, Masaru et al. "'Green Mice' as a Source of Ubiquitous Green Cells." *FEBS Letters* 407.3 (1997): 313–319. Web.

Tiberi, Luca et al. "BCL6 Controls Neurogenesis through Sirt1-Dependent Epigenetic Repression of Selective Notch Targets." *Nature neuroscience* 15.12 (2012): 1627–35. Web.

Chapter 5-Studying the LCR ex-vivo in B-cell Follicular Organoids

5.1 Introduction

If there is anything like a good problem in science, then this is it—the discovery of a phenotype that is so dramatic, so stark that it obliterates the system you wish to detect the defect within. The lack of GC B-cells in the LCR KO mice presented us with such a problem. Our efforts to study the mechanism of LCR engagement and its specific effects on gene regulation refocused our attention to ex-vivo cell culture systems. Our two main options were: 1. Utilize human DLBCL cell lines, or, 2. Culture LCR KO B-cells from the murine spleens ex-vivo. While both approaches have their benefits, each one had its own set of challenges.

We started off with attempts aimed at knocking out the LCR in OCI-Ly7 cells, which are derived from GCB like DLBCL cell lines. While the cell line has a mutation burden which could complicate the process of elucidating the nuances the LCR exhibits in GCBs, it is still useful as the cells have a normal ploidy, wildtype *Bcl6*, *Crebbp*, *Mll4*, *Ezh2* and *Ep300*, and wildtype CGH karyotype (Chang, Blondal, Benchimol, Minden, & Messner, 1995; Mehra, Messner, Minden, & Chaganti, 2002). The doubling time of these cells is approximately 29 hours. However, most attempts to utilize CRISPR to delete the LCR in these cell lines failed (data not shown). While a deletion product was frequently detected via PCR on the larger population of cells, ultimately the isolation of a clone with a deletion failed repeatedly. This was originally attributed to the poor ability of single-cell clones of Ly7 to proliferate after performing limiting dilutions. We hypothesized that the failure might be due to a deleterious effect of the knocked out LCR in these cells.

With the attempts around cell line work largely failing, we switched out attention to ex-vivo B cell cultures. The primary goal of our experiments at this point was to determine if the putative LCR upstream of *Bcl6*, actually regulated expression of *Bcl6*. The results in the next section depict the manner in which the work evolved while highlighting some important realizations about studying chromatin topology and transcriptional regulation in such systems.

5.2 Results

5.2.1 Ex-vivo cultures of murine B-cells

After failing to utilize the human DLBCL cell lines to study the effect of the LCR, we started wondering if the B-cells from the LCR KO mice could be cultured ex-vivo, long enough to test if *Bcl6* expression was indeed influenced. To be able to do this we needed a system that would not only allow for the murine B cells to survive but also show an induction or maintenance of *Bcl6* transcript levels. We started with a simple system where we isolated the B-cells from mouse spleens via CD43 depletion (which is expressed on all leukocytes except immature and mature B-cells) and grew them in RPMI with IL-4, LPS and CD40 antibody. This system has been used for activation and proliferation of Immature B-cells ex-vivo (Haxhinasto & Bishop, 2004; Rush & Hodgkin, 2001).

Unfortunately, the system did not have any appreciable induction or maintenance of *Bcl6* expression (Figure 5.1). While we performed qPCR analysis on a number of genes either shown to contact the LCR (*Klhl6* and *Lpp*) and the *Bcl6* promoter or known to be important in the GC program (*Aicda*, *Cd86*, *Cxcr4*),

however, the analysis did not reveal any appreciable difference in expression between LCR KO and WT B-cells.

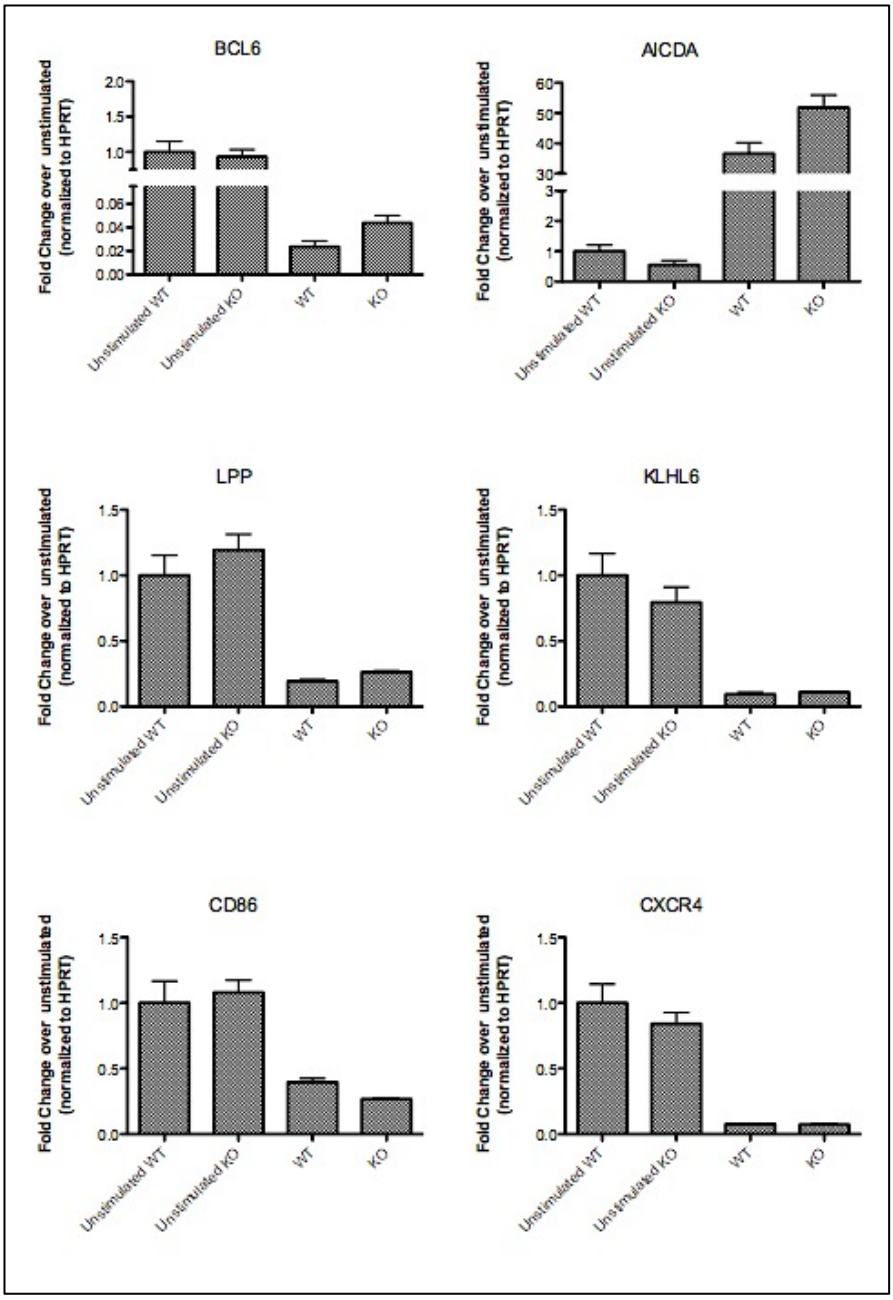

Figure 5.1 qPCR results from the ex-vivo stimulation of CD43 depleted splenocytes. Bars represent average fold change normalized to HPRT and compared to unstimulated WT cells. Error bars are standard deviation.

Our efforts then shifted to a co-culture system with the development of a 3D B-cell follicle organoid. This utilized 3T3 cells engineered to secrete BAFF and express CD40 ligand (CD154) on their surface (Nojima et al., 2011). B-cells cultured with these cells (40LB cells), proliferate rapidly in the presence of IL-4, undergo isotype switching, and even differentiate into cells that resemble GCBs (upregulation of Fas and GL7). An improved version of this culture system, involves the addition of a matrix resembling the consistency of the 3D microenvironment of the Germinal Center. This is achieved by resuspending the B-cells and the 40LB cells in a gelatin-based hydrogel and silicate nanoparticles (Purwada & Singh, 2017). These two versions of this culture system are depicted in figure 5.2.

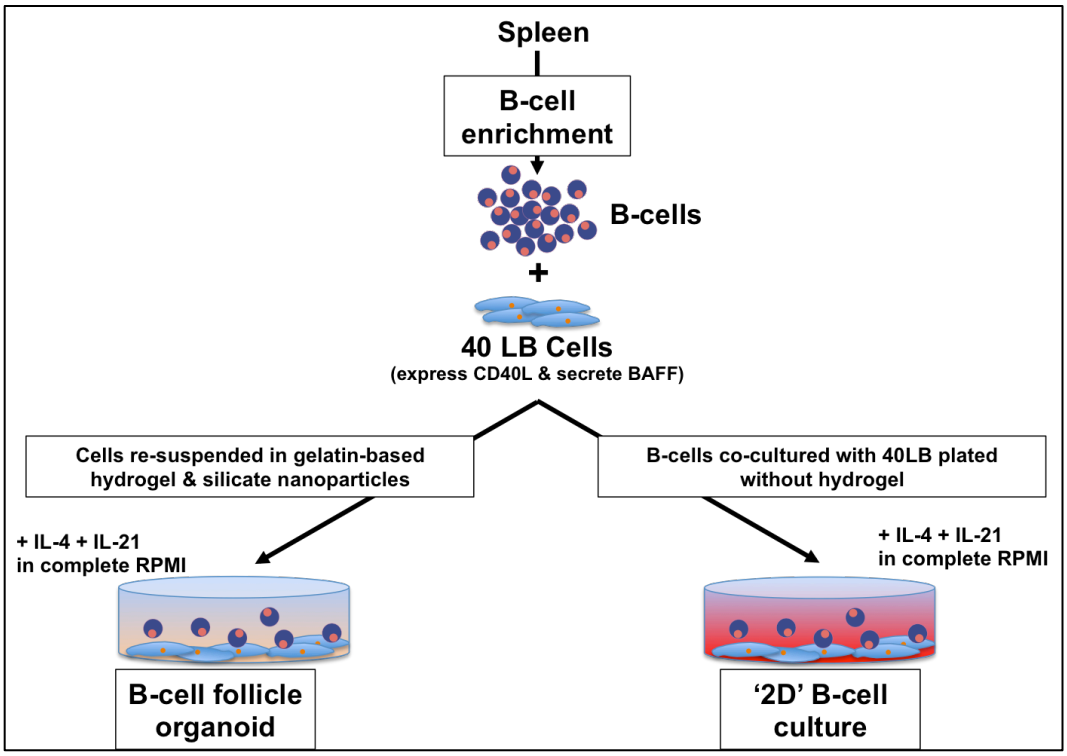

Figure 5.2 Schematic for B-cell follicle culture system with supporting 40LB cells. The left side represents the version where a 3D-matrix is provided in the form of silica nanoparticles and gelatin, whereas the right side lacks this matrix. In early iterations both systems were employed and cytokines were added simultaneously.

The promise of utilizing this system was further highlighted in studies performed by members of our group when they showed that the B-cells in the 3D organoids also undergo somatic hypermutation. Furthermore, at the protein level, both BCL6 and EZH2 levels increase around day 4 post plating of the cells. With this information in hand, we decided to utilize the organoids to determine if the LCR KO B-cells would recapitulate the defect ex-vivo, and more importantly if it would allow us to determine the genes that are affected by the loss of the LCR. The results of these experiments are below.

5.2.2 Utilizing ex-vivo B-cell follicle cultures to study the LCR

Initial efforts with the ex-vivo cultures were to determine if the hypothesized effect of the LCR on *Bcl6* could be captured. If this were possible, the expectation would be that the ex-vivo differentiation of B-cells into GCB-like cells would be somewhat compromised in the B-cells from LCR KO mice as compared to WT mice. Figure 5.3 shows representative flow cytometry plots for Fas+ GL7+ B-cells (B220+ DAPI-) differentiated from splenic B-cells (obtained through CD43 depletion of murine spleens) 3-days post plating for both WT and LCR KO mice. In this experiment, we performed the plating with and without the nanoparticle-gelatin mix. The cells from the nanoparticle-gelatin mix are referred to as ‘organoids’ whereas the ones where the B-cells did not have this matrix are referred to as 2D-cultures. Surprisingly, the ex-vivo system did not show any major defect between the WT and LCR KO mice. The quantification of the GC-like cells from this experiment is shown in Figure 5.4, where the error bars represent standard deviation between three technical replicates for each genotype and condition. P-values are determined with a two-tailed, unpaired t-test.

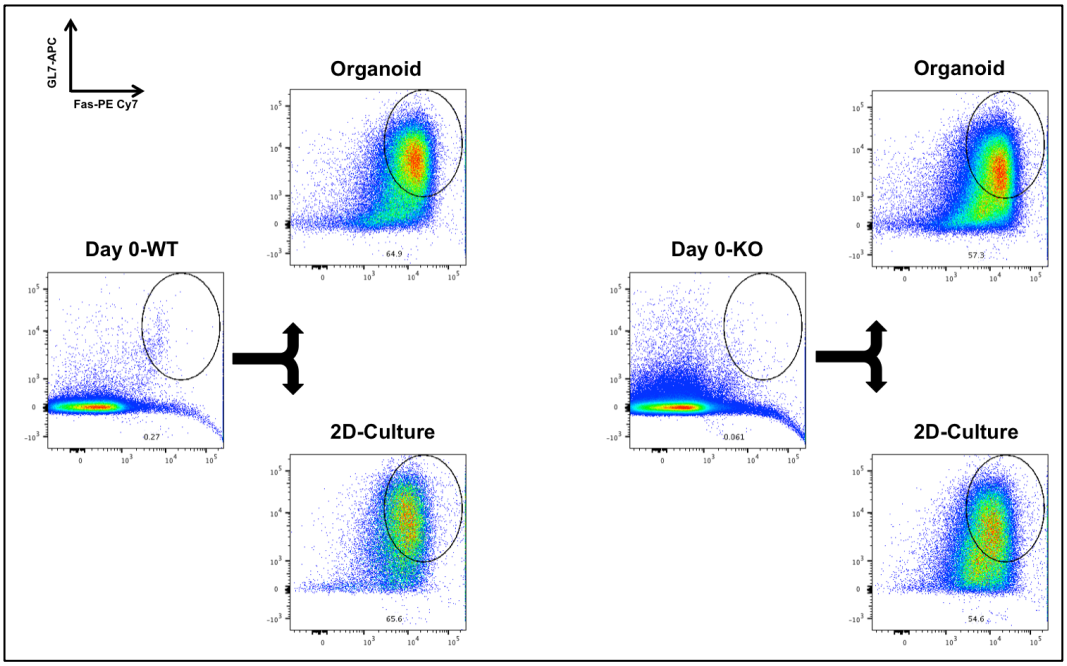

Figure 5.3 Representative flow cytometry plots for GC-like cells from WT (left) and LCR KO B-cells (right). The arrows indicate the differentiated cells 3-days post plating. (Top) organoid cultures, (bottom) 2D-cultures.

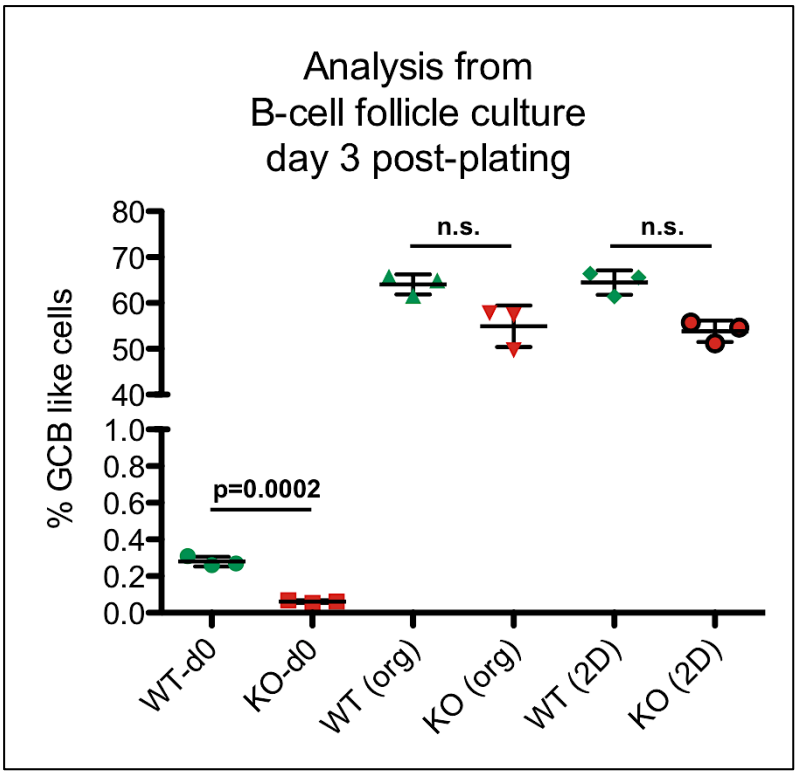

Figure 5.4 Quantification of the GC-like cells from both organoids and 2D cultures. Error bars are standard deviation between technical replicates.

The lack of any defect of GC-like cells in from the LCR KO B-cells led us back to the drawing board for the B-cell cultures. Among the numerous purported reasons for this anomalous observation, one was the idea that the concentration of cytokines being used might be too high. At 50ng/ml of IL-4 and 25 ng/ml of IL-21, we wondered if this amount of stimulation did not mimic physiology.

5.2.3 Optimizing the B-cell follicle culture

We decided to test if significantly lowered concentrations of IL-4 and IL-21 would still allow GC-like cell formation, and if so then we should use those concentrations to study the LCR. Our curiosity about the dynamics of the signalling mechanisms within the organoids led us through a number of experiments where we tested the requirement of the system which were otherwise taken for granted. This included aspects in addition to the cytokine concentrations including the requirement of BAFF and CD154 secreted and expressed by 40-LB cells in the presence of high cytokine concentrations; and the requirement of BCL6 itself (i.e. are the organoids BCL6 dependant or can they differentiate into GC-like cells from BCL6 KO B-cells as well.

We performed an experiment where the organoids were cultured with and without 40LB (control cells used for co-culture were 3T3 cells that are the source cells for 40-LBs but do not secrete BAFF or express CD154 on their surface), and varied concentrations of IL-21 (25 to 0.5 ng/ml). We also tested if 40-LB cells that had been culture for 8 weeks showed any reduction in their ability to support the differentiation of the B-cells as compared to freshly thawed 40-LB cells that had been through fewer passages. Representative flow plots are shown in figure 5.5 below.

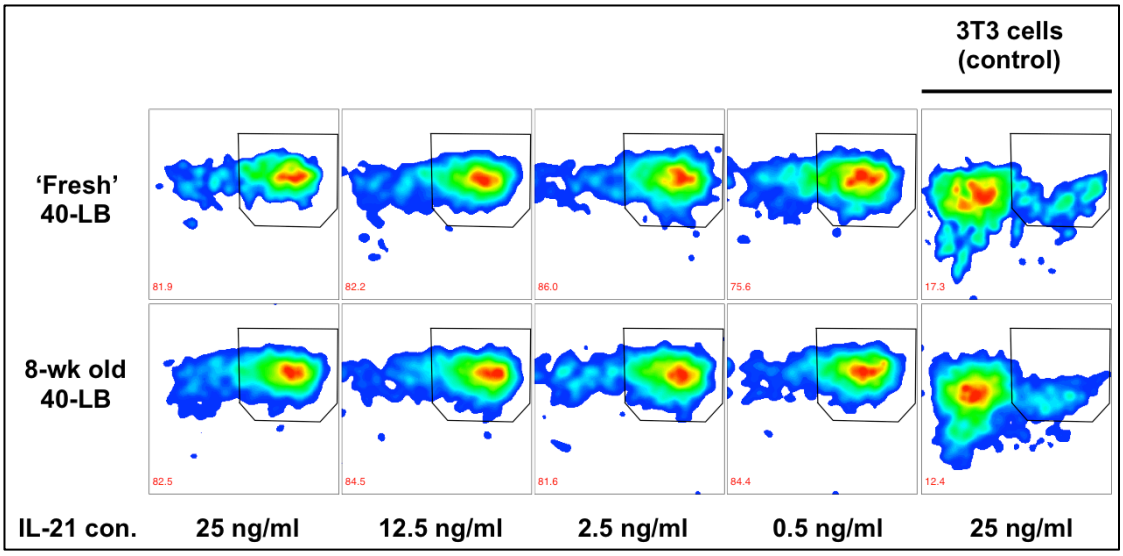

Figure 5.5 Representative flow plots of IL-21 titration in the organoid cultures. 80,000 B-cells were co-cultured with 120,000 40LB or 3T3 cells. (Top) Organoids with freshly thawed 40-LB cells, (bottom) organoids with 8-week old 40-LB cells. Right most plot is with 3T3 cell which do not secrete BAFF and do not express CD154.

As is evident from the figure, lower concentrations of IL-21 did not affect the differentiation of B-cells, and even 0.5ng/ml of IL-21 is sufficient for differentiation. We also confirmed the requirement of BAFF and CD154 (provided by 40LBs) to be critical for this differentiation as the organoids with control 3T3 cells had a significantly lower proportion of B-cells differentiate as compared to the complete organoids. IL-4 concentration for this experiment was maintained at 50ng/ml for all conditions. A separate experiment was performed to determine if lower IL-4 concentrations would be sufficient. That experiment showed similar results, therefore, in subsequent experiments the concentrations of both cytokines were lowered.

Additionally, we tested the requirement of BCL6 in the differentiation process itself. This was achieved by utilizing spleens from mice that had previously been irradiated and transplanted with bone marrow from a BCL6 KO mouse. Surprisingly, the organoids plated from these splenocytes showed normal levels of GC-like cell

formation. This observation made it necessary to test constitutive knockout B-cells directly from a BCL6 KO mouse in culture. Figure 5.6 below shows flow plots for GC like cells from (four technical replicates) for WT and BCL6 KO organoids.

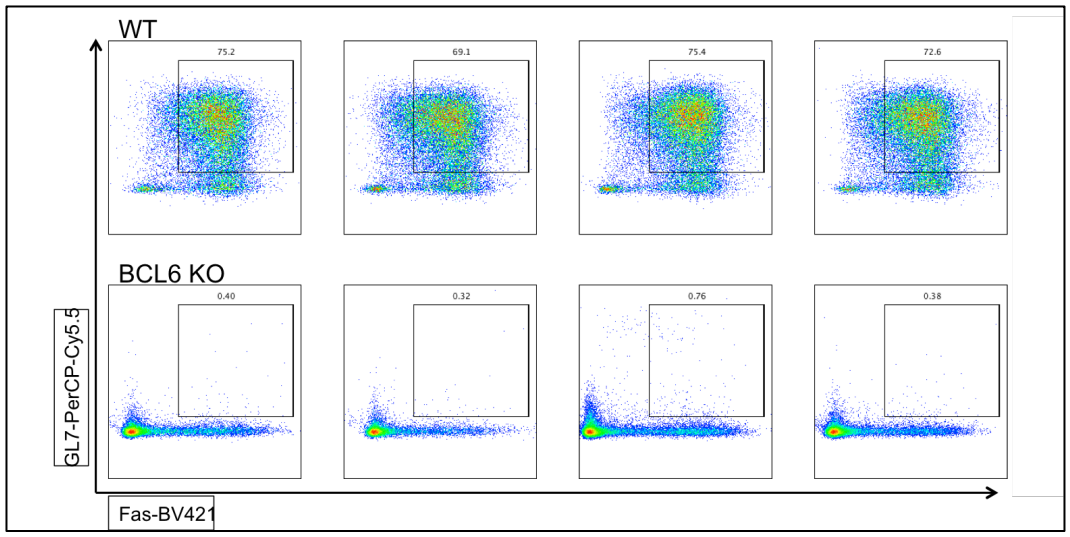

Figure 5.6 Representative flow plots for Fas+GL7+ GC-like cells from (top) WT and (bottom) BCL6 KO B-cells (murine).

The results depicted in figure 5.5 indicate that the organoids are indeed BCL6 dependant. The GC like cells formed from the irradiated mouse with KO bone marrow was most likely due to the incomplete loss of WT bone marrow after irradiation. It is possible that even though the dose of radiation was sufficient for lethality, it did not result in an absolute abrogation of the host bone marrow. With the transplant of the KO bone marrow, the mouse was provided a window of recovery where the KO bone marrow (with compromised fitness compared to host WT bone marrow) ended up co-existing with WT instead of replacing it (akin to a mixed bone marrow chimera). The WT cells might have partially populated the spleens and the resulting organoids resulted in GC like cell formation due to the presence of those WT cells. Our next step was to return to our investigation of the LCR KO mice and test their ability to proliferate; to differentiate or to express Bcl6 was in anyway compromised.

5.2.4 LCR KO B-cells highlight variability of B-cell follicle cultures

With a significantly improved sense of the technical nuances behind the organoid cultures, we restarted experiments with WT and LCR KO B-cells. We labelled the B-cells with eFluor670, a proliferation dye for the B-cells, to follow the rounds of division the cells undergo in culture while differentiating. We also utilized a BCL6-PE antibody for flow cytometry to determine if the LCR KO organoids displayed any lowering of BCL6 protein levels. Figure 5.6 shows results from one of the experiments where the LCR KO cells exhibited an interesting defect.

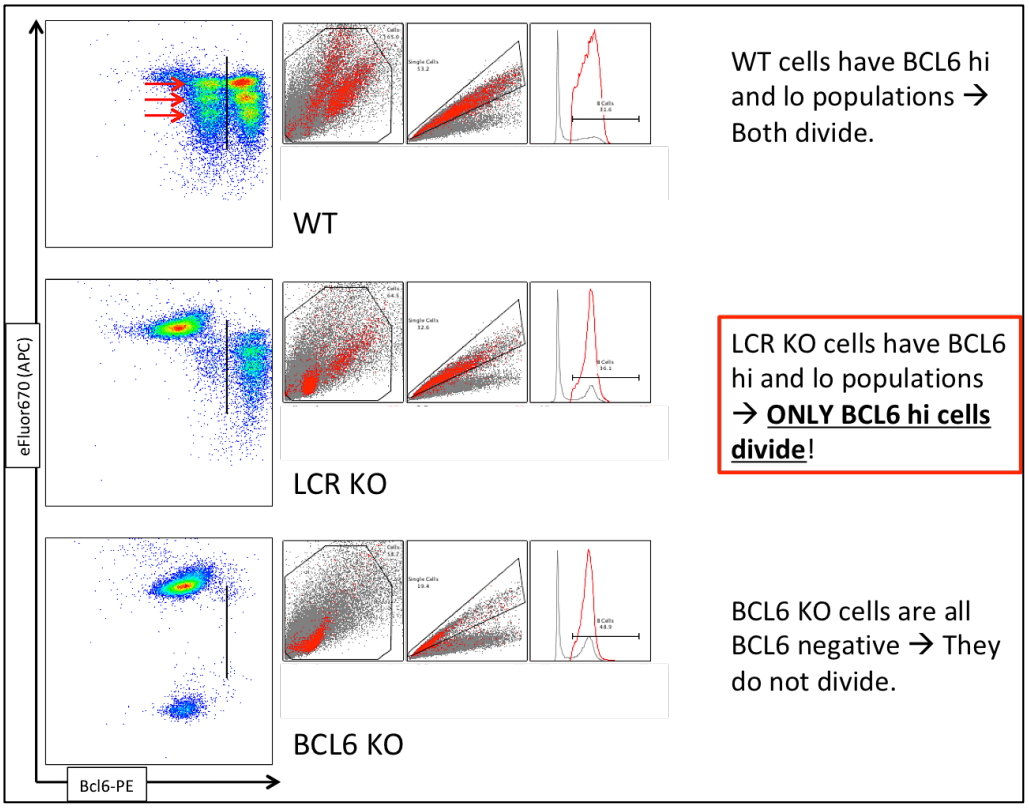

Figure 5.7 Representative flow plots (BCL6 vs. proliferation dye efluor 670) of WT, LCR KO and BCL6 KO B-cells in organoids 4-days post plating. Smaller plots represent the gating (All cells → Singlets → B-cells). Red arrows indicate cell divisions (topmost is undivided).

The results suggested that the LCR KO cells indeed displayed a defect in GC-like cell formation when cultured with lower cytokine concentrations. It also showed

that the LCR KO organoids had two populations: B-cells with and without BCL6. The BCL6 hi cells retained their ability to proliferate normally whereas the sub-population of cells with lo BCL6 did not proliferate and mimicked the BCL6 KO phenotype. In this experiment the overall percentage of GC like cells in LCR KO was significantly less than what was observed for WT cells (figure 5.7).

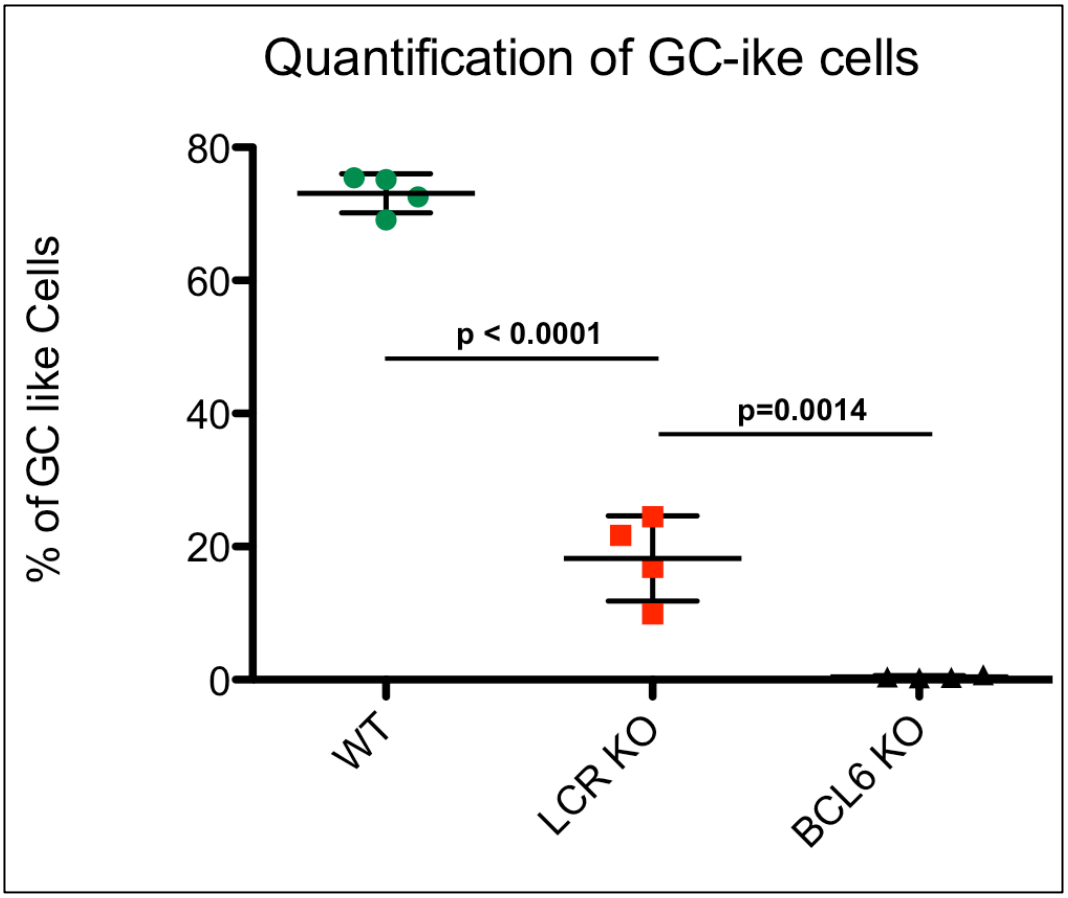

Figure 5.8 Plot quantifying the GC-like cells (% of B220+ cells). Error bars are standard deviation between four technical replicates. P-values are from unpaired, two-tailed t-test.

While these observations were promising, our efforts to replicate this phenotype in culture highlighted an important yet disappointing conclusion. Variability emerged as the key word for germinal center organoids as numerous experiments showed frequently contradicting the observations from figure 5.6 and 5.7.

Figure 5.8 below illustrates one such experiment where the difference between LCR KO and WT organoids was more or less mitigated. Figure 5.9 shows plots where the percentage of GC like cells is plotted for different days along with the level of BCL6 in total B-cells and the GC-like cells. The figure clearly shows that no significant differences were observed in this experiment between WT and KO cells.

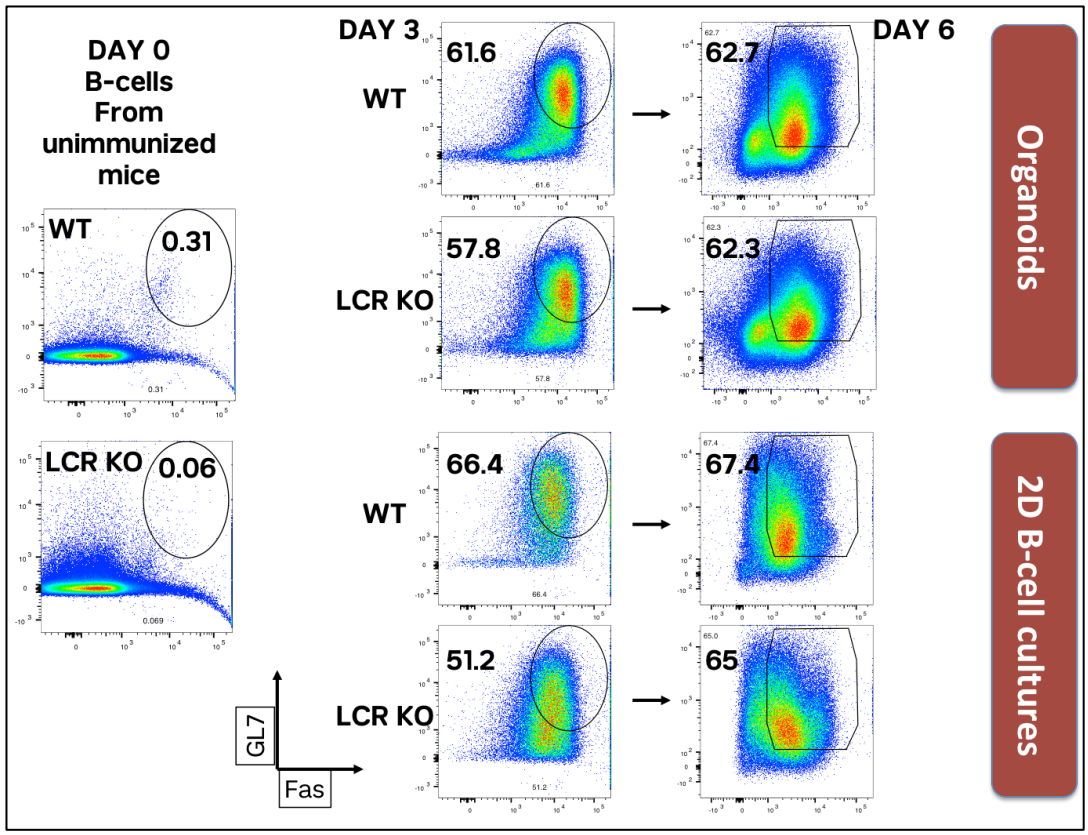

Figure 5.9 Representative flow plots of both B-cell follicle (organoids) and 2D culture from LCR KO and WT B-cells (sorted Naïve B-cells) on day-3 and 6 post plating.

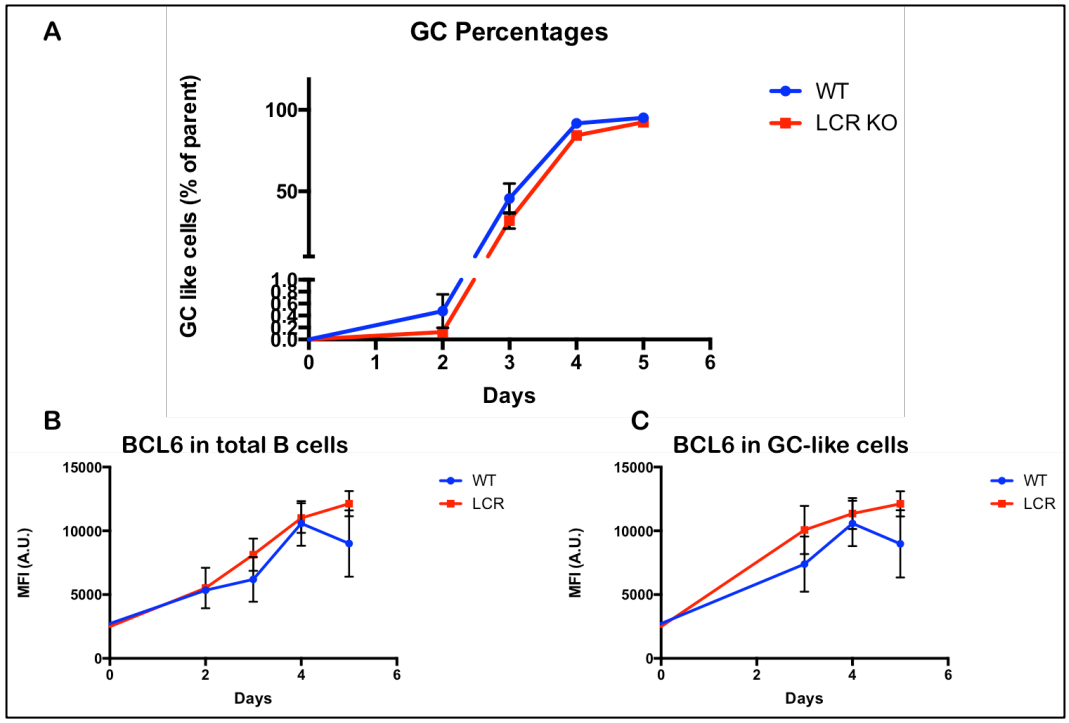

Figure 5.10 (A) Quantifying the percentage of GC-like cells for experiment depicted in figure 5.8. (B) BCL6 levels in all B-cells at different days. (C) BCL6 levels in GC-like cells at different days. No significant differences observed between the two genotypes.

With the issue of variability highlighted through a number of experiments, we decided to try yet another strategy to capture differences between WT and LCR KO organoids. We concluded that to better mimic physiology we should offset the addition of cytokines in the organoids, only plate sorted Naïve B-cells, and also block CD40 signalling through the addition of a blocking antibody. These decisions were influenced not only by literature (Zhang et al., 2017) but also through discussions with experts in the field who had shared unpublished observations in their laboratories. Additionally, we decided to not only test the GC like cell formation trough flow cytometry, but also check the transcript levels of *Bcl6* and other genes relevant to GCB biology via qPCR. We also increased the number of biological replicates by incorporating 3 mice in each group. Finally, based on our previous experiences, we

concluded that the 2D culture (without the nanoparticles and gelatin) would be suitable for the experiment as there no clear reasons to perform the experiment in the 3D setting. We had previously noted that the addition of nanoparticles created a technical challenge during flow assisted sorting of cells, which was needed to get a pure population of cells for cDNA prep. Figure 5.10 below highlights the differences between the two different systems in terms of cytokine addition.

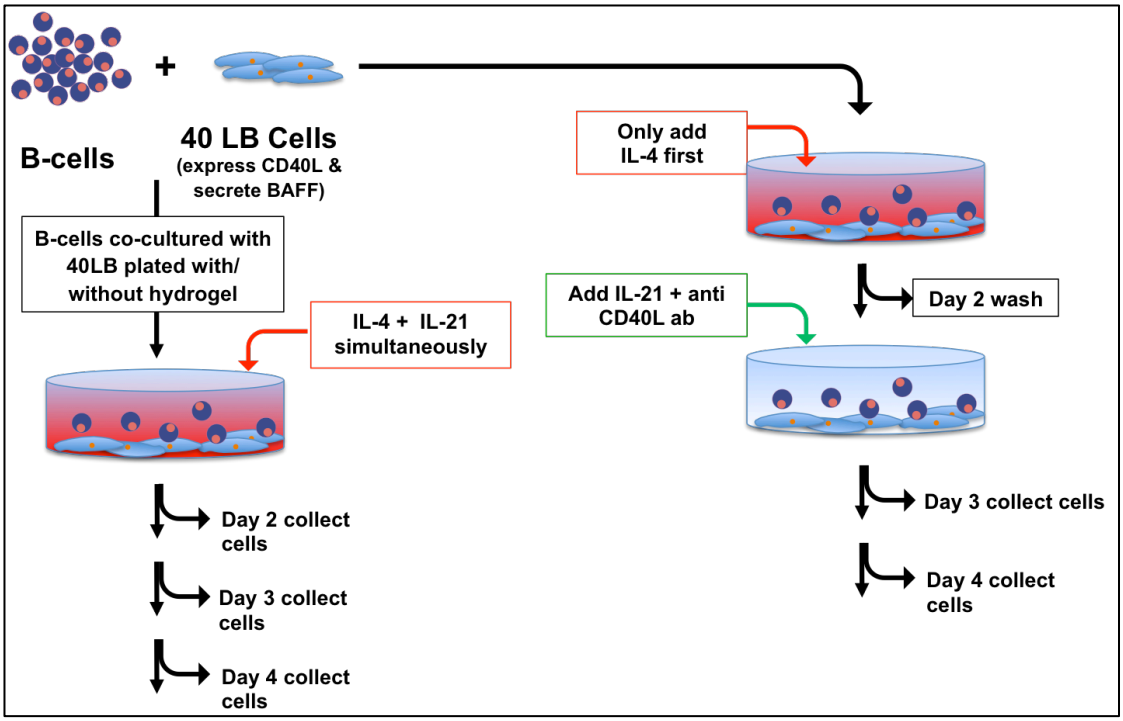

5.11 Schematic for experiment with 2D-culture system where cytokine addition is offset. The left side represents simultaneous cytokine addition, whereas the right side represents the experimental arm where IL-4 was added first and IL-21 two days post plating.

While a pilot experiment with this setup showed promising signs (differences observed at the transcript level of *Bcl6* and other GC genes), the experiment with three biological replicates in each group revealed the true nature of the cells, which was that there were no significant differences between the LCR KO GC-like cells and the WT GC-like cells (Bcl6 transcript levels shown in figure 5.11).

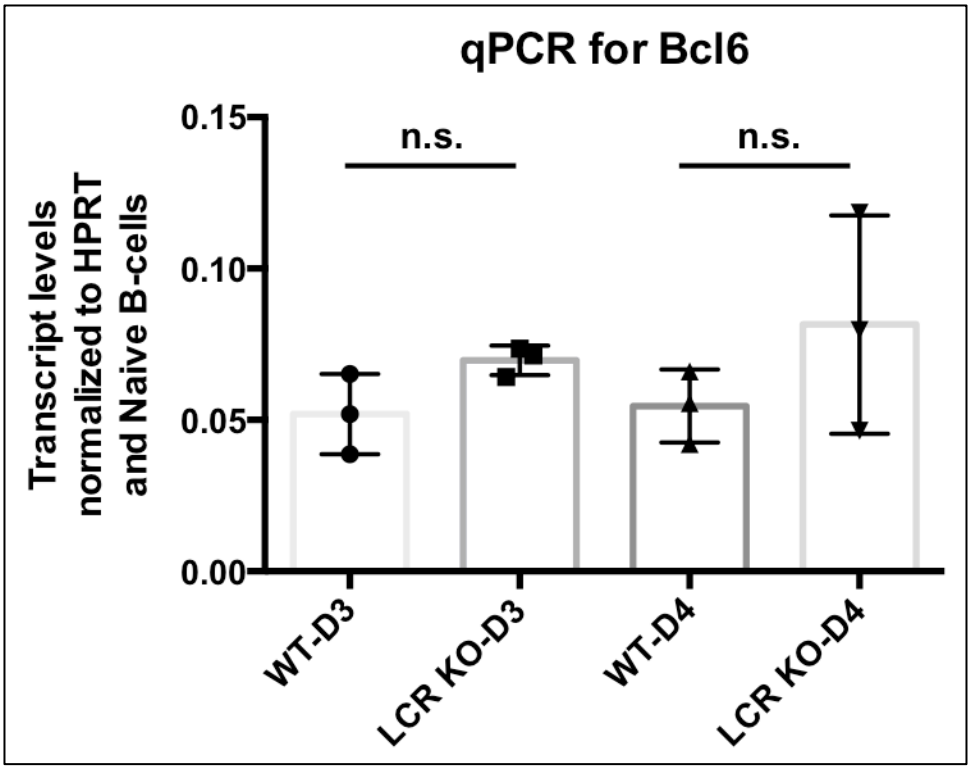

Figure 5.12 qPCR results for Bcl6 levels in WT and LCR KO 2D-cultures (sorted GC-like cells) started with sorted Naïve B-cells. Transcript levels are normalized to HPRT (housekeeping gene) and to the Bcl6 levels at day 0. The error bars are standard error of mean. P-values were calculated via unpaired, two-tailed t-test. No significant differences observed.

5.3 Discussion

Our integrative study comparing the architecture of the genome in human NB and GCB cells reveals a number of mechanisms through which reorganization of chromosomal architecture may accommodate and coordinate the rapid changes in transcriptional programs. The studies revealed a number of fascinating phenomena, which include:

- Loss of inter-arm chromosomal looping in GCB cells (which is likely the basis for the overall nuclear decompaction from NB to GCB.
- The merging of gene neighbourhoods into gene cities, and the concomitant spreading of epigenetic marks across these newly formed gene cities, which is

a potential mechanism to efficiently and quickly coordinate gene expression of multiple genes.

- An increase in overall interactions in key loci revealed through Hi-C and 4C experiments. This includes both the *BCL6* promoter and the upstream LCR experiencing increased connectivity with promoters of other genes relevant to GCB differentiation and enhancers associated with such genes respectively.
- 5' to 3' gene looping for reloading of RNA polymerase II for highly expressed genes.

Through the epigenetic profiling of histone modifications, transcription factor ChIP-seqs, and utilization of chromosomal conformation capture techniques, we identified a putative LCR upstream of *BCL6* which displayed all the features of a cell-specifying regulatory element. The project I undertook to study the potential role of this LCR in a model organism with very little homologous information was, to a certain extent, a leap of faith. While the human data held a lot of promise, the generation of a new mouse model was a step that had to be taken, and it benefitted immensely from the newly available genome editing technique—CRISPR. The successful generation of the LCR KO mouse model was a surprise due to the fact that the expected deletion was unusually large at ~166Kb. The fact that the entire process took less than 6 months is a testament to CRISPR as a technique that is not only allowing us to easily attempt genetic alterations, but also making the entire endeavor achievable at a much faster pace.

The results of my thesis research prove that the enhancer cluster upstream of *Bcl6* is required for germinal center formation in mice, and the extensive phenotyping illustrates that this cluster has the hallmark characteristics of LCRs. Specifically, the

lack of any effect on BCL6 expression in tissues other than GCBs highlights the role of the LCR as a regulatory element that controls the fate of one specific cell type. The mixed bone marrow chimera experiment was performed to determine if the lack of germinal center formation upon SRBC immunization (which should trigger a T-cell dependent immune response) was a GCB autonomous defect or not. The alternative would have been that the T_{FH} cells were primarily affected by the loss of the LCR, which would then have led to a secondary defect in GCB proliferation. The results show that the NB and GCB profiling was pointing in the right direction, i.e. the defect was intrinsic to GCBs and not manifesting primarily through T_{FH} cells. This is especially intriguing, as both GCB and T_{FH} require BCL6 for differentiation. Furthermore, ChIP-seq on T_{FH} cells for histone modifications reveal a degree of H3K27Ac modifications in the locus that represents the LCR in GCBs, albeit to a significantly lower level. It is possible that there is a relatively smaller regulatory role of the LCR in T_{FH} cells, but it does not lead to a complete abrogation of the T_{FH} compartment.

While the LCR is most likely regulating *Bcl6* expression, it has been difficult to provide direct evidence of this specific modality due to the complete loss of GCBs in the LCR KO mice. The experiment where mice with a single copy of the LCR in *trans* with a single functional *BCL6* gene locus exhibit a complete loss of GC formation proved to be an elegant solution to this problem. $BCL6^{+/-}$ mice are known to have a slight defect in overall GC formation compared to WT mice similar to what is observed in $LCR^{+/-}$ mice. While LCRs are known to regulate expression of distal genes, there is also evidence that distance from the LCR is negatively correlated with the level of expression an LCR can induce (Tanimoto, Liu, Bungert, & Engel, 1999). This led us to question if the most proximal gene (in this case *BCL6*) needed to be in

cis with the LCR for it to exert any influence on expression (if it does that at all). When the mice exhibited absolute depletion of the GCB cells in the 'double-hets', that provided, for the first time, a direct link between the LCR and *Bcl6*. If the LCR had no role in regulating *Bcl6* expression, the altered positioning of each locus should not have led to any exacerbation of the otherwise mild defect in GC formation. While establishing the link between the LCR and *Bcl6* is an important step in the project, it is independently an interesting underlying point that such regulatory elements might not function across sister chromosomes. While it is true that an LCR can make far-reaching contacts with multiple distal genes, it might be that those genes need to be on the same chromosome (i.e. be in cis) with the LCR for those interactions to actually occur. The current forms of chromosomal conformation capture techniques do not make this distinction, and thus far this has not been a question that has been of much interest. However, from the perspective of events that occur in the reorganization of the genome between distinct cell stages during differentiation, this could prove to be a critical concern when studying two or more regulatory loci at the same time.

While we tangentially addressed the question of *Bcl6* being regulated by the LCR, our inability to study the GCBs lacking the LCR became a major hurdle. To address this problem, we decided to focus our attention on DLBCL cell lines and primary B-cell cultures from murine splenocytes. Our initial experiments that aimed at deleting the LCR in the OCI-Ly7 cell line proved to unsuccessful. At the time the failure was attributed to the difficulty in obtaining single cell clones from this cell line, which prefers growth in cell clusters. However, subsequent work from other members of the Melnick lab proved that critical regulatory motifs exist within the LCR. These motifs, when individually targeted (via a CRISPR-interference screen) caused those cells to 'drop-out' from culture, thereby highlighting the importance of the LCR. My

attempts at selecting a clone with the entire LCR deleted were retrospectively proven to be a futile experiment.

Switching to B-cell cultures led us into an interesting area of research i.e. the effort to emulate in-vivo conditions of the cell type in question. The work that surrounded the ambitiously named 'GC organoids' proved to be tricky and was plagued by a lack of consistent observations in seemingly consistent culture conditions. In many ways, the decision to study the effect of the LCR on *Bcl6* transcription ex-vivo, acknowledged the fact that the cultures bypass critical physiological cues. For if there existed a hypothetical model that exactly mimicked the phenotype, it would prove to be useless as we would not have any cells left to study the LCR. The formation of ex-vivo GC-like cells with the help of a few critical cytokine signals provided us a chance to attempt a rescue of the cells while still hoping to capture a defect at the transcript level. However, the numerous attempts to discern such an effect proved to be futile. The ever-present reality is that the culture does not capture the temporal nuances, the exact signalling conditions, the true sequence of events occurring in a small fraction of B-cells that form germinal centers in-vivo. The ex-vivo setup strips down the complexity of the actual physiology behind germinal centers to a point where we can only hope to observe the subtleties of locus control region mediated regulation.

Many hypothetical scenarios can be put forth to explain the LCR phenotype which could also include the reasons why we failed to establish a mechanism of action ex-vivo. An important question is the exact moment in B-cell differentiation where presence of the LCR is required. While critical, it is a question that is not going to be easily addressed for some time, as we do not have working models that can be

manipulated in a reliable manner to parse out this particular detail. It is possible that the LCR upstream of *Bcl6* acts as a critical hub (or be one of many) that assimilates the various interleukin and chemokine signals. The convergence of these signals could enable the specific reorganization of genomic architecture that subsequently aids the initiation of the GC transcriptional reprogramming. The engagement of the LCR may be critical at a stage that precedes the events within the germinal center itself i.e. at some extremely early stage post antigen stimulation of Naïve B-cells. This might be aided by signalling events coordinated between different cell types including T_{FH} cells. The fact that the active histone modifications are associated with the LCR in T_{FH} cells is highly suggestive of such a mechanism.

If this hypothesis is true (early LCR engagement model), then our failure to pick up any reliable defects in the organoids and the 2D cultures can be explained. The activation of molecular mechanisms that would allow for effective IL-4 and IL-21 mediated signalling at the appropriate moment in differentiation could be mediated through these potentially early events mediated via the LCR. In the organoids, we might be bypassing this requirement by inundating the cells with signals that would otherwise by downstream of the LCR. Such an act would effectively rescue the phenotype and our observations thus far support such a mechanism. While much of this reads as wild speculation, it is not completely out of the realm of possibility. At the end of the day, the baffling evolutionary gymnastics that led to the existence of the germinal centers surpass what one would imagine being normal, and studying this system is a challenge that allows for such conjecture no matter how far fetched it might seem.

5.4 Materials and Methods

5.4.1 Ex-vivo murine B-cell cultures

Mouse spleens are collected after sacrificing mice post CO_2 mediated euthanasia. Spleens are crushed and filtered through a 70-micron filter and resuspended in 4 ml of cold buffer (PBS, 5mM EDTA and 2% FBS). The filtered splenocytes suspension is gradually layered on top of 3 ml Mouse-Fico-lite in 15 ml falcons at room temperature. The cells are centrifuged at 1500 X g for 20 minutes at 23-degree C. Lymphocytes are collected with a 1 ml pipette by picking up the layer of cells between the two phases. The lymphocytes are transferred to another set of 15 ml falcons with buffer. This second set of tubes is centrifuged at 300 X g for 5 minutes at 4-degree C to wash the cells and rid them of residual ficol. Supernatant is aspirated and cells are resuspended in 5 ml of cold buffer. Cells are counted using a haemocytometer. B-cells are isolated from this suspension using CD43 magnetic beads (Miltenyi Biotec Inc. 130049801). Negative selection with the CD43-MACS beads isolates 'untouched' B-cells that can be cultured ex-vivo. Cells are washed once before plating in complete RPMI (10% FBS, HEPES, L-glutamine and 1X Penicillin/Streptomycin) with LPS (Sigma L4130) at 25µg/ml, IL-4 (R&D # 404-ML-010) at 25ng/ml, and anti-CD40 antibody (eBioscience 16-0402-85) at 1µg/ml. Cells are plated in 6-well plates at 1 million per ml (total 3 ml per well). Cells are sampled at different days for cDNA prep (followed by RNA prep and qPCR) or analysis via flow cytometry.

5.4.2 B-cell Follicle Cultures for Differentiation into 'GCB-Like Cells'

The B-cell follicle culture optimization went through many iterations which involved testing differentiation with and without the gelatin-nanoparticle matrix,

different cytokine concentrations, co-culturing B-cells with 40LB cells or 3T3 cells, and delaying/offsetting cytokine addition. The protocol below describes the steps for assembling the organoids in 96 well plates (Sterile, non-pyrogenic, polystyrene, flat bottom with low evaporation lids- COSTAR 3595 plates) incorporating all the improvements.

40LB cells (BALBc/3T3 cells secreting BAFF and expressing CD154 (or CD40L) are adherent cells which are grown in DMEM (with 10%FBS and 1X Penicillin-Streptomycin). These cells can be cultured in sterile, non-pyrogenic, polystyrene dishes from Corning (Ref# 430167 for 100mm X 20mm, or Ref# 430599 for 150mm X 25mm dishes). Cells are passaged based on cell-confluence, and the day before plating the expected confluency is around 70%. The culture is assembled so as to allow B-cell proliferation and differentiation while preventing the 40LB cells from dividing themselves. This can be achieved through different means. One way to do this is to treat the 40LBs with Mitomycin C (Sigma Aldrich # M0503) at 0.01mg/ml for 55 minutes before co-culturing. Mitomycin C from *Streptomyces caespitosus* is an extremely toxic substance and therefore special care is taken while use as well as for disposal. Another way to do this is to irradiate the 40LB cells with 3000 rads post-trypsinization a few hours prior to the co-culture assembly. The irradiation can be performed in 50 ml falcon tubes or a 150mm culture dish as long as the cells can be transported to the irradiator while maintaining sterile conditions. The irradiator used for our experiments is the he Rad Source Technologies RS 2000 Biological Research X-ray Irradiator. The setting used on this machine to irradiate cells involves placing the tube/plate on level 5 for 6 minutes and 44 seconds.

The B-cells used for culturing are from the spleens of mice. Splenocytes are crushed and filtered through a 70-micron filter before processing with the EasySep™ Mouse B Cell Isolation kit (StemCell Technologies Inc. #19854). The kit employs an immunomagnetic negative selection method that results in the isolation of a >90% pure pan-B-cell population. In recent experiments we have started further isolation of B220+, IgD+ naïve B-cells via FACS to plate a more homogenous population of B-cells. If cell proliferation is also being evaluated then we stain the B-cells with the proliferation dye eFluor-670 (which is detected in the APC channel on a flow cytometer like the BD-Canto II) diluted 1:5000 for 10 minutes at room temperature.

There are two separate forms of the culture based on the addition of a matrix component to the cultures. 1. 3D-organoids which involve the addition of porcine gelatin and silica-based nanoparticles (Laponite XLG) to the culture. This modification is made as an attempt to mimic the extracellular matrix of the B-cell follicles and is touted to be better for proliferation and differentiation of the B-cells. 2. 2D-cultures where the B-cells and 40LB cells are co-cultured in the absence of gelatin and nanoparticles.

To prepare the 3D-organoids, we mix the cells in a 1:1 ratio (i.e. 75000 irradiated 40LB cells are cultured with 75000 sorted naïve B-cells in an organoid in each well). The nanoparticles suspension is prepared separately to a 3% (w/v) stock solution in sterile water. The nanoparticle suspension is made immediately before plating by vortexing the suspension for 3-5 minutes and subsequently filtering the suspension through a 0.45-micron filter (can be done with a syringe). The gelatin solution is a 5% (w/v) stock that is prepared in complete RPMI medium. The solution is mixed and then allowed to dissolve in a 37-degree water bath for 1 hour. The

solution is then filtered through a 0.45-micron filter as well. Both the nanoparticles and gelatin are prepared in sterile conditions.

The cells—which have been mixed together in the required numbers—are first spun down to a pellet by centrifugation at 300 X g for 5 minutes. The supernatant is carefully removed and the cells are gently resuspended in gelatin (20ul of gelatin per organoid) by pipetting. As the gelatin cools down to room temperature it becomes more viscous and therefor difficult to pipette, therefore the cell suspension is placed in a 37-degree water bath or incubator until plating begins. The assembly of an organoid involves pipetting 20ul of the nanoparticle suspension into a well followed by pipetting 20ul of the gelatin-cell suspension into the middle of the nanoparticle suspension. The two are gently mixed together by pipetting, and the appropriate media with or without cytokines is added before placing the plate in a tissue culture incubator set at 37-degree C.

The media that is added to the culture is complete RPMI (with 10% FBS, HEPES, L-glutamine and 1X Penicillin/Streptomycin) with recombinant mouse IL-4 and IL-21. IL-4 concentration ranges from 50 to 0.5 ng/ml. IL-21 concentration ranges from 25 to 2.5 ng/ml (this is specified along with the results for each experiments). 150 to 200ul of media is added to each well. Cells are collected on day 2, 3 and 4 for analysis with flow-cytometry or qPCR.

5.4.3 Fixing, Permeabilizing and Staining Cells for Analysis of Intracellular Proteins

As cells are collected on different days for analysis, we fix the cells with BD Cytofix/Cytoperm buffer and stored at 4-degree C until the day the samples are all stained together. For simple ex-vivo B-cell cultures we wash the cells once with FACS

buffer (PBS with 5mM EDTA and 2% FBS) before fixation. For organoids, we filter the cells once through a 45-micron filter to 'clean up' the cells (remove some of the gelatin and nanoparticles with 40LB cells). The cells are then centrifuged at 400 X g for 5 minutes. If fixation is done in a 96-well v bottom plate then 200ul of the BD cytofix/cytoperm buffer (Cat. No. 554714) is added to each well and the cells are incubated at 4-degree C for 30 minutes. Buffer is washed out via centrifugation an aspiration. This is followed by one round of FACS buffer wash with centrifugation. If cells are to be processed on another day then the cells are resuspended in buffer and can be stored in 4-degree C for up to a week.

If cells are being permeabilized for intracellular staining then the cells are first washed with 1X BD wash buffer (Cat No. 554723). The cells are centrifuged at 900 X g for 5 minutes and supernatant is aspirated. 150ul of cold BD Phosflow buffer III (Cat. No. 558050) is then added slowly (drop-wise) to the wells and the plate is incubated for 30-60 minutes. After the incubation, cells are washed twice with cold FACS buffer. The cells are now ready to be stained. For any intracellular stain (e.g. BCL6-PE or EZH2-AF488) we also ensure the staining of a few wells with an isotype control that is conjugated to the same fluorophore. The typical antigens to be stained for are B220, Fas, GL7 and IgD. If experiment had eFluor670 staining then we leave the APC channel for the proliferation dye.

5.4.4 RNA and cDNA Preparation for Quantitative PCR Analysis of Genes

Cells to be analyzed are resuspended in 1 ml of trizol (100k-1 million cells) and incubated at room temperature for 10 minutes. 200ul of chloroform is added to each tube (RNase free, 1.5 ml eppendorf tubes) and the samples are vigorously shaken before placing them on ice for 15 minutes. Here on all the steps are performed on ice

or at 4-degree C in the centrifuge. Samples are centrifuged at 12000 X g for 15 minutes. The aqueous phase is transferred to another 1.5 ml (RNase free) eppendorf tube for each sample (usually 500-600ul of the aqueous phase is collected). Add 500ul of isopropanol to the aqueous phase and mix by inverting the tubes 2-3 times. Tubes are then transferred to -80-degree C freezer and left overnight to enhance RNA precipitation. The next day the samples are centrifuged at 12000 X g fir 10 minutes. The RNA pellet is washed with 80% ethanol and air dried for 5 minutes before re-suspending in sterile, nuclease free water. RNA concentration is measure via Qubit.

cDNA is prepared for 1ug of the RNA. The RNA concentration should be high enough to have 1ug of RNA in a total of 11ul or less. If RNA concentration for even one of the samples is less than sufficient for this scenario then the cDNA is prepared from a smaller amount (as low as 100ng) for each sample. The verso cDNA synthesis kit (AB1453A) is used for this step. cDNA is prepared in a total reaction volume of 20ul where 11ul is from the sample RNA (we bring up the volume to 11ul with sterile, nuclease free water if needed). The remaining 9ul of the reaction included 4ul of 5X cDNA synthesis buffer, 2ul of dNTP mix, 1 ul of RNA Primer mix (v/v 3 parts random hexamers and 1-part anchored oligo-dT), 1ul of RT enhancer, and 1ul of verso enzyme mix (reverse transcriptase). The tubes (PCR tubes) are vortexed and then spun down. cDNA is prepared in a thermoycler in 1 cycle (42-degree C for 30 minutes →95-degree C for 2 minutes → 4-degree C until samples are removed). The cDNA can then be stored at -20-degree C or diluted 40X for qPCR.

qPCR for genes is performed in a total reaction volume of 10ul in triplicates. We use 384 well plates for the experiment. Primers for the genes to be analyzed are validated prior to the experiment. 100uM stocks of the primers are diluted to 5uM.

The reaction mix per well for qPCR includes 0.5ul of forward and reverse primer mix, 0.5ul of nuclease free water, 5ul of SYBR Green Total, 4ul of diluted cDNA (or water for control). An optical sealing cover is applied on the plate and then the samples are centrifuged at 1000g for 1 minute to remove any bubbles. The qPCR run program includes 1 cycle at 95-degree C for 20 seconds to activate Taq polymerase, followed by 40 cycles of amplification (95-degree C for 20 seconds → 60-degree C for 20 seconds). This is followed by a dissociation curve cycle. Ct values are analyzed with the help of normalizing genes.

Chapter 5 References

Chang, H., Blondal, J. A., Benchimol, S., Minden, M. D., & Messner, H. A. (1995). P53 mutations, c-myc and bcl-2 rearrangements in human non-hodgkin's lymphoma cell lines. *Leukemia and Lymphoma*, *19*(1–2), 165–171. http://doi.org/10.3109/10428199509059672

Haxhinasto, S. a, & Bishop, G. a. (2004). Synergistic B cell activation by CD40 and the B cell antigen receptor: role of B lymphocyte antigen receptor-mediated kinase activation and tumor necrosis factor receptor-associated factor regulation. *The Journal of Biological Chemistry*. http://doi.org/10.1074/jbc.M310628200

Mehra, S., Messner, H., Minden, M., & Chaganti, R. S. K. (2002). Molecular cytogenetic characterization of non-Hodgkin lymphoma cell lines. *Genes, Chromosomes & Cancer*, *33*(May 2001), 225–234. http://doi.org/10.1002/gcc.10025

Nojima, T., Haniuda, K., Moutai, T., Matsudaira, M., Mizokawa, S., Shiratori, I., … Kitamura, D. (2011). In-vitro derived germinal centre B cells differentially generate memory B or plasma cells in vivo. *Nature Communications*, *2*(1). http://doi.org/10.1038/ncomms1475

Purwada, A., & Singh, A. (2017). Immuno-engineered organoids for regulating the kinetics of B-cell development and antibody production. *Nature Protocols*, *12*(1), 168–182. http://doi.org/10.1038/nprot.2016.157

Rush, J. S., & Hodgkin, P. D. (2001). B cells activated via CD40 and IL-4 undergo a division burst but require continued stimulation to maintain division, survival and differentiation. *European Journal of Immunology*. http://doi.org/10.1002/1521-4141(200104)31:4<1150::AID-IMMU1150>3.0.CO;2-V

Tanimoto, K., Liu, Q., Bungert, J., & Engel, J. D. (1999). Effects of altered gene order or orientation of the locus control region on human β-globin gene expression in

mice. *Nature*, *398*, 344. Retrieved from http://dx.doi.org/10.1038/18698

Zhang, T., Gonzalez, D. G., Cote, C. M., Kerfoot, S. M., Deng, S., Cheng, Y., … Haberman, A. M. (2017). Germinal center B cell development has distinctly regulated stages completed by disengagement from T cell help. *ELife*, *6*. http://doi.org/10.7554/eLife.19552